TR-1489-3
(DE84005543)

Energy CONSERVATION

DEVELOPMENT OF MODEL REFERENCE ADAPTIVE CONTROL THEORY FOR ELECTRIC POWER PLANT CONTROL APPLICATIONS

By
Lawrence E. Mabius

September 15, 1982

Work Performed Under Contract No. AC01-78ET29301

The Analytic Sciences Corporation
Reading, Massachusetts

Technical Information Center
Office of Scientific and Technical Information
United States Department of Energy

DISCLAIMER

DISCLAIMER

This report has been reproduced directly from the best available copy.

Available from the National Technical Information Service, U. S. Department of Commerce, Springfield, Virginia 22161.

Price: Printed Copy A04
Microfiche A01

Codes are used for pricing all publications. The code is determined by the number of pages in the publication. Information pertaining to the pricing codes can be found in the current issues of the following publications, which are generally available in most libraries: *Energy Research Abstracts (ERA); Government Reports Announcements* and Index (*GRA* and I); *Scientific and Technical Abstract Reports (STAR);* and publication NTIS-PR-360 available from NTIS at the above address.

Printed in the United States of America
USDOE Technical Information Center, Oak Ridge, Tennessee

TR-1489-3
(DE84005543)
Distribution Category UC-97c

DEVELOPMENT OF MODEL REFERENCE ADAPTIVE CONTROL THEORY FOR ELECTRIC POWER PLANT CONTROL APPLICATIONS

15 September 1982

Prepared Under:

Contract No. AC01-78ET29301

for

DEPARTMENT OF ENERGY
Washington, D.C.

Prepared by:

Lawrence E. Mabius

Approved by:

Charles F. Price
John W. Bartlett

THE ANALYTIC SCIENCES CORPORATION
One Jacob Way
Reading, Massachusetts 01867

ABSTRACT

This report presents the achievements of a three-year research effort in adaptive control design for power plant application. The scope of this effort includes the theoretical development of a multi-input, multi-output (MIMO) Model Reference Control (MRC) algorithm, (i.e., model following control law), Model Reference Adaptive Control (MRAC) algorithm and the formulation of a nonlinear model of a typical electric power plant.

Previous single-input, single-output MRAC algorithm designs have been generalized to MIMO MRAC designs using the MIMO MRC algorithm. This MRC algorithm, which has been developed using Command Generator Tracker methodologies, represents the steady state behavior (in the adaptive sense) of the MRAC algorithm. The MRC algorithm is a fundamental component in the MRAC design and stability analysis. An enhanced MRC algorithm, which has been developed for systems with more controls than regulated outputs, alleviates the MRC stability constraint of stable plant transmission zeroes.

The nonlinear power plant model is based on the Cromby model with the addition of a governor valve management algorithm, turbine dynamics and turbine interactions with extraction flows. An application of the MRC algorithm to a linearization of this model demonstrates its applicability to power plant systems. In particular, the generated power changes at 7% per minute while throttle pressure and temperature, reheat temperature and drum level are held constant with a reasonable level of control. The enhanced algorithm reduces significantly control fluctuations without modifying the output response.

AUTHOR AND CONTRIBUTORS

AUTHOR

Lawrence E. Mabius

CONTRIBUTORS

Alan D. Pisano

Howard Kaufman

Richard V. Monopoli

Kenneth C. Kalnitsky

FOREWORD

This report describes work performed for the Department of Energy under contract No. ET-78-C-01-3392. The authors wish to acknowledge the contributions to this effort of Dr. Howard Kaufman of Rensselaer Polytechnic Institute and Dr. Richard Monopoli of the University of Massachusetts, as consultants.

LIST OF ACRONYMS

CGT - Command Generator Tracker

MIMO - multi-input, multi-output

MRAC - Model Reference Adaptive Control

MRC - Model Reference Control

SISO - single-input, single-output

STR - self-tuning regulator

LIST OF SYMBOLS

Scalars

d_i	relative order index for i^{th} output
$f(s)$	low pass filter in MRAC algorithm
$f_i(s)$	component of $p_i(s)$ $[=h_i(s)f_i(s)]$
$h_i(s)$	component of $p_i(s)$ $[=h_i(s)f_i(s)]$
J_e	enhanced MRC algorithm cost function
ℓ	number of plant outputs
ℓ_s	number of plant measurements
m	number of plant inputs
m_m	number of reference model inputs
n	number of plant states
n_m	number of reference model states
p	number of observer states in MRC algorithm
p_i	number of observer states in MRAC algorithm associated with y_{si} or u_{pi}
$p_i(s)$	s-domain output error dynamics with MRC algorithm
q	number of observer states in MRAC algorithm
$r_{fi}(t)$	i^{th} component of $\underline{r}_f(t)$
$r_i(t)$	i^{th} component of $\underline{r}(t)$
$u_{fi}(t)$	i^{th} component of $\underline{u}_{pf}(t)$
$u_i(t)$	i^{th} component of $\underline{u}_{pl}(t)$
$u_{pi}(t)$	i^{th} component of $\underline{u}_p(t)$
$V(t)$	Lyapunov function
$y_{si}(t)$	i^{th} component of $\underline{y}_s(t)$
α_{ij}	j^{th} pole of $f_i(s)$

Vectors

$\underline{b}$	MRAC algorithm observer control parameters
$\underline{b}_{oi}$	i^{th} column of B_o
$\underline{c}_{oi}^T$	i^{th} row of C_o
$\underline{e}(k)$	DT† state error
$\underline{e}(t)$	CT†† state vector
$\underline{e}_N(t)$	transformed CT state error
$\underline{e}_y(k)$	DT output error
$\underline{e}_y(t)$	CT output error
$\hat{\underline{e}}_y(t)$	CT output error estimate
$\underline{e}_z(k)$	DT observer state error
$\underline{e}_z(t)$	CT observer state error
$\underline{e}_{zf}(t)$	CT filtered state error
$\underline{r}(t)$	CT MRAC algorithm inputs
$\underline{r}_f(t)$	CT filtered MRAC algorithm inputs
$\underline{u}_m(k)$	DT reference model controls
$\underline{u}_m(t)$	CT reference model control
$\underline{u}_p(k)$	DT plant controls
$\underline{u}_p(t)$	CT plant controls
$\underline{u}_{pf}(t)$	CT filtered control
$\underline{u}_{pl}(k)$	subset of $\underline{u}_p(k)$ used in MRC/MRAC algorithm
$\underline{u}_{pl}(t)$	subset of $\underline{u}_p(t)$ used in MRC/MRAC algorithm
$\bar{\underline{u}}_{pl}(k)$	DT MRC algorithm
$\bar{\underline{u}}_{pl}(t)$	CT MRC algorithm
$\underline{u}^*_{pl}(k)$	DT CGT ideal control trajectory
$\underline{u}^*_{pl}(t)$	CT CGT ideal control trajectory
$\underline{u}_{p2}(k)$	Subset of $\underline{u}_p(k)$ used in MRC enhancement
$\underline{u}_{p2}(t)$	Subset of $\underline{u}_p(t)$ used in MRC enhancement
$\underline{w}(t)$	observer state vector in MRAC algorithm
$\underline{w}_i(t)$	i^{th} subset of $\underline{w}(t)$
$\bar{\underline{w}}_i(t)$	decomposition of $\underline{z}(t)$
$\underline{x}_m(k)$	DT reference model state vector
$\underline{x}_m(t)$	CT reference model state vector
$\underline{x}_p(k)$	DT plant state vector
$\underline{x}_p(t)$	CT plant state vector
$\hat{\underline{x}}_p(k)$	DT observer state estimate

$\hat{\underline{x}}_p(t)$ CT observer state estimate

$\underline{x}_p^*(k)$ DT CGT ideal state trajectory

$\underline{x}_p^*(t)$ CT CGT ideal state trajectory

$\underline{y}_m(k)$ DT reference model output

$\underline{y}_m(t)$ CT reference model output

$\underline{y}_p(k)$ DT plant output

$\underline{y}_p(t)$ CT plant output

$\underline{y}_s(k)$ DT plant measurements

$\underline{y}_s(t)$ CT plant measurements

$\underline{z}(k)$ DT observer state (MRC algorithm)

$\underline{z}(t)$ CT observer state (MRC algorithm)

$\underline{\Delta}(t)$ Filter control error (MRAC algorithm)

$\underline{\varepsilon}(t)$ CT augmented error

$\underline{\theta}(k)$ DT CGT filter state

$\underline{\theta}(t)$ CT CGT filter state

Matrices

A State parameters in MRAC algorithm observer dynamics

A_e State parameters in augmented error dynamics

A_m State parameters in CT reference model dynamics

A_N State parameters in transformed error dynamics

A_o State parameters in CT (MRC) observer dynamics

A_p State parameters in CT plant dynamics

A_w State parameters in MRAC observer dynamics

B_N Control parameters in transformed error dynamics

B_o Measurement parameters in MRC observer dynamics

B_p Control parameters in CT plant dynamics

B_{p1} Subset of B_p corresponding to $\underline{u}_{p1}(t)$

B_{p2} Subset of B_p corresponding to $\underline{u}_{p2}(t)$

B_w Measurement parameters in MRAC observer dynamics

C_m State parameters in reference model output

C_N State parameters in output of transformed error

C_o Control parameters in CT MRC observer dynamics

C_p State parameters in plant output

C_w Control parameters in MRAC observer dynamics

E First p rows of W^{-1}

F_m State parameters in DT reference model dynamics

F_o State parameters in DT (MRC) observer dynamics

F_p State parameters in DT plant dynamics

G State feedback gain in enhanced MRC algorithm

G_m Control parameters in DT reference model dynamics

G_o Measurement parameters in DT MRC observer

G_p Control parameters in DT plant dynamics

G_{p1} Subset of G_p corresponding to $\underline{u}_{p1}(k)$

G_{p2} Subset of G_p corresponding to $\underline{u}_{p2}(k)$

G_u Feedforward gain in enhanced MRC algorithm

G_x Feedforward gain in enhanced MRC algorithm

$H(s)$ Output error dynamics (s-domain) with MRC algorithm

H_o Control parameters in DT MRC observer

H_p State parameters in plant measurement

I_p p×p identity matrix

$\bar{K}$ State feedback gain in MRC algorithm

$K_I(t)$ Integral component of adaptive gain

K_{I0} Initial condition on $K_I(t)$

$K_p(t)$ Proportional component of adaptive gain

$\bar{K}_r$ Concatenation of MRC gains

$K_r(t)$ Concatenation of MRAC adaptive gains

$\bar{K}_u$ Feedforward gain ($\underline{u}_m$) in MRC

$K_u(t)$ Adaptive feedforward gain ($\underline{u}_m$) in MRAC

$\bar{K}_{u2}$ Feedforward gain ($\underline{u}_{p2}$) in MRC

$K_{u2}(t)$ Adaptive feedforward gain ($\underline{u}_{p2}$) in MRAC

$\bar{K}_w$ Feedback gain ($\underline{w}$) in MRC

$K_w(t)$ Adaptive feedback gain ($\underline{w}$) in MRAC

$\bar{K}_x$ Feedforward gain ($\underline{x}_m$) in MRC

$K_x(t)$ Adaptive feedforward gain ($\underline{x}_m$) in MRAC

$\bar{K}_y$ Feedback gain ($\underline{y}_s$) in MRC

$K_y(t)$ Adaptive feedback gain ($\underline{y}_s$) in MRAC

L Matrix used to compute MRC gains

$L_I(t)$ Integral component of $L_\Delta(t)$

L_o Nominal value for L

$L_p(t)$ Proportional component of $L_\Delta(t)$

$L_\Delta(t)$ Adaptive gain in output error estimate (MRAC)

N Matrix used to compute MRC gains

p^0_ℓ $p \times \ell$ null matrix

P Positive definite matrix in Lyapunov function

Q Feedback gain in transformed error dynamics

Q_e Positive definite Lyapunov derivative matrix

Q_L Gain matrix in MRAC

R_1 $\underline{u}_{p1}$ weighting matrix in J_e

R_2 $\underline{u}_{p2}$ weighting matrix in $J_{\dot{e}}$

R_{11} R_{21}
R_{12} R_{22}
R_{13} R_{23}
} DT ideal trajectory parameters

S_K Lyapunov function parameter

S_L Lyapunov function parameter

S_{11} S_{21}
S_{12} S_{22}
S_{13} S_{23}
} CT ideal trajectory parameters

T_i i^{th} subset of T_w

T_{KI} $K_I(t)$ adaptation parameters in MRAC

T_{KP} $K_p(t)$ adaptation parameters in MRAC

T_{LI} $L_I(t)$ adaptation parameters in MRAC

T_{LP} $L_p(t)$ adaptation parameters in MRAC

W Transformation from observer states to plant state estimates

W_1 $\underline{z}(t)$ component of W

W_2 $\underline{y}_s(t)$ component of W

Λ_{11} Λ_{12}
Λ_{21} Λ_{22}
} Partitions of DT quad inverse

Ω_{11} Ω_{12}
Ω_{21} Ω_{22}
} Partitions of CT quad inverse

†DT discrete-time

††CT continuous-time

TABLE OF CONTENTS

LIST OF FIGURES

LIST OF TABLES

1.0 INTRODUCTION

The objective of this project has been to extend the technology of Model Reference Adaptive Control (MRAC) for multi-input, multi-output (MIMO) systems in such a way as to make the technology applicable to the control of electric generating plants. In working toward these objectives this project has been divided into two phases. The first phase has been to develop an MRAC algorithm for MIMO systems. An important component in this phase has been the development of the MIMO Model Reference Control (MRC) algorithm. The MRC algorithm is the nonadaptive counterpart of the MRAC algorithm and represents the steady state (in the adaptive sense) behavior of the MRAC algorithm. The second phase has been the validation and understanding of the algorithms using a power plant model. An important development in this phase is the nonlinear model of Philadelphia Electric's Cromby No. 2 Unit. A linearization of this model has been used to test and evaluate the MRC algorithm.

2.0 BACKGROUND

The electric power plant control problem is characterized by multiple plant inputs and outputs. That is, a set of controls (e.g., coal mill feeder stroke, feed water and governor valve positions, spray flows and burner positions) must be manipulated such that the power generated will track load demand while other plant variables (e.g., drum level, steam temperatures and pressures) remain within specified constraints. The relationships between the outputs (power generated and regulated plant variables) and the controls are highly nonlinear with each output possibly influenced by a number of controls. Modern multivariable control design techniques are well suited for this type of problem.

Current industry-wide control designs are based on single-loop principles relating each output to a single control. These designs include feedforward commands which may attempt to coordinate some of the single-loop structures (see Fig. 1-1 where u_1, u_2 ... are the controls and y_1, y_2,... are the outputs); however, performance is limited by the lack of coordination or "direct communication" between feedback controllers. This lack of feedback coordination leads to hunting as each controller responds to process changes on an individual basis. Modern control approaches, which intrinsically account for loop interactions (see Fig. 1-2 where Command Generator Tracker is a feedforward/feedback multiloop coordinator), promise improved performance capabilities, as demonstrated by control-related performance improvements in many aerospace designs and at least one utility simulation -- the Cromby study.

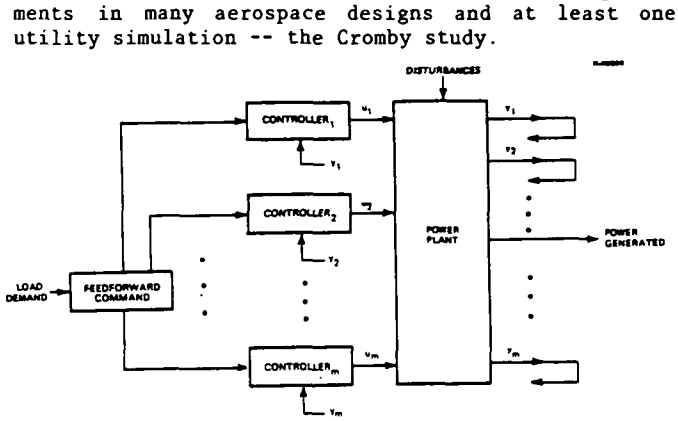

Figure 1-1 Current Control Designs for Power Plant

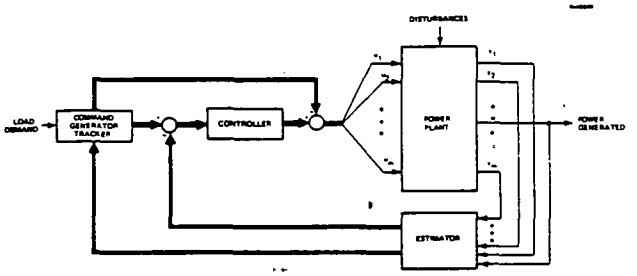

Figure 1-2 Modern Multivariable Control Design for Power Plant

Electric generating plant performance and response have been improved in the past primarily through advancements in plant and controller hardware. Controller hardware evolution is exemplified by the change in turbine governors from mechanical to analog-electro-hydraulic and to digital-electro-hydraulic designs (Ref. 1). However, the enhancement in hardware has not been accompanied by corresponding advances in control strategies. Single-loop control strategies continue to be used, despite the significant advantages associated with modern multivariable control.

The very fact that coordination of controls is inherent to the success of modern control algorithms is, ironically, the reason for doubting the practical value of such algorithms in utility applications. These control algorithms are dependent on models of the systems to be controlled and the performance of the coordinated controls depends on the accuracy with which the models predict the behavior of the system. Due to the complex and diverse nature of utility-type systems, their models have limited accuracy. As a result, the improved performance generated by modern control algorithms is diminished.

The overall objective of this project has been to develop a multi-input, multi-output (MIMO) Model Reference Adaptive Control (MRAC) algorithm which exhibits reduced sensitivity to modeling errors and measurement noise. MRAC algorithms intrinsically adapt to changes in plant parameters and hence offer enhanced robustness of the control system which improves performance under less-than-ideal conditions. The robustness of the MRAC algorithm with uncertain system parameters is assumed through a Lyapunov stability analysis.

3.0 ACCOMPLISHMENTS

An extensive review of the literature has shown that existing adaptive control schemes are of two general types: either the self-tuning regulator (STR) or the model reference adaptive controller. Although STRs have fewer restrictions and thus wider applicability, unlike MRACs they cannot guarantee closed loop stability. Previous MRAC algorithms which have been designed for single-input, single-output (SISO) systems have global stability properties that cause output errors to asymptotically approach zero. MRAC algorithms which have previously been designed for MIMO systems are globally stable but only result in state errors being bounded. The goal of this effort has been to develop MIMO MRAC algorithms with characteristics similar to the SISO MRAC algorithms.

The fundamental achievement in this project has been the development of the MIMO Model Reference Control (MRC) algorithm (or model following control

algorithm) using the Command Generator Tracker methodology. The MRC algorithm has been developed for linear multi-input, multi-output (MIMO) time-invariant continuous- and discrete-time systems with known parameters. The MRC algorithm is the nonadaptive (requiring knowledge of the plant parameters) counterpart to the MRAC algorithm. The MRC algorithm development is a significant achievement in this research because: (1) it is a unique model following control algorithm and (2) represents the steady state behavior (or ideal goal) of the MRAC. That is, the MRAC algorithm adjusts the control gains toward the MRC algorithm gains. Once the gains reach their MRC values, no more adaptation will occur. Thus, the MRC algorithm is an important component in the MRAC algorithm analysis.

Model Reference Control (MRC) is based upon matching the response of a system having known parameters to that of a reference model which has desirable design specifications incorporated within it. For example, the outputs to a step input might be characterized by specified rise times, overshoots, and/or damping ratios. The controller and reference model work together to incorporate these characteristics into the plant outputs. The reference inputs are fed into the reference model, the outputs of which respond in accordance with the design specifications that have been built into it. The control system is designed such that the inputs to the plant drive the outputs of the plant to equal the outputs of the reference model.

The second major accomplishment has been the development of the MRAC algorithm for linear MIMO time-invariant and continuous-time systems with unknown parameters. The adaptive algorithm is an extension of the MRAC algorithm, previously developed by Mabius and Kaufman (Ref. 2), using the MRC algorithm described above. The algorithm is also an extension to MIMO systems of previously developed single-input, single-output (SISO) MRAC algorithms (Ref. 3). In fact, the MRAC algorithm presented here degenerates into the SISO algorithm if the number of inputs and outputs is one. The fundamental difference in the approach taken here is that the MRC algorithm and most of the MRAC algorithm are formulated in state-space and matrix format (as opposed to input/output differential equation format). The MRC algorithm is implementable if the plant parameters are unknown, whereas the MRAC algorithm is applicable when the plant parameters are unknown.

Since the MRAC algorithm is derived from a Lyapunov function, the resulting system is globally stable. The application of this algorithm is restricted by one aspect of the design which is required to complete the stability analysis. The author feels this restriction on the design can be overcome with continued research on the algorithm. Other MRAC algorithms have been developed earlier in this contract. These algorithms are similar in nature to the previously developed MIMO MRAC algorithms resulting in bounded error stability and requiring a more stringent constraint for stability.

The third major accomplishment is development of a boiler-turbine-generator power plant model of Philadelphia Electric Company's Cromby No. 2 Unit used to study and validate the control algorithms. This model is a nonlinear, state-space representation of the Cromby plant and has been developed from first-principle considerations (Refs. 4 and 5). Since test data are available for validation, this model is considered to be highly realistic with regard to predicting plant behavior.

The fourth major accomplishment of this project has been validating the continuous-time MRC algorithm with a linearization of the power plant model behavior near 190 MW. In this application, five controls have been designed to maintain throttle pressure and temperature, reheater output temperature and drum level at a fixed level. At the same time, generated power response to load demand rate has been included in the reference model as a first order lag and integator. The regulating controls are mill feeder stroke, superheater burner tilt, reheater burner tilt, feedwater valve area and throttle valve area. With the MRC algorithm, the output of the linear model responds exactly as designed (no output variations except generated power which has very smooth 7% of load demand per minute response) and the controls remain within their designed bounds. This result is important since the MRC algorithm represents the behavior of the MRAC once adaptation is complete. In effect, the applicability of the MRAC algorithm in the (adaptive) steady-state has been verified.

The final major achievement of this project has been the enhancement of the MRC algorithm. The application previously described is characterized by rapid and large variations in the controls. This result has been dramatically improved by introducing the remaining power plant controls, air flow, feedwater valve area, and governor valve lift. In the enhanced MRC algorithm these controls are optimally chosen to balance the efforts of all the controls in an outer loop control system around the inner loop MRC algorithm. If the MRAC algorithm were similarly enhanced, these outer loop controls would not be adaptive.

4.0 RECOMMENDATIONS

Future efforts in this area of research should deal with the MRC algorithm high feedback gain characteristics. In spite of the excellent performance reported in Section 3.0 above, the feedback gains are relatively high. This causes large fluctuations in the controls when unmodeled disturbances enter the system or initial condition errors are significant. This problem may not have occurred if the control system could be applied to a lower order model of the power plant. However, the MRC and MRAC stability theory do not deal with unmodeled dynamics. Hence, the stability problem with unmodeled dynamics is an important topic for future research with respect to the MRAC algorithm.

Future efforts on the MRAC algorithm should also deal with the structural constraints necessary to establish stability. As noted above, the algorithm is limited to plants satisfying limiting structural constraints, necessary to complete the stability analysis. The author feels that, without much difficulty, future efforts should be able to modify the algorithm or the stability analysis to eliminate this restriction.

5.0 REFERENCES

1. Osborne, R.L., "Controlling Central Station Steam Turbine-Generators," Instruments and Control Systems, Vol. 48, No. 11, November 1975, pp. 29-32.

2. Mabius, L.E., and Kaufman, H., "An Adaptive Flight Controller for the F-8 Without Explicit Parameter Identification," Proceedings of the 1976 IEEE Conference on Decision and Control (Clearwater), December 1976, pp. 9-14.

1.0 INTRODUCTION

1.1 BACKGROUND

The electric power plant control problem is characterized by multiple plant inputs and outputs. That is, a set of controls (e.g., coal mill feeder stroke, feed water and governor valve positions, spray flows and burner positions) must be manipulated such that the power generated will track load demand while other plant variables (e.g., drum level, steam temperatures and pressures) remain within specified constraints. The relationships between the outputs (power generated and regulated plant variables) and the controls are highly nonlinear with each output possibly influenced by a number of controls. Modern multivariable control design techniques are well suited for this type of problem.

Current industry-wide control designs are based on single-loop principles relating each output to a single control. These designs include feedforward commands which may attempt to coordinate some of the single-loop structures (see Fig. 1.1-1 where u_1, u_2, ... are the controls and y_1, y_2, ... are the outputs); however, performance is limited by the lack of coordination or "direct communication" between feedback controllers. This lack of feedback coordination leads to hunting as each controller responds to process changes on an individual basis. Modern control approaches, which intrinsically account for loop interactions (see Fig. 1.1-2 where Command Generator Tracker is a feedforward/feedback multiloop coordinator), promise improved performance capabilities, as demonstrated by control-related performance improvements in many aerospace designs and at least one utility simulation -- the Cromby study (see Chapter 5).

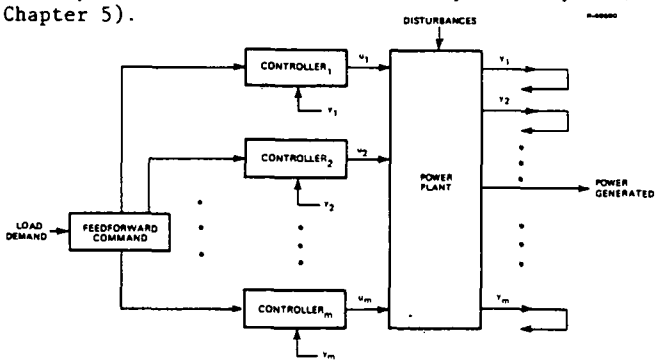

Figure 1.1-1 Current Control Design for Power Plants

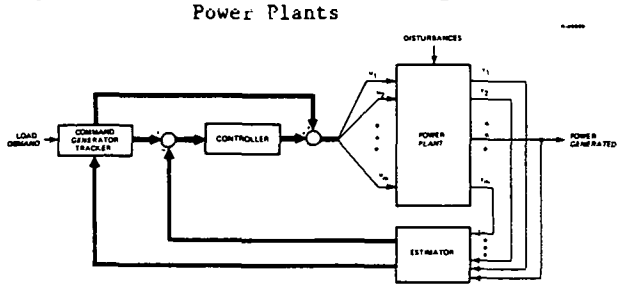

Figure 1.1-2 Modern Multivariable Control Design for Power Plants

Electric generating plant performance and response have been improved in the past primarily through advancements in plant and controller hardware. Controller hardware evolution is exemplified by the change in turbine governors from mechanical to analog-electro-hydraulic and to digital-electro-hydraulic designs (Ref. 1). However, the enhancement in hardware has not been accompanied by corresponding advances in control strategies. Single-loop control strategies continue to be used, despite the significant advantages associated with modern multivariable control.

The very fact that coordination of controls is inherent to the success of modern control algorithms is, ironically, the reason for doubting the practical value of such algorithms in utility applications. These control algorithms are dependent on models of the systems to be controlled and the performance of the coordinated controls depends on the accuracy with which the models predict the behavior of the system. Due to the complex and diverse nature of utility-type systems, their models have limited accuracy. As a result, the improved performance generated by modern control algorithms is diminished.

1.2 OBJECTIVES

The overall objective of this project has been to develop a multi-input, multi-output (MIMO) Model Reference Adaptive Control (MRAC) algorithm which exhibits reduced sensitivity to modeling errors and measurement noise. MRAC algorithms intrinsically adapt to changes in plant parameters and hence offer enhanced robustness of the control system which improves performance under less-than-ideal conditions The robustness of the MRAC algorithm with uncertain system parameters is assumed through a Lyapunov stability analysis.

Research by Monopoli (Ref. 2) and others (Ref.3) on single-input, single-output (SISO) MRAC design procedures has led to adaptive algorithms which cause the plant and model outputs to converge asymptotically. These algorithms do not require any positive real constraints on the plant and only output (not full state) feedback. However, due to their formulation, it is cumbersome to extend the algorithms to multivariable systems.

An approach for designing model reference adaptive controllers for multivariable linear systems was originally proposed by Mabius and Kaufman (Refs. 4, 5, 6). The applicability of this adaptive controller has been demonstrated using the linearized equations of motion for a typical fighter aircraft (Ref. 5). Results showed the algorithm to be capable of sufficiently rapid adjustment of control gains to compensate for instantaneous altitude and velocity changes. However, the algorithm was limited by:

- The guarantee of only a bounded error between the plant and model state vector
- The need for the order of the model to be the same as the order of the plant
- The requirement that the plant satisfy a positive real constraint to achieve stability
- The requirements of full state feedback.

The specific objective of this effort has been to generalize the SISO MRAC algorithms to MIMO systems. First, previous work at TASC on Command Generator Tracker (CGT) algorithms (Refs. 7, 8) has led to the development of the MIMO Model Reference Control (MRC) algorithm. This algorithm then provides the basis for the MIMO MRAC design. The evolution of the latter is analogous to the development of Monopoli's

SISO MARC design from early SISO model-following control ideas.

1.3 ACCOMPLISHMENTS

The fundamental achievement in this project has been the development of the MIMO Model Reference Control (MRC) algorithm (or model following control algorithm) using the Command Generator Tracker methodology. This algorithm represents the steady state (in terms of adaptation) behavior of the Model Reference Adaptive Control (MRAC) algorithm and hence is a fundamental component in its design and analysis. The MRC algorithm has been developed for linear multi-input, multi-output (MIMO) time-invariant continuous- and discrete-time systems with known parameters.

The second major accomplishment has been the development of the MRAC algorithm for linear MIMO continuous-time systems with unknown parameters. Since the algorithm is derived from a Lyapunov function the resulting system is globally stable. The algorithm is formulated around the continuous-time MRC algorithm, and in some aspects is a generalization of Monopoli's algorithm. The fundamental difference in the generalized approach is that the MRC algorithm and most of the MRAC algorithm are formulated in state-space and matrix format (as opposed to input/output differential equation format). The application of this algorithm is restricted by one aspect of the design which is required to complete the stability analysis. The author feels this restriction on the design can be overcome with continued research on the algorithm. Other MRAC algorithms have been developed earlier in this contract. These algorithms are similar in nature to the previously developed MIMO MRAC algorithms resulting in bounded error stability and requiring a more stringent constraint for stability.

The third major accomplishment is development of a boiler-turbine-generator power plant model of Philadelphia Electric Company' Cromby No. 2 Unit used to study and validate the control algorithms. This model is a nonlinear, state-space representation of the Cromby plant and has been developed from first-principle considerations (Refs. 9 and 10). Since test data are available for validation, this model is considered to be highly realistic with regard to predicting plant behavior.

The fourth major accomplishment of this project has been validating the continuous-time MRC algorithm with a linearization of the power plant model behavior near 190 MW. In this application, five controls have been designed to maintain throttle pressure and temperature, reheater output temperature and drum level at a fixed level. At the same time, generated power response to load demand rate has been included in the reference model as a first order lag and integrator. The regulating controls are mill feeder stroke, superheater burner tilt, reheater burner tilt, feedwater valve area and throttle valve area. With the MRC algorithm, the output of the linear model responds exactly as designed (no output variations except generated power which has very smooth 7% of load demand per minute response) and the controls remain within their designed bounds. This result is important since the MRC algorithm represents the behavior of the MRAC once adaptation is complete. In effect, the applicability of the MRAC algorithm in the (adaptive) steady-state has been verified.

The final major achievement of this project has been the enhancement of the MRC algorithm. The application previously described is characterized by rapid and large variations in the controls. This result has been dramatically improved by introducing the remaining power plant controls, air flow, feedwater valve area, and governor valve lift. In the enhanced MRC algorithm these controls are optimally chosen to balance the efforts of all the controls in an outer loop control system around the inner loop MRC algorithm. If the MRAC algorithm were similarly enhanced, these outer loop controls would not be adaptive.

This report presents a detailed description of the achievements summarized above. A literature review of adaptive control and a formulation of model reference adaptive control appears in Chapter 2. The basic MRC algorithm and its enhancement are detailed in Chapter 3 along with analysis of the plant/model error with the MRC algorithm. Chapter 4 presents the MRAC algorithm and a stability analysis using the Lyapunov approach. Other MRAC algorithms developed during this contract and reported in previous Topical Reports are included in Appendix E. Chapter 5 presents a summary of the Cromby model; a detailed development is given in Appendix A. The application of the MRC algorithm to a linearization of the power plant appears in Chapter 6.

2.0 ADAPTIVE CONTROL PROBLEM FORMULATION

2.1 BACKGROUND

As discussed in Chapter 5 and detailed (using a representative example) in Appendix A, the power plant is a system which, when modeled in state variable format, has nonlinear dynamics and measured outputs which are nonlinear combinations of states. As a result, it is not easy to apply modern control theory (largely a linear system technology) directly to power plant control design. Usually, however, each control can be computed as the sum of an open loop control and an incremental control. The open loop control, which can be computed a priori, drives the plant to a given (usually constant) state referred to as the operating point. The incremental control responds to deviations of the system about the operating point. Since the system behavior near the operating point can be described approximately by a linear model, the incremental control design can be formulated using linear modern control theory.

Due to their nature, the incremental controls are feedback-type controls. They serve to stabilize the system about the operating point and regulate transient performance when small changes in the operating point are required. In nonlinear systems such as the power plant, the following problems can arise.

- The parameters of the linear incremental model may change as the operating point changes
- The nonlinear dynamics of the power plant may change with time (e.g., due to aging)
- The linear incremental model only approximates the nonlinear behavior of the plant near the operating point.

In many cases these problems can be overcome by the incremental control design technique because

- The robust property of the incremental control design causes the system stability to be insensitive in a local sense to small parameter changes and disturbances
- The control design gains are scheduled as functions of the operating point.

However, large uncertainty of the parameters (often the case in power plants) can result in undesirable transient performance and even global instability.

The problem of performance regulation in the face of unknown system parameters has been heavily addressed by adaptive control for single-input, single-output systems; however, the corresponding problem for the more general multi-input, multi-output (MIMO) nonlinear system such as the power plant has not yet received much emphasis. Since theoretical advances in adaptive control may lead to its application in power plant control design, TASC's goal is to extend adaptive control theory in such a way as to make it applicable to the particular problems of the power plant control discussed above. This chapter and Chapters 3 and 4 address the progress we have made toward these goals. Section 2.2 presents a review of previous results that are relevant to our study. In Section 2.3, a formulation of the linear MIMO model reference adaptive control problem is presented.

2.2 REVIEW OF PREVIOUS WORK

Although the ultimate goal of our work is applying adaptive control to the power plant system, the intent of this report is a theoretical development. Hence, this review of the theoretical work includes a brief description of the literature on application of the technology.

Most of the research in adaptive control has been devoted to linear systems with either continuous- or discrete-time representations. A significant part of this research has concentrated on single-input, single-output (SISO) systems. Within the class of linear SISO systems two promising approaches have emerged: the self-tuning regulator (STR) (Ref. 11) and the Model Reference Adaptive Controller (MRAC) (Ref. 3). The STR approach adjusts the control parameters based on explicit estimates of the system parameters which are obtained through a parameter identification scheme. MRAC directly adjusts the control law parameters using a Lyapunov-based scheme which ensures that the resulting closed loop system is stable. In the current literature STR's are more easily designed and less restricted but generally do not guarantee stability, whereas, MRAC's are complex structures and have restricted applications, but guarantee a stable closed loop system.

The first step in designing adaptive control schemes is the development of a parameterized control law such that, given complete knowledge of the system to be controlled, the control law parameters can readily be chosen. The model reference controller (MRC), which serves this purpose adequately, is an intrinsic part of MRAC designs (Ref. 11 and 12) and is commonly used in STR designs. It is, however, restricted to minimum phase systems. Aström has proposed an alternative controller (similar to MRC) which the more flexible STR can use, and which is not restricted to minimum phase systems.

The development of adaptive controllers for multi-input, multi-output (MIMO) systems has been very minimal. For the MRAC approach, the results to date are extremely restrictive in their application. Landau (Ref. 12) has proposed a continuous time solution that requires "perfect model following" conditions for stability. (He has also proposed a discrete-time solution of the MIMO problem in Ref. 13). Mabius and Kaufman (Refs. 4, 5 and 6) have relaxed these conditions and achieved stability with a bounded-state-error tracking result. However, the application is restricted to positive real systems, which is more limiting than the minimum phase condition. Monopoli attempted to extend his SISO approach (Ref. 14) to MIMO systems (Ref. 15); however, the formulation is rather cumbersome and is not sufficiently general for the power plant application. The results to be discussed in this report are a continuation of the Mabius-Kaufman and Monopoli work.

Applications of STR and MRAC that appear in the literature are generally based on Aström's STR or Landau's discrete time MRAC. A number of applications of STR's and MRAC's to power systems, aircraft systems and process control appear in Ref. 16. Reference 17 presents an STR application to chemical process control, and Ref. 18 a MRAC application to a pointing system control. Reference 19 discusses the use of minicomputers in a STR application. Reference 20 discusses a MRAC algorithm with output errors that can be made arbitrarily small during transient periods of adaptation. TASC has previously applied adaptive control to the missile guidance problem (Ref. 21).

2.3 PROBLEM FORMULATION

As discussed in Section 2.1, this report presents theoretical developments in Model Reference Control (MRC) and Model Reference Adaptive Control (MRAC) as applied to multi-input, multi-output (MIMO) systems. MRAC is an adaptive version of MRC that is implemented when the system parameters are unknown. This section presents a formulation of the MRC/MRAC problem for continuous and discrete time-domain representations of linear systems, beginning by formulating the MRC problem.

Model Reference Control (MRC) is based upon matching the response of a system having known parameters to that of a reference model which has desirable design specifications incorporated within it. For example, the outputs to a step input might be characterized by specified rise times, overshoots, and/or damping ratios. The controller and reference model work together to incorporate these characteristics into the plant outputs. The reference inputs are fed into the reference model, the outputs of which respond in accordance with the design specifications that have been built into it. If the control system is designed properly, the inputs to the plant drive the outputs of the plant to equal the outputs of the reference model.

The continuous-time plant (system) is described by a set of linear differential equations with m inputs $\underline{u}_p(t)$,

$$\dot{\underline{x}}_p(t) = A_p \underline{x}_p(t) + B_p \underline{u}_p(t) \qquad (2.3\text{-}1a)$$

$$\underline{y}_p(t) = C_p \underline{x}_p(t) \qquad (2.3\text{-}1b)$$

$$\underline{y}_s(t) = H_p \underline{x}_p(t) \qquad (2.3\text{-}1c)$$

where

$\underline{x}_p(t)$ is a $n \times 1$ state vector

$\underline{u}_p(t)$ is a $m \times 1$ input vector

$\underline{y}_p(t)$ is a $\ell \times 1$ output vector

$\underline{y}_s(t)$ is a $\ell_s \times 1$ measurement vector

The outputs $\underline{y}_p(t)$ are those quantities (linear combinations of the states) that are manipulated by the controls to be equal to the reference model outputs. The variable $\underline{y}_s(t)$ represents those linear combinations of states that are measured. The matrices A_p, B_p, C_p and H_p are constant, of appropriate dimensions, and contain the plant parameters. These parameters are assumed to be known in the MRC problem and unknown, but bounded, in the MRAC problem.

It is assumed that the number of outputs, ℓ, is less than or equal to the number of inputs, m. Generally, only ℓ inputs are required to regulate ℓ outputs. If $m>\ell$, Eq. 2.3-1a is expanded to

$$\dot{\underline{x}}_p(t) = A_p \underline{x}_p(t) + B_{p1} \underline{u}_{p1}(t) + B_{p2} \underline{u}_{p2}(t) \qquad (2.3\text{-}2)$$

where

$\underline{u}_{p1}(t)$ is a $\ell \times 1$ input vector

$\underline{u}_{p2}(t)$ is a $(m-\ell) \times 1$ input vector

and the matrices B_{p1} and B_{p2} are subsets of B_p.

The first set of controls $\underline{u}_{p1}(t)$ is used in the MRC and MRAC algorithms and compensates for plant/model errors generated by $\underline{u}_{p2}(t)$. The second set of controls $\underline{u}_{p2}(t)$ can be arbitrary but they are used in the enhanced MRC algorithm to balance the efforts of $\underline{u}_{p1}(t)$.

The discrete-time plant is described by a set of linear difference equations representing the inputs, outputs, measurements and states at discrete (equally spaced) points in time. The numbers of inputs, outputs, measurements and states are the same as in the continuous-time formulation (Eq. 3.3-1) and k is a time-index. Thus,

$$\underline{x}_p(k+1) = F_p \underline{x}_p(k) + G_p \underline{u}_p(k) \qquad (2.3\text{-}3a)$$

$$\underline{y}_p(k) = C_p \underline{x}_p(k) \qquad (2.3\text{-}3b)$$

$$\underline{y}_s(k) = H_p \underline{x}_p(k) \qquad (2.3\text{-}3c)$$

where the matrices F_p and G_p (like A_p and B_p) are constant matrices of appropriate dimensions containing the plant parameters. As in the continuous time case if $m>\ell$ then Eq. 2.3-3a is expanded to

$$\underline{x}_p(k+1) = F_p \underline{x}_p(k) + G_{p1} \underline{u}_{p1}(k) + G_{p2} \underline{u}_{p2}(k) \qquad (2.3\text{-}4)$$

where G_{p1} and G_{p2} are subsets of G_p.

If the plant is described in continuous-time format (Eq. 3.3-1), the reference model is described by a set of n_m linear differential equations with m_m inputs and ℓ outputs (i.e. the plant and reference model have the same number of outputs),

$$\dot{\underline{x}}_m(t) = A_m \underline{x}_m(t) + B_m \underline{u}_m(t) \qquad (2.3\text{-}5a)$$

$$\underline{y}_m(t) = C_m \underline{x}_m(t) \qquad (2.3\text{-}5b)$$

where

$\underline{x}_m(t)$ is a $n_m \times 1$ state vector

$\underline{y}_m(t)$ is a $\ell \times 1$ output vector

$\underline{u}_m(t)$ is a $m_m \times 1$ input vector

The constant matrices A_m, B_m and C_m are of appropriate dimensions. Note that $\underline{u}_m(t)$ is the reference model command and $\underline{y}_m(t)$ is the desired plant response (achieved by appropriately picking the reference model parameters). Since the reference model is synthesized by the controller all its states and inputs are known quantities.

If the plant is described in discrete-time format (Eqs. 2.3-2), the reference model is also. The number of inputs, outputs and states is the same as in the continuous formulation. Thus,

$$\underline{x}_m(k+1) = F_m \underline{x}_m(k) + G_m \underline{u}_m(k) \qquad (2.3\text{-}6a)$$

$$\underline{y}_m(k) = C_m \underline{x}_m(k) \qquad (2.3\text{-}6b)$$

where F_m, G_m and C_m are matrices of appropriate dimensions containing constant parameters.

In terms of the plant and model, the solution to the MRC or MRAC problem is a plant control, $\underline{u}_p(t)$ or $\underline{u}_p(k)$, that causes the plant output, $\underline{y}_p(t)$ or $\underline{y}_p(k)$, to approach the reference model output, $\underline{y}_m(t)$ or $\underline{y}_m(k)$, asymptotically. The difference between the MRC and MRAC problem is that in the former the plant parameters (A_p, B_p, C_p, F_p, G_p, H_p) are known while in the latter they are unknown.

3.0 MODEL REFERENCE CONTROL

This chapter presents the Model Reference Control (MRC) algorithm solutions to the control problem posed in Chapter 2. The MRC algorithm is the nonadaptive (requiring knowledge of the plant parameters) counterpart to the MRAC algorithm. The MRC algorithm development is a significant achievement in this research because: (1) it is a unique model following control algorithm and (2) represents the steady state behavior (or ideal goal) of the MRAC. That is, the MRAC algorithm adjusts the control gains toward the MRC algorithm gains. Once the gains reach their MRC values, no more adaptation will occur. Thus, the MRC algorithm is an important component in the MRAC algorithm analysis.

Model Reference Control (MRC) is based upon matching the response of a system having known parameters to that of a reference model which has desirable design specifications incorporated within it. For example, the outputs to a step input might be characterized by specified rise times, overshoots, and/or damping ratios. The controller and reference model work together to incorporate these characteristics into the plant outputs. The reference inputs are fed into the reference model, the outputs of which respond in accordance with the design specifications that have been built into it. The control system is designed such that the inputs to the plant drive the outputs of the plant to equal the outputs of the reference model.

3.1 CONTINUOUS-TIME ALGORITHM

The continuous-time MRC algorithm is based on continuous-time Command Generator Tracker (CGT) methodology and a continuous-time observer. Before presenting the algorithms in section 3.1.3, these two technologies are reviewed.

3.1.1 Command Generator Tracker Methodology

The controls developed from CGT technology (Ref. 7) are based on the so-called idealized or *-trajectories. The ideal plant state trajectory, $\underline{x}_p^*(t)$, represents that trajectory which the plant state follows when the plant output, $\underline{y}_p(t)$, equals the reference model output, $\underline{y}_m(t)$, for all time. The idealized plant control trajectory, $\underline{u}_{p1}^*(t)$, represents the control that will cause the plant state to follow the ideal plant state trajectory for any arbitrary, $\underline{u}_{p2}(t)$. That is, for all time

$$C_p \underline{x}_p^*(t) = \underline{y}_m(t) \tag{3.1-1a}$$

and

$$\dot{\underline{x}}_p^*(t) = A_p \underline{x}_p^*(t) + B_{p1} \underline{u}_{p1}^*(t) + B_{p2} \underline{u}_{p2}(t) \tag{3.1-1b}$$

In Appendix C, expressions for the *-trajectories as linear functions of $\underline{x}_m(t)$, $\underline{u}_m(t)$, $\underline{u}_{p2}(t)$ and $\underline{\theta}(t)$ (a filtered version of $\underline{u}_m(t)$) are derived. The expressions for $\underline{x}_p^*(t)$, $\underline{u}_p^*(t)$ and $\underline{\theta}(t)$ are given by

$$\underline{x}_p^*(t) = S_{11} \underline{x}_m(t) + S_{12} \underline{u}_m(t) + S_{13} \underline{u}_{p2}(t) + \Omega_{11} \dot{\underline{\theta}}(t) \tag{3.1-2a}$$

$$\underline{x}_p^*(0) = S_{11} \underline{x}_m(0) + \underline{\theta}(0) \tag{3.1-2b}$$

$$\underline{u}_{p1}^*(t) = S_{21} \underline{x}_m(t) + S_{22} \underline{u}_m(t) + S_{23} \underline{u}_{p2}(t) + \Omega_{21} \dot{\underline{\theta}}(t) \tag{3.1-2c}$$

$$\underline{\theta}(t) - \Omega_{11} \dot{\underline{\theta}}(t) = S_{12} \underline{u}_m(t) + S_{13} \underline{u}_{p2}(t) \tag{3.1-2d}$$

The filter initial condition, $\underline{\theta}(0)$, is arbitrary as long as there exists a $\dot{\underline{\theta}}(0)$ which satisfies Eq. 3.1-2d for t=0. Realization of Eq. 3.1-2d involves a complex reformulation, but subsequent developments eliminate this filter from the MRC algorithm.

The coefficients in Eq. 3.1-2 are partitions of the S and Ω matrices, which satisfy

$$\begin{bmatrix} A_p & B_{p1} \\ C_p & 0 \end{bmatrix} \begin{bmatrix} S_{11} & S_{12} & S_{13} \\ S_{21} & S_{22} & S_{23} \end{bmatrix} = \begin{bmatrix} S_{11}A_m & S_{11}B_m & -B_{p2} \\ C_m & 0 & 0 \end{bmatrix} \tag{3.1-3a}$$

$$\begin{bmatrix} A_p & B_{p1} \\ C_p & 0 \end{bmatrix} \begin{bmatrix} \Omega_{11} & \Omega_{12} \\ \Omega_{21} & \Omega_{22} \end{bmatrix} = \begin{bmatrix} I_n & 0 \\ 0 & I_\ell \end{bmatrix} \tag{3.1-3b}$$

Equation 3.1-3a has a solution if none of the plant transmission zeros are equal either to zero or to any of the reference model poles (Ref. 22). Equation 3.1-3b has a solution if none of the plant transmission zeros are equal to zero (Ref. 23).

The MRC algorithm is defined in terms of these *-trajectories and an estimate of the plant state, $\underline{x}_p(t)$. If H_p is of full rank (with ℓ_s=n) then the estimate, $\hat{\underline{x}}_p(t)$ is given by

$$\hat{\underline{x}}_p(t) = H_p^{-1} \underline{y}_s(t) \tag{3.1-4}$$

If H_p is less than full rank (let the rank be p=n-ℓ_s) then the estimate is the output of a minimal order observer given by*

$$\dot{\underline{z}}(t) = A_o \underline{z}(t) + B_o \underline{y}_s(t) + C_o \underline{u}_p(t) \tag{3.1-5}$$

$$\hat{\underline{x}}_p(t) = W_1 \underline{z}(t) + W_2 \underline{y}_s(t) \tag{3.1-6}$$

where

A_o is a p×p matrix with left half plane eigenvalues

B_o is a p×ℓ_s matrix

C_o is a p×m matrix

W_1 is a n×p matrix

W_2 is a n×ℓ_s matrix

*Subsequent discussion of the observer will refer to Eqs. 3.1-5 and 3.1-6 rather than Eq. 3.1-4. If H_p is nonsingular, the results are equally relevant with $W_2 = H_p^{-1}$ and all terms associated with $\underline{z}(t)$ being eliminated.

These matrices satisfy the following equalities*

$$[A_o \quad B_o] = [I_p \quad p0_{\ell_s}] \, W^{-1} \, A_p \, W \tag{3.1-7}$$

$$C_o = [I_p \quad p0_{\ell_s}] \, W^{-1} \, B_p \tag{3.1-8}$$

$$[\ell_s 0_p \quad I_p] = H_p \, W \tag{3.1-9}$$

$$W = [W_1 \quad W_2] \tag{3.1-10}$$

A few notes on observers.

- It can be shown there exists a matrix E such that

$$W^{-1} = \begin{bmatrix} E \\ H_p \end{bmatrix} \tag{3.1-11}$$

- If

$$\underline{e}_z(t) = \underline{z}(t) - E\underline{x}_p(t) \tag{3.1-12}$$

then

$$\dot{\underline{e}}_z(t) = A_o \underline{e}_z(t) \tag{3.1-13a}$$

and

$$\hat{\underline{x}}_p(t) - \underline{x}_p(t) = W_1 \underline{e}_z(t) \tag{3.1-13b}$$

3.1.2 MRC Algorithm Formulation

The MRC algorithm, $\bar{\underline{u}}_{p1}(t)$, is defined in terms of the CGT gains and the observer output. Thus,

$$\bar{\underline{u}}_{p1}(t) = -\bar{K}\hat{\underline{x}}_p(t) + \bar{K}_x \underline{x}_m(t) + \bar{K}_u \underline{u}_m(t) + \bar{K}_{u2} \underline{u}_{p2}(t) \tag{3.1-14}$$

$$\dot{\underline{z}}(t) = A_o \underline{z}(t) + B_o \underline{y}_s(t) + C_o \underline{u}_p(t) \tag{3.1-15a}$$

$$\hat{\underline{x}}_p(t) = W_1 \underline{y}_s(t) + W_2 \underline{z}(t) \tag{3.1-15b}$$

where

$$\bar{K}_x = S_{21} + \bar{K} S_{11} \tag{3.1-16a}$$

$$\bar{K}_u = S_{22} + \bar{K} S_{12} \tag{3.1-16b}$$

$$\bar{K}_{u2} = S_{23} + \bar{K} S_{13} \tag{3.1-16c}$$

and $\bar{K}$ satisfies

$$(\bar{K}\Omega_{11} + \Omega_{21}) \, \dot{\underline{\theta}}(t) = \underline{0} \tag{3.1-17a}$$

and

$$A_p - B_{p1}\bar{K} \text{ has stable eigenvalues.} \tag{3.1-17b}$$

This algorithm is shown graphically in Fig. 3.1-1.

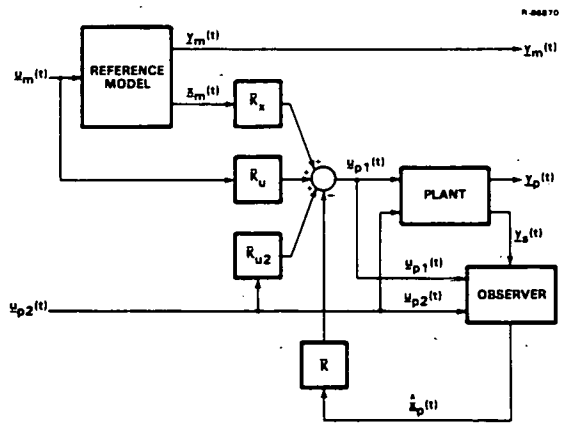

Figure 3.1-1 Model Reference Control Algorithm

Appendix D presents a methodology for constructing a matrix $\bar{K}$ satisfying Eqs. 3.1-17. This method depends on:

- Structural constraints on the reference model (analogous to the relative order constraints in Refs. 3 and 14)
- Structural constraints on $\underline{u}_{p2}(t)$ which limit its relative order to be greater than $\underline{u}_{p1}(t)$. This can be satisfied by the appropriate partitioning of controls into $\underline{u}_{p1}(t)$ and $\underline{u}_{p2}(t)$
- Frequency domain constraints on the transmission zeroes between $\underline{u}_{p1}(t)$ and $\underline{u}_{p2}(t)$ in that they must lie in the left half plane. This can be a significant restriction on the use of the algorithm but can be corrected by the appropriate choice of $\underline{u}_{p2}(t)$* (see Section 3.3).

Also presented in Appendix D is a mechanism for constructing $\bar{K}_x$, $\bar{K}_u$, $\bar{K}_{u2}$ without using the S_{ij} matices as in Eq. 3.1-16.

3.1.3 Stability Analysis

In this section, the stability and asymptotic performance of the MRC algorithm are demonstrated. In particular, if the control, $\underline{u}_{p1}(t)$, is set equal to the MRC algorithm, $\bar{\underline{u}}_{p1}(t)$ (Eq. 3.1-14), then the plant output, $\underline{y}_p(t)$, will asymptotically approach the reference model output, $\underline{y}_m(t)$. The error dynamics derived in this analysis are an important component in the subsequent MRAC stability analysis (Section 4.3).

The first step in analyzing the MRC algorithm performance is to note from Eqs. 3.1-2, 3.1-14, 3.1-16 and 3.1-17 that

---

*I_p is a $p \times p$ identity matrix

$p0_{\ell_s}$ is a $p \times \ell$ null matrix.

*If the number of controls m equals the number of outputs ℓ then $\underline{u}_{p2}(t)$ does not exist and if the transmission zeroes are unstable the algorithm cannot be applied.

$$\bar{u}_{p1}(t) = u^*_{p1}(t) + \bar{K}[x^*_p(t) - \hat{x}_p(t)] \qquad (3.1\text{-}18)$$

Now, the errors, $e(t)$ and $e_z(t)$ (Eq. 3.1-12), are defined

$$e(t) \equiv x^*_p(t) - x_p(t) \qquad (3.1\text{-}19)$$

$$e_z(t) \equiv z(t) - E\,x_p(t) \qquad (3.1\text{-}20)$$

Replacing the x_p terms in Eq. 3.1-18 with the errors in Eqs. 3.1-19 and 3.1-20 (using Eq. 3.1-13b) yields

$$\bar{u}_{p1}(t) = u^*_{p1}(t) + \bar{K}[e(t) - W_1 e_z(t)] \qquad (3.1\text{-}21)$$

Differentiating Eqs. 3.1-19 and substituting Eqs. 2.3-2 and 3.1-1b results in

$$\dot{e}(t) = A_p e(t) + B_{p1}[u^*_{p1}(t) - u_{p1}(t)] \qquad (3.1\text{-}22)$$

Finally, solving Eq. 3.1-21 for $u^*_{p1}(t)$ and substituting into Eqs. 3.1-22 yields

$$\dot{e}(t) = (A_p - B_{p1}\bar{K})\,e(t) + B_{p1}[\bar{u}_{p1}(t) - u_{p1}(t)] + B_{p1}\bar{K}\,W_1 e_z(t) \qquad (3.1\text{-}23a)$$

Reiterating Eq. 3.1-13a for completeness

$$\dot{e}_z(t) = A_o e_z(t) \qquad (3.1\text{-}23b)$$

and stating initial conditions

$$e(0) = x^*_p(0) - x_p(0) \qquad (3.1\text{-}24a)$$

$$e_z(0) = z(0) - E\,x_p(0) \qquad (3.1\text{-}24b)$$

Equations 3.1-23 and 3.1-24 define the dynamics for the error vectors, $e(t)$ and $e_z(t)$. Of particular importance to the stability analysis is the behavior of the error when $u_{p1}(t) = \bar{u}_{p1}(t)$ (i.e., the MRC algorithm). Given that both $A_p - B_{p1}\bar{K}$ and A_o have stable eigenvalues, then, as $t \to \infty$, $e(t) \to 0$. Multiplying Eq. 3.1-19 by C_p and substituting Eqs. 3.1-1a and 2.3-1b yields the output error, $e_y(t)$.

$$C_p e(t) = y_m(t) - y_p(t) \equiv e_y(t) \qquad (3.1\text{-}25)$$

Hence as $t \to \infty$, $y_p(t) \to y_m(t)$ which is the desired result. In summary, if the transfer function from $u_p(t)$ to $y_p(t)$ has no right half plane finite transmission zeroes, $\bar{K}$ is chosen as described in Appendix D and the observer is designed to be stable, then the continuous-time algorithm causes the plant output to asymptotically track the reference model output.

3.2 DISCRETE-TIME ALGORITHM

The discrete-time MRC algorithm for the system described in Eqs. 2.3-3, is based on the discrete-time Command Generator Tracker (CGT) methodology (Ref. 8) and discrete-time observer. Before presenting the algorithm in section 3.2.3, these two technologies are reviewed.

3.2.1 Command Generator Tracker Methodology

As with the continuous-time formulation, the controls developed from discrete-time CGT technology are based on the idealized or *-trajectories. The ideal plant state trajectory, $x^*_p(k)$, represents that trajectory which the plant state follows when the plant output, $y_p(k)$, equals the reference model output, $y_m(k)$, for all time. The idealized plant control trajectory, $u^*_{p1}(k)$, represents the control that will cause the plant state to follow the ideal plant state trajectory for arbitrary $u_{p2}(k)$. That is, for all time

$$C_p\,x^*_p(k) = y_m(k) \qquad (3.2\text{-}1a)$$

and

$$x^*_p(k+1) = F_p\,x^*_p(k) + G_{p1}\,u^*_{p1}(k) + G_{p2}\,u_{p2}(k) \qquad (3.2\text{-}1b)$$

In Appendix C, expressions for the *-trajectories as linear functions of $x_m(k)$, $u_m(k)$ and $\theta(k)$ (a filtered version of $u_m(k)$) are derived. The expressions for $x^*_p(k)$, $u^*_{p1}(k)$ and $\theta(k)$ are given by

$$x^*_p(k) = R_{11}\,x_m(k) + R_{12}\,u_m(k) + R_{13}\,u_{p2}(k) + \Lambda_{11}\,[\theta(k+1) - \theta(k)] \qquad (3.2\text{-}2a)$$

$$x^*_p(0) = R_{11}\,x_m(0) + \theta(0) \qquad (3.2\text{-}2b)$$

$$u^*_{p1}(k) = R_{21}\,x_m(k) + R_{22}\,u_m(k) + R_{23}\,u_{p2}(k) + \Lambda_{21}\,[\theta(k+1) \quad \theta(k)] \qquad (3.2\text{-}2c)$$

$$\theta(k) - \Lambda_{11}\,[\theta(k+1) - \theta(k)] = R_{12}\,u_m(k) + R_{13}\,u_{p2}(k) \qquad (3.2\text{-}2d)$$

As with continuous time formulation, the filter initial condition, $\theta(0)$, is arbitrary as long as there exists a $\theta(1)$ which satisfies Eq. 3.2-2c for k=0. Realization of Eq. 3.2-2d involves a complex formulation, but subsequent developments eliminate this filter from the MRC algorithm.

The coefficients in Eq. 3.2-2 are partitions of the R and Λ matrices, which satisfy

$$\begin{bmatrix} F_p - I_n & G_{p1} \\ C_p & 0 \end{bmatrix} \begin{bmatrix} R_{11} & R_{12} & R_{13} \\ R_{21} & R_{22} & R_{23} \end{bmatrix} = \begin{bmatrix} R_{11}(F_m - I_{n_m}) & R_{11}G_m & -G_{p2} \\ C_m & 0 & 0 \end{bmatrix} \qquad (3.2\text{-}3a)$$

$$\begin{bmatrix} F_p - I_n & G_p \\ C_p & 0 \end{bmatrix} \begin{bmatrix} \Lambda_{11} & \Lambda_{12} \\ \Lambda_{21} & \Lambda_{22} \end{bmatrix} = \begin{bmatrix} I_n & 0 \\ 0 & I_\ell \end{bmatrix} \qquad (3.2\text{-}3b)$$

Equation 3.2-3a has a solution if none of the plant transmission zeros are equal either to unity or to any of the reference model poles. Equation 3.2-3b has a solution if none of the plant transmission zeros are equal to unity (Ref. 23).

3.2.2 Observer Formulation

As in the continuous-time case, the MRC algorithm is defined in terms of these *-trajectories and an estimate of the plant state, $\underline{x}_p(k)$. If H_p is of full rank (with ℓ_s=n) then the estimate is given by

$$\hat{\underline{x}}_p(k) = H_p^{-1}\, \underline{y}_s(k) \qquad (3.2\text{-}4)$$

If H_p is less than full rank (let p=n-ℓ be the rank deficiency) then the state estimate is the output of a minimal order observer given by*

$$\underline{z}(k+1) = F_o\, \underline{z}(k) + G_o\, \underline{y}_s(k) + H_o\, \underline{u}_p(k) \qquad (3.2\text{-}5)$$

$$\hat{\underline{x}}_p(k) = W_1\, \underline{z}(k) + W_2\, \underline{y}_s(k) \qquad (3.2\text{-}6)$$

where

F_o is a p×p matrix with left half plane eigenvalues

G_o is a p×ℓ matrix

H_o is a p×m matrix

W_1 is a n×p matrix

W_2 is a n×ℓ matrix

These matrices satisfy the following equalities*

$$[F_o \;\; G_o] = [I_p \;\; p0_{\ell_s}]\, W^{-1} F_p\, W \qquad (3.2\text{-}7)$$

$$H_o = [I_p \;\; p0_{\ell_s}]\, W^{-1} B_p \qquad (3.2\text{-}8)$$

$$[\ell_s 0_p \;\; I_p] = H_p\, W \qquad (3.2\text{-}9)$$

$$W = [W_1 \;\; W_2] \qquad (3.2\text{-}10)$$

A few notes on observers

- There exists a matrix E such that

$$W^{-1} = \begin{bmatrix} E \\ H_p \end{bmatrix} \qquad (3.2\text{-}11)$$

- If

$$\underline{e}_z(k) = \underline{z}(k) - E\, \underline{x}_p(k) \qquad (3.2\text{-}12)$$

then

$$\underline{e}_z(k+1) = F_o\, \underline{e}_z(k) \qquad (3.2\text{-}13a)$$

and

$$\hat{\underline{x}}_p(k) - \underline{x}_p(k) = W_1\, \underline{e}_z(k) \qquad (3.2\text{-}13b)$$

*See footnote on page 7.

3.2.3 MRC Algorithm Formulation

The MRC algorithm, $\bar{\underline{u}}_{p1}(k)$, is defined in terms of CGT gains and observer outputs. That is

$$\bar{\underline{u}}_{p1}(k) = \bar{K}\, \hat{\underline{x}}_p(k) + \bar{K}_y\, \underline{u}_m(k) + \bar{K}_x\, \underline{x}_m(k) + \bar{K}_{u2}\, \underline{u}_{p2}(k) \qquad (3.2\text{-}14)$$

$$\underline{z}(k+1) = F_o\, \underline{z}(k) + G_o\, \underline{y}_s(k) + H_o\, \underline{u}_p(k) \qquad (3.2\text{-}15a)$$

$$\hat{\underline{x}}_p(k) = W_1 \underline{y}_s(k) + W_2 \underline{z}(k) \qquad (3.2\text{-}15b)$$

where

$$\bar{K}_x = R_{21} + \bar{K}\, R_{11} \qquad (3.2\text{-}16a)$$

$$\bar{K}_u = R_{22} + \bar{K}\, R_{12} \qquad (3.2\text{-}16b)$$

$$\bar{K}_{u2} = R_{23} + \bar{K}\, R_{13} \qquad (3.2\text{-}16c)$$

and $\bar{K}$ satisfies

$$(\bar{K}\Lambda_{11} + \Lambda_{21})\, [\underline{\theta}(k+1) - \underline{\theta}(k)] = \underline{0} \qquad (3.2\text{-}17a)$$

and

$$F_p - G_{p1}\, \bar{K} \text{ has stable eigenvalues} \qquad (3.2\text{-}17b)$$

A matrix $\bar{K}$ satisfying Eqs. 3.1-17 can be constructed in a method similar to that described in Appendix D. This method would depend on:

- Structural constraints on the reference model (analogous to the relative order constraints in Refs. 3 and 14)
- Structural constraints on $\underline{u}_{p2}(k)$ which limit its relative order to be greater than $\underline{u}_{p1}(k)$. This can be satisfied by the appropriate choice of controls in $\underline{u}_{p1}(k)$ and $\underline{u}_{p2}(k)$
- Frequency domain constraints on the transmission zeroes between $\underline{u}_{p1}(k)$ and $\underline{u}_{p2}(k)$ in that they must lie in the unit circle. This can be a significant restriction on the use of the algorithm but can be corrected by the appropriate choice of $\underline{u}_{p2}(k)$*.

3.2.4 Stability Analysis

In this section, the stability and asymptotic performance of the MRC algorithms are demonstrated. As with the continuous-time algorithm, if the control, $\underline{u}_{p1}(k)$, is set equal to the MRC algorithm, $\bar{\underline{u}}_{p1}(k)$ (Eq. 3.2-14), then the plant output, $\underline{y}_p(k)$ will asymptotically approach the reference model output, $\underline{y}_m(k)$.

*If the number of controls m equals the number of outputs ℓ then $\underline{u}_{p2}(k)$ does not exist and if the transmission zeroes are unstable the algorithm cannot be applied.

The first step in analyzing the MRC algorithm performance is to note from Eqs. 3.2-2, 3.2-14, 3.2-16 and 3.2-17 that

$$\bar{u}_{p1}(k) = u^*_{p1}(k) + \bar{K}[x^*_p(k) - \hat{x}_p(k)] \qquad (3.2\text{-}18)$$

Define $e(k)$ and $e_z(k)$ (see Eq. 3.2-12)

$$e(k) = x^*_p(k) - x_p(k) \quad (3.2\text{-}19)$$

$$e_z(k) = z(k) - E\, x_p(k) \qquad (3.2\text{-}20)$$

Replacing the x_p terms in Eq. 3.2-18 with the error in Eqs. 3.2-19 and 3.2-20 (using Eq. 3.2-13b) yields

$$\bar{u}_{p1}(k) = u^*_{p1}(k) + \bar{K}[e(k) - W_1\, e_z(k)] \qquad (3.2\text{-}21)$$

Using Eqs. 2.3-4 and 3.2-1b with Eq. 3.2-19 results in

$$e(k+1) = F_p\, e(k) + G_{p1}[u^*_{p1}(k) - u_{p1}(k)] \qquad (3.2\text{-}22)$$

Finally, solving Eq. 3.2-21 for $u^*_{p1}(k)$ and substituting into Eq. 3.1-22 yields

$$e(k+1) = (F_p - G_{p1}\bar{K})\, e(k) + G_{p1}[\bar{u}_{p1}(k) - u_{p1}(k)] + G_{p1}\, W_1\, e_z(k) \qquad (3.2\text{-}23a)$$

Reiterating Eq. 3.2-13a for completeness

$$e_z(k+1) = F_o\, e_z(k) \qquad (3.2\text{-}23b)$$

and stating initial conditions

$$e(0) = x^*_p(0) - x_p(0) \qquad (3.2\text{-}24a)$$

$$e_z(0) = z(0) - E\, x_p(0) \qquad (3.2\text{-}24b)$$

Equations 3.2-23 and 3.2-24 define the dynamics for the error vectors, $e(k)$ and $e_z(k)$. Of particular importance is the behavior of the error when $u_{p1}(k) = \bar{u}_{p1}(k)$ (i.e., the MRC algorithm). Given that $F_p - G_{p1}\bar{K}$ and F_o have stable eigenvalues then as $t \to \infty$, $e(k) \to 0$. Multiplying Eq. 3.2-19 by C_p and substituting Eqs. 3.2-1a and 2.3-3b yields the output error, $e_y(k)$.

$$C_p\, e(k) = y_m(k) - y_p(k) \equiv e_y(k) \qquad (3.2\text{-}25)$$

Hence as $t \to \infty$, $y_p(k) \to y_m(k)$ which is the desired result.

In summary, if all finite transmission zeroes of the transfer function from $u_{p1}(k)$ to $y_p(k)$ are inside the unit circle, $\bar{K}$ is chosen in a procedure analogous to that described in Appendix D and the observer is designed to be stable, then the discrete-time MRC algorithm causes the plant output to asymptotically track the reference model output.

3.3 ENHANCED MRC ALGORITHM

The previous two sections presented continuous- and discrete-time MRC algorithms that cause the plant outputs to track the reference model outputs provided that

- the reference model and u_{p2} satisfy (mild) structural constraints analogous to relative order constraints
- the transmission zeroes of the transfer function from u_{p1} to y_p are stable.

This section presents the continuous-time enhanced MRC algorithm which deals the latter of these constraints.

The reason the plant transmission zeroes must be stable is because for each transmission zero, one eigenvalue of $A_p - B_{p1}\bar{K}$ ($F_p - G_{p1}\bar{K}$) equals that transmission zero. Hence, if one transmission zero is unstable so is $A_p - B_{p1}\bar{K}$ and the criteria for MRC stability is not satisfied. A less serious problem occurs if the transmission zero is marginally stable. In this case, the MRC algorithm causes the system to be marginally stable which leads asymptotically to y_p perfectly tracking the y_m after initial oscillations. However, the controls, u_{p1}, exhibit large oscillations at the transmission zero frequencies. This problem is demonstrated in Chapter 6.

The enhancement of the MRC algorithm presented in this section alleviates this problem for systems with more inputs than outputs ($m > \ell$ see Eq. 2.3-1). Only the continuous-time enhancement is presented, however, the discrete-time equivalent can be developed in an analogous fashion.

The derivation of this enhanced algorithm is based on the closed loop plant dynamics with the MRC algorithm. In particular assume $u_{p1}(t) = \bar{u}_{p1}(t)$. From Eq. 3.1-14

$$u_{p1}(t) = -\bar{K}\, \hat{x}_p(t) + \bar{K}_x\, x_m(t) + \bar{K}_u\, u_m(t) + \bar{K}_{u2}\, u_{p2}(t) \qquad (3.3\text{-}1)$$

Substituting Eq. 3.3-1 into the plant dynamics, Eq. 2.3-2

$$\dot{x}_p(t) = A_p\, x_p(t) + B_{p1}[-\bar{K}\, \hat{x}_p(t) + \bar{K}_x\, x_m(t) + \bar{K}_u\, u_m(t) + \bar{K}_{u2}\, u_{p2}(t)] + B_{p2}\, u_{p2}(t) \qquad (3.3\text{-}2)$$

If the observer is assumed to be in steady state (i.e., $e_z(t)=0$) then Eqs. 3.3-1 and 3.3-2 become

$$u_{p1}(t) = -\bar{K}\, x_p(t) + \bar{K}_x\, x_m(t) + \bar{K}_u\, u_m(t) + \bar{K}_{u2}\, u_{p2}(t) \qquad (3.3\text{-}3)$$

$$\dot{x}_p(t) = (A_p - B_{p1}\bar{K})\, x_p(t) + (B_{p1}\bar{K}_{u2} + B_{p2})\, u_{p2}(t) + B_{p1}[\bar{K}_x\, x_m(t) + \bar{K}_u\, u_m(t)] \qquad (3.3\text{-}4)$$

Consider these two equations as representing a dynamic system with $\underline{u}_{p2}(t)$ as an input, $\underline{x}_m(t)$ and $\underline{u}_m(t)$ as disturbances, and $\underline{u}_{p2}(t)$ as an output. If the transmission zeroes of the plant are unstable or marginally stable this system (open-loop) is unstable or marginally stable, respectively. Hence, the objective in designing the enhanced algorithm is to choose $\underline{u}_{p2}(t)$ to stabilize the above system and minimize the excursions of $\underline{u}_{p1}(t)$. (Recall that any choice of $\underline{u}_{p2}(t)$ preserves the MRC algorithm). Taking the standard optimal control approach, the following cost function is used.

$$J_e = \int_0^\infty [\underline{u}_{p1}^T(t)\, R_1\, \underline{u}_{p1}(t) + \underline{u}_{p2}^T(t)\, R_2\, \underline{u}_{p2}(t)]dt \qquad (3.3\text{-}5)$$

The resulting choice of $\underline{u}_{p2}(t)$ is of the form (note $\underline{x}_p(t)$ is replaced by its estimate)

$$\underline{u}_{p2}(t) = G\, \hat{\underline{x}}_p(t) + G_x\, \underline{x}_m(t) + G_u\, \underline{u}_m(t) \qquad (3.3\text{-}6)$$

The MRC algorithm acts as inner loop and the enhancement acts as outer loop (see Fig. 3.3-1). The cost function (Eq. 3.3-5) causes the action of the controls, $\underline{u}_{p1}(t)$ and $\underline{u}_{p2}(t)$, to balance each other (with appropriate weighting factors) without disturbing the action of the MRC algorithm in driving $\underline{y}_p(t)$ toward $\underline{y}_m(t)$. At the same time the closed loop system is stabilized. This enhanced algorithm is demonstrated in Chapter 6.

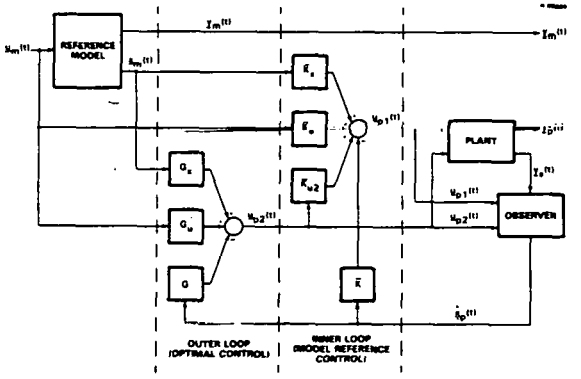

Figure 3.3-1 Enhanced Model Reference Control Algorithm

4.0 MODEL REFERENCE ADAPTIVE CONTROL

This chapter presents the multi-input multi-output (MIMO) Model Reference Adaptive Control (MRAC) algorithm and a stability analysis of the resulting closed loop system. The adaptive algorithm is an extension of the MRAC algorithm previously developed by Mabius and Kaufman (Ref. 3) using the MRC algorithm described in Chapter 3. The algorithm is also an extension to MIMO systems of previously developed single-input, single-output (SISO) MRAC algorithms (Ref. 15). In fact, the MRAC algorithm presented here degenerates into the SISO algorithm if the number of inputs and outputs is one. One limitation to the stability proof (described in Section 4.3) limits the use of this algorithm. However, future efforts should readily eliminate this restriction and make the algorithm generally applicable.

The MRC algorithm presented in Chapter 3 is implementable if the plant parameters are unknown, the MRAC algorithm described here is applicable because it adjusts the gains to account for unknown plant parameters. The gains adapt to the MRC gains described in Chapter 3 at which point the plant/model is driven to zero. Since the adaptation is driven by this error, the gains remain fixed and as with the MRC algorithm the plant output tracks the reference model output.

Section 4.1 presents a reformulation of the observer necessary to put the MRC algorithm into a context amenable to adaptation. The MRAC algorithm appears in Section 4.2 and stability analysis appears in Section 4.3.

4.1 OBSERVER MODIFICATION

The key to the adaptive algorithm discussed in the next section is that the control must be a linear combination of known quantities. Note that the observer term in the MRC algorithm (Eq. 3.1-14) is dependent on $\underline{z}(t)$, that is

$$\bar{K}\,\hat{\underline{x}}_p(t) = \bar{K}\,W_1\,\underline{z}(t) + \bar{K}\,W_2\,\underline{y}_s(t) \qquad (4.1\text{-}1)$$

But $\underline{z}(t)$ is computed using B_o and C_o (Eq. 3.1-5) both of which are dependent on unknown plant parameters; hence, $\underline{z}(t)$ is "unknown". In this section the observer state $\underline{z}(t)$ is redesigned to be a linear combination of known quantities.

Recall that $\underline{z}(t)$ is a p×1 vector ($p=n-\ell_s$) and is governed by (Eq. 3.1-5)

$$\dot{\underline{z}}(t) = A_o\,z(t) + B_o\,\underline{y}_c(t) + C_o\,\underline{u}_p(t) \qquad (4.1\text{-}2)$$

Let the elements of $\underline{y}_s(t)$ and $\underline{u}_p(t)$ be $y_{si}(t)$ ($i=1\ldots\ell_s$) and u_{pi} ($i=1\ldots m$), respectively, and let the columns of B_o and C_o be $\underline{b}_{oi}$ ($i=1\ldots\ell_s$) and $\underline{c}_{oi}$ ($i=1\ldots m$), respectively. Then, Eq. 4.1-2 becomes

$$\dot{\underline{z}}(t) = A_o\,\underline{z} + \sum_{i=1}^{\ell_s} \underline{b}_{oi}\,y_{si}(t) + \sum_{i=1}^{m} \underline{c}_{oi}\,u_{pi}(t)$$

Define $\bar{\underline{w}}_i(t)$ as a p×1 vector governed by

$$\begin{aligned}\dot{\bar{\underline{w}}}_i(t) &= A_o\,\bar{\underline{w}}_i(t) + \underline{b}_{oi}\,y_{si}(t) \quad i=1\ldots\ell_s \\ &= A_o\,\bar{\underline{w}}_i(t) + \underline{c}_{oj}\,u_{pj}(t) \quad i=\ell_s+1\ldots\ell_s+m,\ j=i-\ell_s\end{aligned} \qquad (4.1\text{-}3)$$

That is, there are ℓ_s+m p×1 vectors $\bar{\underline{w}}_i(t)$.

If $\bar{\underline{w}}_i(0)$ is chosen to satisfy

$$\sum_{i=1}^{\ell_s+m} \bar{\underline{w}}_i(0) = \underline{z}(0) \qquad (4.1\text{-}4)$$

then for all t

$$\underline{z}(t) = \sum_{i=1}^{\ell_s+m} \bar{\underline{w}}_i(t) \qquad (4.1\text{-}5)$$

Each set of dynamics in Eq. 4.1-3 can be transformed into (Ref. 24)

$$\begin{aligned}\dot{\underline{w}}_i(t) &= A\,w_i(t) + \underline{b}\,y_{ci}(t) \quad i=1\ldots\ell_s \\ &= A\,\underline{w}_i(t) + \underline{b}\,u_{pj}(t) \quad i=\ell_s+1\ldots\ell_s+m,\ j=i-\ell_s\end{aligned} \qquad (4.1\text{-}6)$$

where

$$\bar{\underline{w}}_i(t) = T_i\,\underline{w}_i(t) \qquad i=1\ldots\ell_s+m \qquad (4.1\text{-}7)$$

The matrix A has the same eigenvalues as A_o and the vector $\underline{b}$ is independent of index i. Thus

$$\underline{z}(t) = \sum_{i=1}^{\ell_s+m} T_i\,\underline{w}_i(t) \qquad (4.1\text{-}8)$$

and $\underline{w}_i(t)$ is a "known" quantity independent of the plant parameters.

Equations 4.1-6 and 4.1-8 can be consolidated into two vector equations given by

$$\dot{\underline{w}}(t) = A_w\,\underline{w}(t) + B_w\,\underline{y}_s(t) + C_w\,\underline{u}_p(t) \qquad (4.1\text{-}9a)$$

$$\underline{z}(t) = T_w\,\underline{w}(t) \qquad (4.1\text{-}9b)$$

where $\underline{w}(t)$ is q×1 [$q = (\ell_c+m)p$] vector given by

$$\underline{w}(t) = \begin{bmatrix} \underline{w}_1(t) \\ \underline{w}_2(t) \\ \vdots \\ \underline{w}_{\ell_s+m}(t) \end{bmatrix} \qquad (4.1\text{-}10)$$

and the matrices are defined as follows

$$A_w = \begin{bmatrix} A & 0 & \cdots & 0 \\ 0 & A & \cdots & 0 \\ \vdots & \vdots & & \vdots \\ 0 & 0 & \cdots & A \end{bmatrix} \quad \text{a } q\times q \text{ matrix} \qquad (4.1\text{-}11)$$

$$B_w = \begin{bmatrix} \underline{b} & 0 & \cdots & 0 \\ 0 & \underline{b} & \cdots & 0 \\ \vdots & \vdots & & \vdots \\ 0 & 0 & \cdots & \underline{b} \\ 0 & 0 & \cdots & 0 \\ \vdots & \vdots & & \vdots \\ 0 & 0 & & 0 \end{bmatrix} \quad \text{a } q\times \ell_s \text{ matrix} \qquad (4.1\text{-}12)$$

$$C_w = \begin{bmatrix} 0 & 0 & \cdots & 0 \\ \vdots & \vdots & & \vdots \\ 0 & 0 & \cdots & 0 \\ \underline{b} & 0 & \cdots & 0 \\ 0 & \underline{b} & \cdots & 0 \\ \vdots & \vdots & & \vdots \\ 0 & 0 & \cdots & \underline{b} \end{bmatrix} \quad \text{a } q\times m \text{ matrix} \qquad (4.1\text{-}13)$$

$$T_w = [T_1 \quad T_2 \cdots T_{\ell_s} \quad T_{\ell_s+1} \cdots T_{\ell_s+m}] \quad \text{a } p\times q \text{ matrix} \qquad (4.1\text{-}14)$$

In summary, the p^{th} order dynamics of $\underline{z}(t)$ (Eq. 4.1-2) have been transformed into the system defined by Eq. 4.1-9 with q^{th} order dynamics (Eq. 4.1-9b). The size of q can be reduced if the observed structure is somewhat decoupled. In particular, the individual systems described in Eq. 4.1-3 may be of order less than p, say p_i'. In this case

$$q = \sum_{i=1}^{\ell_s+m} p_i' < p(\ell_s+m) \qquad (4.1\text{-}15)$$

But the basic result is that observer term in the MRC algorithms (Eq. 3.1-14) is given by

$$\bar{K}\, \hat{\underline{x}}_p(t) = \bar{K}\, W_1\, T_w\, \underline{w}(t) + \bar{K}\, W_2\, \underline{y}_s(t) \qquad (4.1\text{-}16)$$

where both $\underline{w}(t)$ and $\underline{y}_s(t)$ are "known" quantities (independent of the plant parameters).

4.2 MRAC ALGORITHM FORMULATION

The Model Reference Adaptive Control (MRAC) algorithm presented here has the same structure as the MRC algorithm described in Chapter 3. Only the continuous-time algorithm is presented while the discrete-time counterpart is very similar in structure. The enhanced algorithm (feedback to $\underline{u}_{p2}(t)$) is not adaptive and thus is not included in the equations. The stability of the MRAC (see Section 4.3) depends on the MRC being stable.

As mentioned in Section 4.1, the MRAC algorithm is different than the MRC algorithm in that the observer described in Eq. 4.1-9 replaces the MRC observer. Substituting Eq. 4.1-15 into Eq. 3.1-14 yields the following

$$\underline{u}_{p1}(t) = \bar{K}_w\, \underline{w}(t) + \bar{K}_y\, \underline{y}_s(t) + \bar{K}_x\, \underline{x}_m(t) + \bar{K}_u\, \underline{u}_m(t) + \bar{K}_{u2}\, \underline{u}_{p2}(t) \qquad (4.2\text{-}1)$$

where $\underline{w}(t)$ is defined by Eq. 4.1-9a and

$$\bar{K}_w = \bar{K} W_1 T_w \qquad (4.2\text{-}2a)$$

$$\bar{K}_y = \bar{K} W_2 \qquad (4.2\text{-}2b)$$

The MRAC algorithm has the same structure as Eq. 4.2-1 and is given by

$$\underline{u}_{p1}(t) = K_w(t)\, \underline{w}(t) + K_y(t)\, \underline{y}_s(t) + K_x(t)\, \underline{x}_m(t) + K_u(t)\, \underline{u}_m(t) + K_{u2}(t)\, \underline{u}_{p2}(t) \qquad (4.2\text{-}3)$$

As in Mabius-Kaufman algorithm in Ref. 4, the quantities $\underline{r}(t)$ and $\underline{K}_r(t)$ are now defined to provide more compact notation for the adaptive controller, viz,

$$\underline{r}(t) = \begin{bmatrix} \underline{w}(t) \\ \underline{y}_s(t) \\ \underline{x}_m(t) \\ \underline{u}_m(t) \\ \underline{u}_{p2}(t) \end{bmatrix} \qquad (4.2\text{-}4)$$

$$K_r(t) = [K_w(t),\ K_y(t),\ K_x(t),\ K_u(t),\ K_{u2}(t)] \qquad (4.2\text{-}5)$$

$K_r(t)$ represents a concatenation of the adaptive gains. With these definitions

$$\underline{u}_{p1}(t) = K_r(t)\, \underline{r}(t) \qquad (4.2\text{-}6)$$

The mechanism by which $K_r(t)$ is adapted is defined by

$$K_r(t) = K_p(t) + K_I(t) \qquad (4.2\text{-}7a)$$

$$K_p(t) = Q_L\, \underline{\varepsilon}(t)\, \underline{r}_f^T(t)\, T_{KP} \qquad (4.2\text{-}7b)$$

$$K_I(t) = Q_L\, \underline{\varepsilon}(t)\, \underline{r}_f^T(t)\, T_{IP} \qquad (4.2\text{-}7c)$$

$$K_I(0) = K_{I0} \qquad (4.2\text{-}7d)$$

where the augmented error is given by

$$\underline{\varepsilon}(t) = \underline{e}_y(t) - \hat{\underline{e}}_y(t) \qquad (4.2\text{-}8)$$

the output error is given by

$$\underline{e}_y(t) = \underline{y}_m(t) - \underline{y}_p(t) \qquad (4.2\text{-}9)$$

the output error estimate is given by

$$\frac{d}{dt}\,\hat{\underline{e}}_y(t) = A_e\,\hat{\underline{e}}_y(t) + L_\Delta(t)\,\underline{\Delta}(t) \qquad (4.2\text{-}10)$$

and finally

$$L_\Delta(t) = L_P(t) + L_I(t) \qquad (4.2\text{-}11a)$$

$$L_P(t) = \underline{\varepsilon}(t)\,\underline{\Delta}^T(t)\,T_{LP} \qquad (4.2\text{-}11b)$$

$$\dot{L}_I(t) = \underline{\varepsilon}(t)\,\underline{\Delta}^T(t)\,T_{LI} \qquad (4.2\text{-}11c)$$

$$L_I(0) = L_{I0} \qquad (4.2\text{-}11d)$$

$$\underline{\Delta}(t) = K_r(t)\,\underline{r}_f(t) - \underline{u}_{pf}(t) \qquad (4.2\text{-}12)$$

The matrices T_{KP}, T_{KI}, T_{LP} and T_{LI} are positive definite, Q_L is any nonsingular $\ell \times \ell$ matrix that satisfies a constraint described in Section 4.3 and K_{I0} and L_{I0} are initial guesses at $\bar{K}_r$ and L. Note that $K_P(t)$ is a proportional gain and $K_I(t)$ is an integral gain, and the choice of T_{KP} and T_{KI} affects the transient behavior of the adaptive algorithm. The matrix A_e is a stable system matrix which satisfies constraints specified in Section 4.3.

The quantities $\underline{r}_f(t)$ and $\underline{u}_{pf}(t)$, which are defined in Section 4.3, are filtered versions of $\underline{r}(t)$ and $\underline{u}_{pl}(t)$ respectively. This algorithm is summarized in Figs. 4.2-1 and 4.2-2.

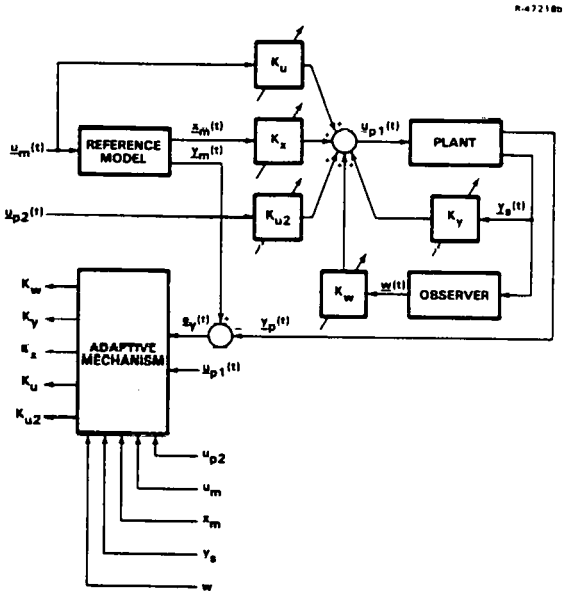

Figure 4.2-1 Model Reference Adaptive Control Algorithm

The algorithm is greatly simplified if the filter f(s) is unity (see Section 4.3). In this case $\underline{u}_{pf}(t) = \underline{u}_p(t)$ and $\underline{r}_f(t) = \underline{r}(t)$ and thus $\underline{\Delta}(t) = 0$ and $\hat{\underline{e}}_y(t) = \underline{0}$. The governing equations are then

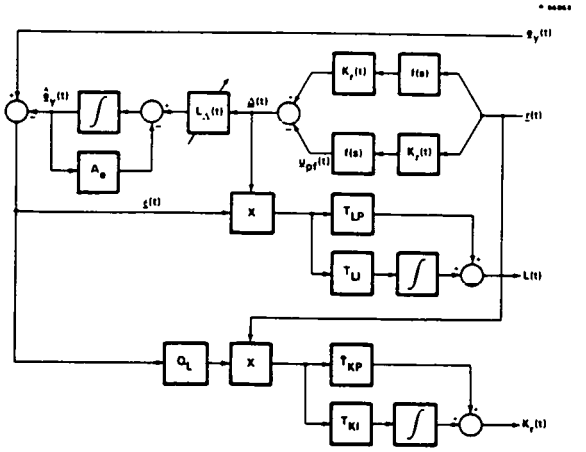

Figure 4.2-2 Model Reference Adaptive Control Adaptive Mechanism

$$K_r(t) = K_P(t) + K_I(t) \qquad (4.2\text{-}13a)$$

$$K_P(t) = Q_L\,\underline{e}_y(t)\,\underline{r}^T(t)\,T_{KP} \qquad (4.2\text{-}13b)$$

$$\dot{K}_I(t) = Q_L\,\underline{e}_y(t)\,\underline{r}^T(t)\,T_{IP} \qquad (4.2\text{-}13c)$$

$$K_I(0) = K_{I0} \qquad (4.2\text{-}13d)$$

which is the previous result appearing in Appendix E.

The stability analysis in the next section shows that $\underline{\varepsilon}(t)$, $\hat{\underline{e}}_y(t)$, $\underline{\Delta}(t)$ and thus, $\underline{e}_y(t)$, approach zero, asymptotically. Given sufficient excitation of the system, the gains $K_I(t)$ and $L_I(t)$ approach $\bar{K}_r$ and L (defined in Appendix D) respectively. Once these gains are reached further excitation does not cause $\underline{e}_y(t)$ to deviate from zero. Similarly, $\hat{\underline{e}}_y(t)$ remains at zero and thus, $\underline{\varepsilon}(t)$ is zero and no further adaptation takes place.

4.3 STABILITY ANALYSIS

This section presents a stability analysis of the system described in Chapter 2 (Eqs. 2.3-1 and 2.3-2) with the input $\underline{u}_{pl}(t)$ defined by Eq. 4.2-6 and gain adaptation defined by Eqs. 4.2-7 to 4.2-12. First, the filters used to compute $\underline{r}_f(t)$, $\underline{u}_{pf}(t)$ and $\hat{\underline{e}}_y(t)$ (i.e., $(sI\text{-}Ae)^{-1}$) are defined. Then, the augmented error, $\underline{\varepsilon}(t)$, dynamics are derived, a Lyapunov function is defined and finally, the stability is verified.

In Eq. 4.2-9, the output error, $\underline{e}_y(t)$, is defined. In Section 3.1, the dynamics governing these errors are shown to be

$$\underline{e}_y(t) = C_p\,\underline{e}(t)$$

$$\dot{\underline{e}}(t) = (A_p - B_{pl}\bar{K})\,\underline{e}(t) + B_{pl}[\bar{\underline{u}}_{pl}(t) - \underline{u}_{pl}(t)] + B_{pl}\bar{K}\,W_1\,\underline{e}_z(t) \qquad (4.3\text{-}1)$$

In Appendix D, these equations are shown to be equivalent to

$$\underline{e}_y(t) = C_N \underline{e}_N(t)$$
$$\dot{\underline{e}}_N(t) = (A_N - B_N Q)\, \underline{e}_N(t) + B_N L[\bar{\underline{u}}_{pl}(t) - \underline{u}_{pl}(t)] + B_N L \bar{K} W_1 \underline{e}_z(t) \quad (4.3\text{-}2)$$

where

$$\underline{e}_N(t) = N \underline{e}(t) \quad (4.3\text{-}3)$$

and the matrices A_N, B_N, C_N, L, N and Q are defined in Appendix D. The matrices A_N, B_N, C_N and Q are known (independent of the plant parameters) and in particular, the choice of Q is arbitrary.

From the definitions of A_N, B_N and C_N, Q can be chose such that the $\ell \times \ell$ transfer function matrix H(s), given by

$$H(s) = C_N (sI - A_N + B_N Q)^{-1} B_N \quad (4.3\text{-}4)$$

is diagonal, given by

$$H(s) = \mathrm{diag}[h_1(s), h_2(s) \ldots h_\ell(s)] \quad (4.3\text{-}5)$$

with each element of the diagonal of the form

$$h_i(s) = p_i(s) \cdot f_i(s) \quad (4.3\text{-}6)$$

where

$$p_i(s) = \frac{1}{(s+\alpha_{i0})} \qquad i=1 \ldots \ell \quad (4.3\text{-}7)$$

$$f_i(s) = \frac{1}{(s+\alpha_{i1})(s+\alpha_{i2}) \ldots (s+\alpha_{id_i})} \qquad i=1 \ldots \ell \quad (4.3\text{-}8)$$

The relative order index d_i is

$$0 \le d_i \le n \quad (4.3\text{-}9)$$

and if $d_i = 0$

$$f_i(s) = 1 \quad (4.3\text{-}10)$$

In order to prove that the algorithm defined in Section 4.2 is stable, Q must be selected such that the filters $f_i(s)$ satisfy

$$f_1(s) = f_2(s) = \ldots = f_\ell(s) = f(s) \quad (4.3\text{-}11)$$

This can be true only if the plant is structured so that

$$d_1 = d_2 = \ldots = d_\ell \quad (4.3\text{-}12)$$

This is a serious restriction on the use of the algorithm, however, the author feels this restriction can be eliminated by an alternate stability proof or by prefiltering the inputs. In the subsequent analysis, it is assumed Eq. 4.3-11 is true.

The filter f(s) is a stable filter of order $d_i (= d_1 = d_2$, etc.) and the filters $p_i(s)$ are stable first order low pass filters. These filters define H(s)

$$H(s) = (sI - A_e)^{-1} f(s) \quad (4.3\text{-}13)$$

and as described above define Q. Furthermore, these filters define the matrix A_e (Eq. 4.2-10) to be a diagonal $\ell \times \ell$ matrix

$$A_e = \mathrm{diag}[-\alpha_{10}, -\alpha_{20} \cdots -\alpha_{\ell 0}]$$

Also the elements of $\underline{r}_f(t)$ are defined as the output of a filter with the respective elements of $\underline{r}(t)$ as the input. In particular

$$r_{fi}(t) = f(s) \cdot r_i(t) \quad (4.3\text{-}14)$$

where $r_{fi}(t)$ is the i^{th} element of $\underline{r}_f(t)$ and $r_i(t)$ is the i^{th} element of $\underline{r}(t)$. The elements of $\underline{u}_{pf}(t)$ are defined as

$$u_{fi}(t) = f(s) \cdot u_i(t) \quad (4.3\text{-}15)$$

where $u_{fi}(t)$ is the i^{th} element of $\underline{u}_{pf}(t)$ and $u_i(t)$ is the i^{th} element of $\underline{u}_{pl}(t)$.

With these definitions we can derive the dynamics of the augmented error, $\underline{\varepsilon}(t)$ (defined in Eq. 4.2-8), upon which the stability proof is based. From Eq. 4.3-13 the output error dynamics Eq. 4.3-2 can be rewritten as

$$\dot{\underline{e}}_y(t) = A_e \underline{e}_y(t) + f(s) L[\bar{\underline{u}}_{pl}(t) - \underline{u}_{pl}(t)] + f(s) L \bar{K} W_1 \underline{e}_z(t) \quad (4.3\text{-}16)$$

Defining $\bar{K}_r$ analogous to $K_r(t)$

$$\bar{K}_r = [\bar{K}_w, \bar{K}_y, \bar{K}_x, \bar{K}_u, \bar{K}_{u2}] \quad (4.3\text{-}17)$$

$\bar{\underline{u}}_{pl}(t)$ can be written as

$$\bar{\underline{u}}_{pl}(t) = \bar{K}_r \underline{r}(t) \quad (4.3\text{-}18)$$

Defining $\underline{e}_{zf}(t)$ as

$$\underline{e}_{zf}(t) = f(s) \underline{e}_z(t) \quad (4.3\text{-}19)$$

and using Eqs. 4.3-14, 4.3-15, 4.3-18 and 4.3-19, the ouptut error dynamics, Eq. 4.3-16, become

$$\dot{\underline{e}}_y(t) = A_e \underline{e}_y(t) + L[\bar{K}_r \underline{r}_f(t) - \underline{u}_{pf}(t)] + L \bar{K} W_1 \underline{e}_{zf}(t) \quad (4.3\text{-}20)$$

From the definition of $\underline{\Delta}(t)$, Eq. 4.2-12, note that the bracketed quantity in Eq. 4.3-20 satisfies the identity

$$\bar{K}_r \underline{r}_f(t) - \underline{u}_{pf}(t) = \underline{\Delta}(t) + [\bar{K}_r - K_r(t)] \underline{r}_f(t) \quad (4.3\text{-}21)$$

Hence, Eq. 4.3-20 becomes

$$\dot{\underline{e}}_y(t) = A_e \underline{e}_y(t) + L \underline{\Delta}(t) + L[\bar{K}_r - K_r(t)] r_f(t) + L \bar{K} W_1 \underline{e}_{zf}(t) \quad (4.3\text{-}22)$$

Recall that the augmented error, $\underline{\varepsilon}(t)$, is the difference between the output errors, $\underline{e}_y(t)$ and the output error estimate, $\hat{\underline{e}}_y(t)$, as defined in Eq. 4.2-10. Hence, using Eq. 4.2-10, and 4.3-20

$$\dot{\underline{\varepsilon}}(t) = A_e\,\underline{\varepsilon}(t) + L[\bar{K}_r - K_r(t)]\,\underline{r}_f(t) + [L - L_\Delta(t)]\,\underline{\Delta}(t) + L\,\bar{K}\,W_1\,\underline{e}_{zf}(t) \tag{4.3-23}$$

The cornerstone of all MRAC algorithms is the Lyapunov function from which the algorithms are derived. Deriving the algorithms with the Lyapunov function assures their global stability. Although this MRAC algorithm has been presented first, it has been derived from the augmented error dynamics, Eq. 4.3-23, and the Lyapunov function V(t).

$$V(t) = \underline{\varepsilon}^T(t)P\,\underline{\varepsilon}(t) + \mathrm{Tr}\{S_K[\bar{K}_r - K_I(t)]T_{KI}^{-1}[\bar{K}_r - K_I(t)]^T S_K^T\} + \mathrm{Tr}\{S_L[L - L_I(t)]T_{LI}^{-1}[L - L_I(t)]S_L^T\} \tag{4.3-24}$$

where S_K and S_L are nonsingular matrices and P is a positive definite symmetric matrix. The matrices must satisfy the constraints discussed below.

It can be shown that if

$$P = S_L^T S_L \tag{4.3-25}$$

and

$$PL = Q_L^T S_K^T S_K \tag{4.3-26}$$

then

$$\dot{V}(t) = \underline{\varepsilon}^T(t)\,[PA_e + A_e^T P]\,\underline{\varepsilon}(t) - 2\underline{\varepsilon}^T(t)\,Q_L^T S_K^T S_K\,Q_L\,\underline{\varepsilon}(t)\,\underline{r}_f^T(t)\,T_{KP}\,\underline{r}_f(t) - 2\underline{\varepsilon}^T(t)\,S_L^T S_L\,\underline{\varepsilon}(t)\,\underline{\Delta}^T(t)\,T_{LP}\,\underline{\Delta}(t) - 2\underline{\varepsilon}^T(t)\,P\,L\,\bar{K}\,W_1\,\underline{e}_{zf}(t) \tag{4.3-27}$$

An analysis analogous to that in Ref. 4 shows that if V(t) is positive definite in $\underline{\varepsilon}(t)$ and $\dot{V}(t)$ is negative definite* in $\underline{\varepsilon}(t)$, then $\underline{\varepsilon}(t)$ will approach zero asymptotically. By its definition, Eq. 4.3-24, V is positive definite in $\underline{\varepsilon}(t)$. If Q_e, defined as

$$PA_e + A_e^T P = -Q_e \tag{4.3-28}$$

is positive definite then $\dot{V}(t)$ is negative definite in $\underline{\varepsilon}(t)$ and the augmented error $\underline{\varepsilon}(t)$ is asymptotically stable to zero; hence, $\hat{\underline{e}}_y(t) \to \underline{e}_y(t)$. This result along with the structure of $\dot{V}(t)$ implies that $\underline{e}_y(t) \to 0$ (i.e., $\underline{y}_p(t) \to \underline{y}_m(t)$) as discussed in Ref. 2. In this reference, the stability discussion refers to single-input, single-output systems. However, for the algorithm discussed here the reasoning is the same. In particular, $\underline{\varepsilon}(t)$ is bounded and from the structure of $\dot{V}(t)$, $\underline{r}_f(t)$ can be shown to be bounded.

To summarize, the MRAC algorithm presented in Eqs. 4.2-5, 7, 8, 9, 10 and 11 is stable provided that the constraints presented in Eqs. 4.3-25, 26 and 28 are satisfied. Unlike constraints on previous algorithms generated in this effort (Appendix E) these constraints are much easier to satisfy. Let L_0 be a nominal value of L, then choose $Q_L = L_0^{-1}$ and $S_K = L_0$ and the constraints become

$$P = S_L^T S_L \tag{4.3-29}$$

$$PL = L_0 \tag{4.3-30}$$

$$PA_e + A_e^T P = -Q_e \tag{4.3-31}$$

where P and Q are positive definite. If $L = L_0$, $P = I_p$, $Q_e = -A_c - A_c^T$ is an obvious solution. Thus, a solution exists everywhere in the neighborhood of $L = L_0$.

*The term $\underline{e}_{zf}(t)$ asymptotically approaches zero; hence, after some time, the quadratic terms in $\underline{\varepsilon}(t)$ dominate these linear terms.

5.0 POWER PLANT MODEL

5.1 BACKGROUND

Modern control system design procedures are predicated on models of the system being controlled. The model reference adaptive control theory being developed in this project will likewise lead to a model-dependent design methodology. To enhance the understanding of the theory and implications of various design options that may arise, TASC has developed a realistic power plant model.

The model chosen to aid in studying the theory is that of Philadelphia Electric Company's Cromby No. 2 Unit. A nonlinear, state-space model of this plant has been developed from first-principle considerations (Refs. 9 and 10). Moreover, test data are available for validation and, therefore, this model is considered to be highly realistic with regards to predicting (restricted) operating conditions. A linearization of this nonlinear model has been used to validate the applicability of MRC algorithms (and thereby MRAC algorithms) as described in Chapter 6. For various reasons discussed below, TASC has extended the capabilities of this model as part of the research effort.

5.2 MODEL DEVELOPMENT

The major objective of the model development task has been to extend the capabilities of the mathematical model for the Cromby No. 2 Unit which consists of a fossil-fired reheat boiler-turbine-generator. These extensions include:

- Restructuring the turbine model to improve extraction flow modeling
- Providing representation of governor-valve overlap
- Increasing the range of thermodynamic state relations.

5.2.1 The Cromby Model

TASC has been engaged in building a simulation from portions of the Cromby model as documented in Ref. 10. In particular, a model of the boiler has been established. This includes (according to nomenclature of Ref. 10)

- Feedwater valve/boiler feed pumps
- Downcomers
- Waterwalls
- Drum
- Primary superheater (steam side)
- Superheat spray
- Secondary superheater (steam side)
- Reheat spray
- Reheater section (steam side)
- Mills
- Combustion
- Superheat furnace
- Reheat furnace.

Two major assumptions about the plant cycle were made in the original work, and all are adopted herein, they significantly impact the final model formulation. The first is that dynamic phenomena related to air and hot gases are much faster than those that occur in the steam cycle. Consequently, these dynamics are ignored; their inclusion would lead only to computational difficulties during simulation without contributing to overall control analysis capability. For similar reasons, the second assumption made was that feedwater train and economizer dynamics could also be omitted. Building a model based on Ref. 10 entails resolving simultaneous nonlinear algebraic equations, and establishing the order for implementing the resolved equations. The resolved equations are presented in Appendix A. The 14 state variables used to model the boiler are tabulated in Table 5.2-1. Additional state variables will be defined for the turbine model; control and output variables are discussed in Section 5.3.

TABLE 5.2-1
CROMBY MODEL BOILER STATE-VARIABLES

Drum steam density
Drum water volume
Fractional mill volume occupied by coal
Crusher-zone coal mass
Superheat-furnace waterwall tube temperature
Reheat-furnace waterwall tube temperature
Primary-superheater steam density
Primary-superheater steam enthalpy
Secondary-superheater average steam density
Secondary-superheater average steam enthalpy
Secondary-superheater outlet steam enthalpy
Reheater average steam density
Reheater average steam enthalpy
Reheater outlet steam enthalpy

5.2.2 Model Extensions

Modifications of the Cromby model have been included as part of this TASC effort in order to develop a more generic power plant model. These modifications are centered around substitution of the dynamic turbine model developed in Ref. 25 for that originally used in the Cromby model. Incorporation of the dynamic turbine affords more realistic representation of the following:

- turbine steam dynamics
- governor valve operation
- effects of turbine back-pressure.

These items are important from the viewpoint of turbine control in the presence of balance-of-plant interactions.

Turbine steam dynamics - The original Cromby turbine model was developed under the assumption of reaction-turbine flow being proportional to inlet pres-

sure; that is, sonic flow prevails throughout the turbine over the entire load range. This model represents the reaction-turbine flow as being algebraically related to superheater outlet flow. The dynamic model of Ref. 25, however, allows for steam mass and energy storage in the high-pressure turbine which in turn facilitates the use of Stodola's flow equation. Since this flow equation is equally valid for sonic and subsonic turbine flow, the dynamic model is less restrictive than the algebraic one.

Governor valve operation - The model of Ref. 25 also incorporates an algorithm to represent governor valve overlap. Governor valve overlap is an operating practice which is used to reduce the impulse-like flow disturbances introduced upon opening of a governing valve. The practice is carried out by opening successive valves before previously opened valves are fully opened. The procedure is reversed upon closure.

The implications of overlap are that some valves may be passing sonic flow while others operate subsonically. These mixed conditions and model capabilities are alluded to in the original Cromby work and extended in Ref. 25.

Effects of turbine back-pressure - The original assumption of algebraic reaction-turbine flow limits the capability to model effects of turbine back-pressure. This can be ameliorated by use of the Stodola equation which explicitly relates turbine flow and turbine exit pressure. Therefore, representations of turbine extraction flows can be modeled and interactions with feedwater-train heaters can be approximated.

In addition to the model structure modifications discussed above, extensions to the modeled thermodynamic steam relations have been developed. This modification has extended the power-plant model capabilities to represent an operating regime of about 25% to 110% of turbine rating. This allows control studies over extended load ranges, as well as with alternative operating modes such as variable pressure operation.

5.3 IMPLICATIONS OF ADVANCED CONTROL DESIGNS

The power plant is characterized as a multi-input multi-output system as depicted in Fig. 5.3-1. The inputs or control variables are:

- Mill feeder stroke
- Throttle valve position
- Feedwater valve position
- Air flow (inlet louver drive)
- Superheater and reheater attemperator spray flows
- Superheater and reheater burner tilts.

The (conventionally) controlled output variables are:

- Power output
- Throttle pressure and temperature
- Combustion (air-fuel ratio)

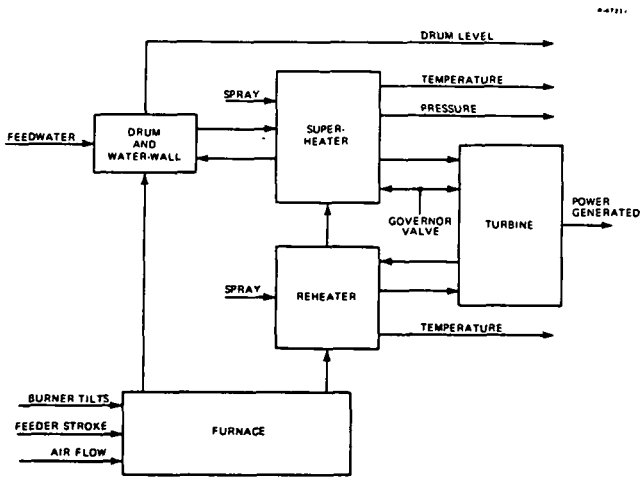

Figure 5.3-1 Power Plant Model

- Reheater outlet temperature
- Steam flow
- Drum water level.

The control of power output is directly related to steam flow control. The attemperator sprays and burner tilts are both used to control superheater and reheater outlet temperatures and therefore are somewhat redundant. Thus, there are essentially six principal control devices and six major controlled variables. These are conventionally paired as shown in Table 5.3-1, which is typical of boiler-follow* operation.

TABLE 5.3-1
CONTROL INPUT-OUTPUT RELATIONS

CONTROL INPUT	CONTROL OUTPUT	COMMENTS
Mill feeder stroke	Throttle pressure	Alternatively steam flow
Throttle valve position	Steam flow (power)	Alternatively throttle pressure
Feedwater valve position	Drum level	Three-element controller
Air flow	Furnace conditions	
Attemperator sprays and burner tilts	Superheat and Reheat temperature	Sprays used when tilts reach limits

Pairing of input-output variables as in Table 5.3-1 is based upon predominant cause-and-effect relations. In fact, there are many interactions exhibited

*Boiler-follow operation refers to the fact that boiler controls respond to load-demand changes directly, and the throttle valves respond to pressure fluctuations.

among the variables of Table 5.3-1 and conventional control systems are designed in ad hoc fashion to account for them. The advantage of modern multivariable control system designs is that these interactions can be accounted for in a harmonious manner which is completely complementary to control of the dominant plant interactions. In addition, the Model Reference Adaptive Controller provides the capability of varying pre-selected control gains which may be dependent upon time-varying and/or uncertain plant parameters, e.g., fuel heat-content or changing heat coefficients due to slag buildup.

6.0 CONTROL APPLICATION

The final objective of this project has been to apply the control theory discussed in the first four chapters of this report to the power plant model described in Chapter 5. The first step in this effort has been the application of the MRC algorithm (with and without the enhancement) to a linearization of the power plant model near 190 MW generation. This application demonstrates that the MRC algorithm achieves its objectives, i.e., the MRC algorithm causes the plant outputs to perfectly track the reference model outputs. The enhanced MRC algorithm demonstrates this goal can be achieved (by both the MRC and MRAC algorithms) with moderate levels of control. The limitations of the MRAC theory (see discussion of f(s) filters in section 4.3) as well as the sensitivity of the MRC algorithm to parameter changes forces this effort to be limited to the above results. The remainder of this chapter discusses in more detail these results.

The first step in this process is to identify the 190 MW operating point. The operating point is defined as the steady state conditions necessary for all outputs to achieve desired constant values. The constant controls required to achieve this operating point are the open loop controls. Each control is computed as the sum of an open loop control and an incremental control (computed from the MRC algorithm). The incremental control causes the system to respond to deviations about the operating point. The steady state operating point outputs are defined in Table 6-1.

TABLE 6-1
OUTPUTS FOR 190 MW OPERATING POINT

OUTPUT NO.	DESCRIPTION	VALUE
1	Throttle Pressure	1830 psia
2	Throttle Temperature	1460°
3	Reheater Outlet Temperature	1460°
4	Generated Power	190 MW
5	Drum Water Level Deviation	0 in.

Values for all the system states, the two burner tilts, the feeder stroke, feedwater valve and governor value are found such that these outputs are achieved as well as all the system state derivatives are zero. Table 6-2 lists all these values. Note that there are five outputs (ℓ=5) and eight controls (m=8), hence, the controls must be divided into $\underline{u}_{p1}$ (5 elements) and $\underline{u}_{p2}$ (3 elements). This selection is designated by the prefix of the control number, P1 designates element of $\underline{u}_{p1}$ and P2 designates elements of $\underline{u}_{p2}$. The linear system describing the power plant behavior near the operating point described in Tables 6-1 and 6-2 has been obtained by empirically differentiating the dynamic equations described in Appendix A about this operating point.

The relative order indices (see Appendix D) for this linear system are given in Table 6-3.

TABLE 6-2
OPEN LOOP CONTROLS FOR 190 MW OPERATING POINT

CONTROL NO.	DESCRIPTION	VALUE
P1-1	Mill Feeder Stroke	0.6362
P1-2	Superheater Spray	0.003 klb/sec
P1-3	Reheater Burner Tilt	6.336°
P1-4	Feedwater Valve Area	0.7072
P1-5	Throttle Valve Area	5.527
P2-1	Superheater Burner Tilt	20.13°
P2-2	Furnace Airflow	454.0 lb/sec
P2-3	Reheater Spray	0.003 klb/sec

TABLE 6-3
RELATIVE ORDER INDICES

i	d_i
1	1
2	1
3	1
4	0
5	1

The matrix Q is chosen to keep the output error dynamics diagnonal. In particular

$$Q = \begin{bmatrix} 0.01 & 0.2 & 0 & 0 & 0 & 0 & 0 & 0 & 0 \\ 0 & 0 & 0.01 & 0.2 & 0 & 0 & 0 & 0 & 0 \\ 0 & 0 & 0 & 0 & 0.01 & 0.2 & 0 & 0 & 0 \\ 0 & 0 & 0 & 0 & 0 & 0 & 0.1 & 0 & 0 \\ 0 & 0 & 0 & 0 & 0 & 0 & 0 & 0.01 & 0.2 \end{bmatrix}$$

Thus, all the eigenvalues for the closed loop dynamics are at -0.1. All but the fourth output have second order error dynamics and the fourth output (power generated) has first order error dynamics. The error dynamics refer to the output behavior with the MRC algorithm.

The reference model parameters are defined as follows.

$$A_m = \begin{bmatrix} 0.0 & 1.0 \\ 0.0 & -0.1 \end{bmatrix} \quad B_m = \begin{bmatrix} 0.0 \\ 0.1 \end{bmatrix} \qquad (6\text{-}1)$$

$$C_m = \begin{bmatrix} 0 & 0 \\ 0 & 0 \\ 0 & 0 \\ 1 & 0 \\ 0 & 0 \end{bmatrix}$$

where the reference model outputs are the desired trajectory of the derivations from nominal of throttle pressure, temperature, reheat outlet temperature, power generated and drum level. The command inputs are the desired rate of change of power

generated. Note that all the desired trajectories are constants except power generated. The latter is the integral of a low pass filter with time constant of 10 sec. This output is a second order lag from the reference model input and hence has relative order index of one, which is greater than the relative order index of power enerated ($d_4 = 0$).

The observer in the MRC algorithm has a significant inpact on performance of the nonlinear system. In the linear system analysis in which the design and analysis models are the same, the observer has no effect except in its initial transient response. Thus, it has been assumed in this study that

$$\hat{\underline{x}}_p(t) = \underline{x}_p(t) \qquad (6\text{-}2)$$

The initial simulation results are generated with $\underline{u}_{p2}(t) = \underline{0}$ and the continuous MRC algorithm described in section 3.1 is used.

The power generated response to a reference command given by

$$\underline{u}_m(t) = \begin{cases} 0.0 & t < 1 \text{ sec} \\ 0.26 & 1 \text{ sec} \leq t \leq 41 \text{ sec} \\ 0.0 & 41 \text{ sec} < t \end{cases} \qquad (6\text{-}3)$$

is shown in Fig. 6-1. This trajectory is identical to the fourth output of the reference model. Note that the power changes at 15 mW/min or approximately 7% total capacity per minute. At the same time all the other outputs remained constant (within numerical accuracy). More significant are the control trajectories, two of which are depicted in Figs. 6-2, 6-3, 6-4, 6-5 and 6-6.

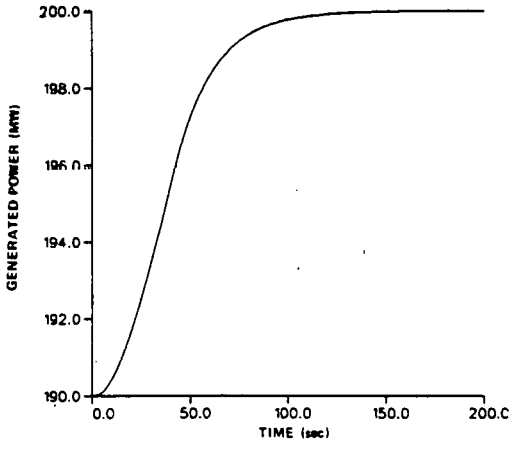

Figure 6-1 Generated Power vs. Time with the MRC Algorithm

Note that these controls have rather large oscillations. The introduction of the enhanced MRC algorithm (section 3.3) allows the use of these controls to be balanced off against the $\underline{u}_{p2}(t)$ controls (see Table 6-2). Recall that the cost function used to compute $\underline{u}_{p2}(t)$ is given by

$$J_e = \int_0^\infty \{\underline{u}_{p1}^T(t)\, R_1\, \underline{u}_{p1}(t) + \underline{u}_{p2}^T(t)\, R_2\, \underline{u}_{p2}(t)\}dt \qquad (6\text{-}4)$$

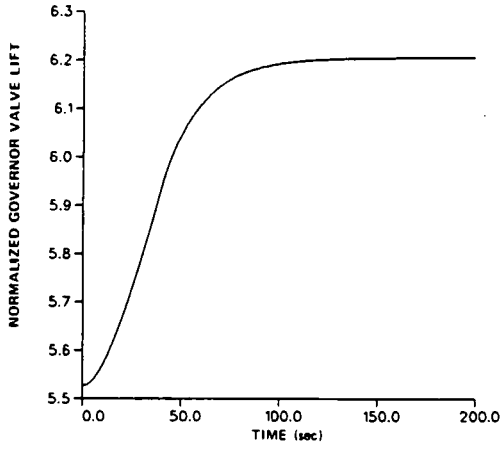

Figure 6-2 Governor Valve Lift vs. Time for the MRC Algorithm

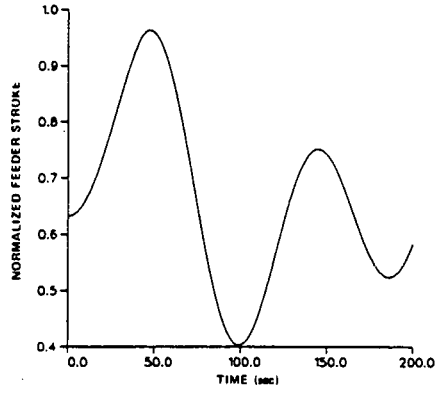

Figure 6-3 Feeder Stroke vs. Time for the MRC Algorithm with $\underline{u}_{p2} = \underline{0}$

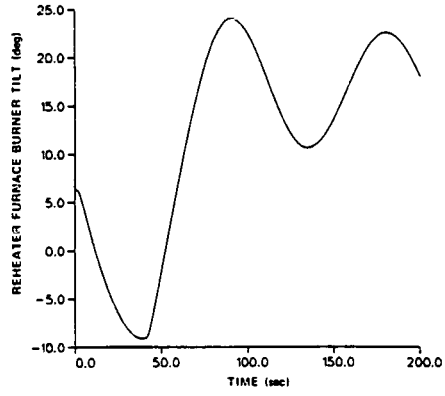

Figure 6-4 Reheater Furnace Burner Tilt vs. Time for the MRC Algorithm with $\underline{u}_{p2} = \underline{0}$

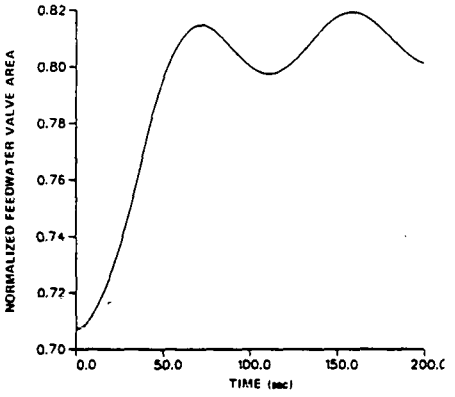

Figure 6-5 Feedwater Valve Area vs. Time for the MRC Algorithm with $\underline{u}_{p2} = \underline{0}$

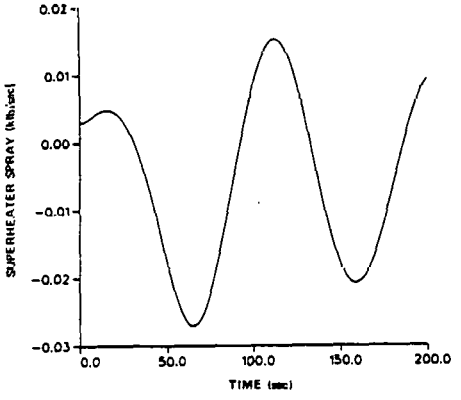

Figure 6-6 Superheater Spray vs. Time for the MRC Algorithm with $\underline{u}_{p2} = \underline{0}$

In this case

$$R_1 = \begin{bmatrix} 100 & 0 & 0 & 0 & 0 \\ 0 & 0.01 & 0 & 0 & 0 \\ 0 & 0 & 10^{-4} & 0 & 0 \\ 0 & 0 & 0 & 1.0 & 0 \\ 0 & 0 & 0 & 0 & 10^{6} \end{bmatrix} \quad (6\text{-}5)$$

$$R_2 = \begin{bmatrix} 10^{4} & 0 & 0 \\ 0 & 4.0 & 0 \\ 0 & 0 & 4.0\times10^{-4} \end{bmatrix} \quad (6\text{-}6)$$

The diagonal elements of the R matrices are inversely proportional to the square of the magnitudes of the maximum deviations of the controls. Minimizing the cost functions Eq. 6-2 subject to Eqs. 3.3-3 and 3.3-4 yield an optimal feedback and feedforward control algorithm for $\underline{u}_{p2}(t)$. Since $\underline{u}_{p1}(t)$ compensates for any $\underline{u}_{p2}(t)$, in terms of output following, the output response is the same. However, the control response is dramatically improved as shown in Figs. 6-7 through 6-10 (the governor valve response is not significantly modified). At the same time the controls $\underline{u}_{p2}(t)$ are not exhibiting significant changes themselves. That is, actions of $\underline{u}_{p1}(t)$ and $\underline{u}_{p2}(t)$ have been optimally balanced.

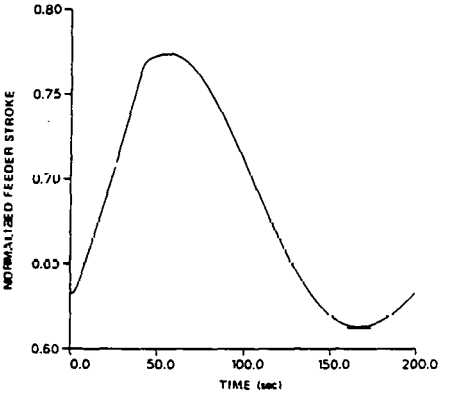

Figure 6-7 Feeder Stroke vs. Time for the MRC Algorithm with $\underline{u}_{p2}$ Chosen Optimally

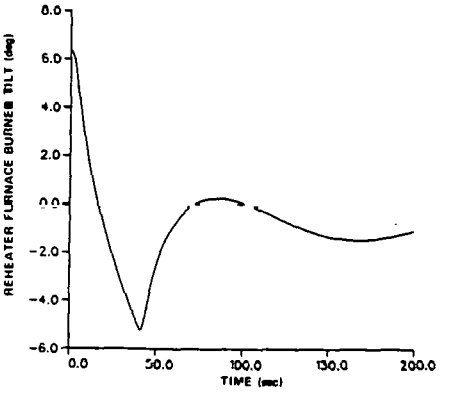

Figure 6-8 Reheater Furnace Burner Tilt vs. Time for the MRC Algorithm with $\underline{u}_{p2}$ Chosen Optimally

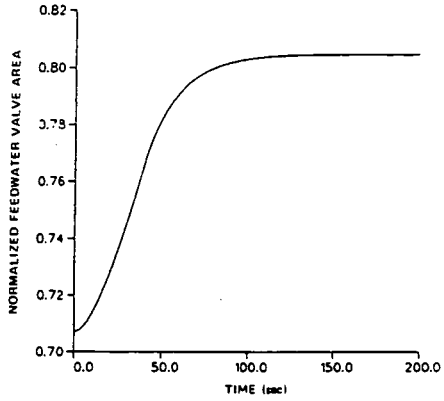

Figure 6-9 Feedwater Valve Area vs. Time for the MRC Algorithm with $\underline{u}_{p2}$ Chosen Optimally

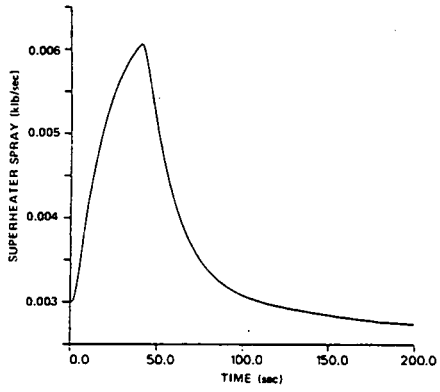

Figure 6-10 Superheater Spray vs. Time for the MRC Algorithm with $\underline{u}_{p2}$ Chosen Optimally

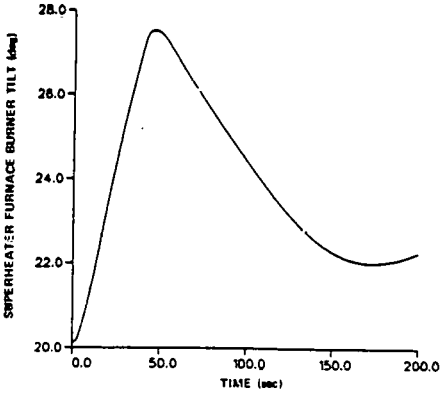

Figure 6-11 Superheater Furnace Burner Tilt vs. Time for the MRC Algorithm with $\underline{u}_{p2}$ Chosen Optimally

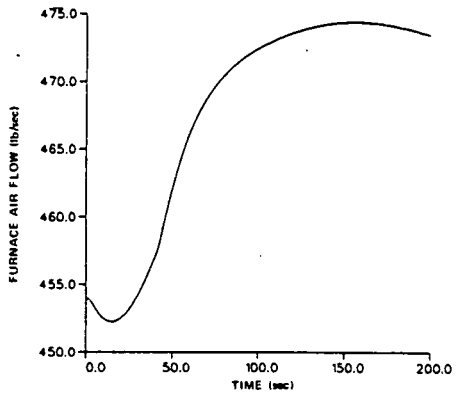

Figure 6-12 Furnace Air Flow vs. Time for the MRC Algorithm with $\underline{u}_{p2}$ Chosen Optimally

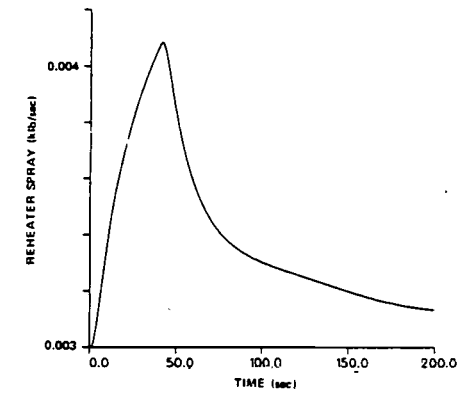

Figure 6-13 Reheater Spray vs. Time for the MRC Algorithm with $\underline{u}_{p2}$ Chosen Optimally

7.0 CONCLUSIONS AND RECOMMENDATIONS

7.1 SUMMARY AND CONCLUSIONS

This report presents the achievements of a three-year research effort in Model Reference Control (MRC) and Model Reference Adaptive Control (MRAC) theory for multi-input, multi-output (MIMO) electric power plant control applications. Current industry-wide power plant control designs relate each plant output to a single control (i.e., multiple single-input, single-output algorithms). This approach is sometimes enhanced with feedforward commands which coordinate some of the single-loop structures, but does not coordinate feedback networks which ultimately limits system performance. Since MRC and MRAC approaches intrinsically account for loop interactions, they promise improved performance capabilities.

An extensive review of the literature has shown that existing adaptive control schemes are of two general types: either the self-tuning regulator (STR) or the model reference adaptive controller. Although STRs have fewer restrictions and thus wider applicability, unlike MRACs they cannot guarantee closed loop stability. Previous MRAC algorithms which have been designed for single-input, single-output (SISO) systems have global stability properties that cause output errors to asymptotically approach zero. MRAC algorithms which have previously been designed for MIMO systems are globally stable but only result in state errors being bounded. The goal of this effort has been to develop MIMO MRAC algorithms with characteristics similar to the SISO MRAC algorithms.

The first step towards the goal has been to find a control algorithm which is the steady state (in the adaptive sense) of the MIMO MRAC algorithm. This non-adaptive MRC algorithm has been developed for MIMO linear continuous- and discrete-time systems using Command Generator Tracker methodology (Sections 3.1 and 3.2). The existence and stability of the MRC algorithm depends on structural conditions in the reference model and depends on stable transmission zeros in the plant. This latter constraint is alleviated for systems with more inputs than outputs with the enhanced MRC algorithm (Section 3.3). These algorithms require knowledge of the plant parameters and serve as a foundation for the MRAC algorithm development and stability analysis.

The MRAC algorithm differs from the MRC algorithm in that it is applicable to systems with unknown parameters. The initial MIMO MRAC algorithms developed in this effort are improvements to the previous MIMO algorithms which yielded bounded state error performance and required various positive real constraints (see Appendix E). The final MIMO MRAC algorithm, presented in Chapter 4, is a generalization of SISO algorithms described in Ref. 2. The performance of this algorithm is such that the plant output asymptotically approaches the reference model output. The algorithm requires no positive real constraints but only that a stable MRC algorithm exist, (i.e., that the plant transmission zeroes be stable) and structural constraint on the plant (all the relative order indices must be the same). Although the latter constraint limits the MRAC applications continuing research should readily alleviate this restriction.

In order to enhance the understanding of the MRC and MRAC algorithms, a realistic power plant model has been developed. A nonlinear, state-space model of Philadelphia Electric Company's Cromby No. 2 Unit has been developed from first-principle considerations (Refs. 9 and 10). Since test data are available for validation, this model is considered to be highly realistic with regard to predicting plant dynamics at different operating conditions. This model is detailed in Chapter 5 and Appendices A and B. The Cromby model is a multi-input, multi-output nonlinear system, with measurements which are nonlinear functions of the states.

The final phase of this project has been the implementation of the MRC algorithm in a linearization of the Cromby model representing the plant behavior near 190 MW. The inputs and outputs of this system are listed in Table 7-1.

TABLE 7-1
POWER PLANT CONTROLS AND OUTPUTS

CONTROLS	REGULATED OUTPUTS
1) Coal Feeder Stroke	1) Throttle Pressure
2) Superheat Spray	2) Throttle Temperature
3) Reheat Burner Tilt	3) Reheat Output Steam Temperature
4) Feedware Valve Area	4) Power Generated
5) Governor Valve Lift	5) Drum Level
6) Air Flow	
7) Superheater Burner Tilt	
8) Reheat Spray	

For this effort all the states are assumed to be measured. The reference model input is load demand rate and its outputs which are the desired response of the outputs (Table 7-1) are all held fixed, except for generated power. The latter is a first order lag and integral of load demand rate.

Initial results using the basic MRC algorithm (with the first five controls in Table 7-1) are very good with respect to system outputs; i.e., they perfectly matched reference model outputs. In particular the generated power changes at a rate of 7% (of full load) per minute while all other outputs are held fixed. However, the feedback gains are very large and the controls are very noisy with large amplitudes. The control behavior is dramatically improved by introducing the enhanced MRC algorithm which introduces the remaining three controls and uses optimal control technology to optimally balance all the control trajectories.

Thus the project accomplishment are

- Development of a MIMO MRC algorithm for linear continuous- and discrete-time systems with known parameters
- Development of a MIMO MRAC algorithm for linear continuous-time systems with unknown parameters which drives output errors asymptotically to zero
- Development of a nonlinear model of the boiler-turbine-generator Cromby power plant unit

- Validation of the MRC algorithm with a linearization of the Cromby model

- Development of an enhanced MRC algorithm which dramatically improves the control response characteristics of the plant.

7.2 RECOMMENDATIONS

Future efforts in this area of research should deal with the MRC algorithm high feedback gain characteristics. In spite of the excellent performance reported in the application section, the feedback gains are relatively high. This causes large fluctuations in the controls when unmodeled disturbances enter the system or initial condition errors are significant. This problem may not have occurred if the control system could be applied to a lower order model of the power plant. However, the MRC and MRAC stability theory do not deal with unmodeled dynamics. Hence, the stability problem with unmodeled dynamics is an important topic for future research with respect to the MRAC algorithm.

Future efforts on the MRAC algorithm should also deal with the structural constraints necessary to establish stability. As noted above, the algorithm is limited to plants satisfying limiting structural constraints, necessary to complete the stability analysis. The author feels that, without much difficulty, future efforts should be able to modify the algorithm or the stability analysis to eliminate this restriction.

APPENDIX A
RESOLUTION OF POWER PLANT MODEL EQUATIONS

A.1 CROMBY MODEL EQUATIONS

References 9 and 10 describe the modeling process and results obtained regarding the development of the Cromby No. 2 Unit mathematical model. These references give some explanation of the underlying principles and assumptions governing the model formulation. However, the form of the model presented is not readily usable because of the existence of several unresolved nonlinear simultaneous equations. This appendix presents the results of resolving these equations into a form suitable for simulation.

The equations are grouped and ordered into self-consistent (program) modules. Each module essentially contains all the equations needed to define a particular portion of the plant (superheater, turbine, etc.). The development of any module is based on the assumption that initial conditions of state-variables and control variables are known. This assumption permits breaking of implicit loops. That is, the equations can be ordered by defining a "starting place" for the ordering process. Figure A.1-1 is a solution diagram that illustrates the interfacing between modules and thus defines the order of solution. State variables are shown as outputs of the defining modules and are indicated by double-headed arrows.

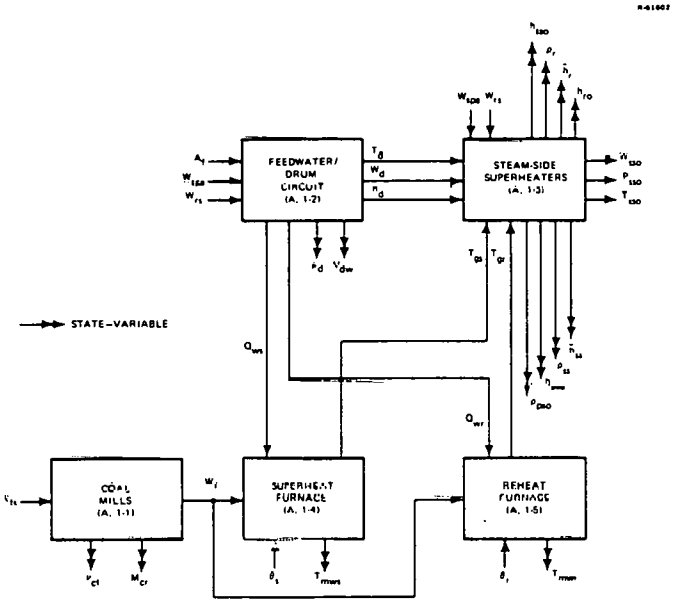

Figure A.1-1 Power-Plant Model Solution Diagram

The modules are presented in Tables A.1-1 through A.1-5. Titles given to the tables roughly describe the major power plant components that are modeled by the set of equations in the table. Each table contains the resolved equations used to define a given module, corresponding equation numbers (Ref. 10) of the defining equations, and comments pertaining to assumptions. The nomenclature used is that of Ref. 9 and is explained in Appendix B.

TASC has implemented a quartic solution for flow resolution which is not presented in Ref. 10. This algorithm is discussed in Section A.2.

TABLE A.1-1
COAL MILLS

RESOLVED EQUATIONS	REFERENCE 10 DEFINING EQUATIONS
$W_{pao} = W_{ao} + K_{wfs}\ell_{fs}$	13-3
$W_f = W_{pao}\left(\frac{\rho_{cf}}{\rho_a}\right)\frac{v_{cf}}{1-v_{cf}}$	13-3 (Assumes all mills are operational)
$\frac{d}{dt} v_{cf} = \frac{1}{\rho_{cf} V}(K_{cf} M_{cr} - W_f)$	13-2
$\frac{d}{dt} M_{cr} = K_{fs}\ell_{fs} - K_{cf}M_{cr}$	13-1

TABLE A.1-2
WATER-SIDE FEEDWATER-DRUM CIRCUIT SOLUTION

RESOLVED EQUATIONS	REFERENCE 10 DEFINING EQUATIONS
$\alpha_{hd} = \left(\frac{\partial h_d}{\partial \rho_d}\right)_{SAT}$	4-4 (Assumed Constant)
$\alpha_{hdW} = \left(\frac{\partial h_{dW}}{\partial \rho_{dW}}\right)_{SAT}$	4-4 (Assumed Constant)
$\alpha_{\rho_{dW}} = \left(\frac{\partial \rho_{dW}}{\partial \rho_d}\right)_{SAT}$	4-4 (Assumed Constant)
$\rho_{dW} = f_{4,1}(\rho_d)$	4-3
$T_d = f_{4,2}(\rho_d)$	4-3
$P_d = f_{4,3}(\rho_d)$	4-3
$h_{dW} = f_{4,4}(\rho_d)$	4-3
$h_d = f_{4,5}(\rho_d)$	4-3
$g_1 = \frac{\alpha_{hd}\rho_d(V_d - V_{dW}) + \alpha_{hdW}\rho_{dW}V_{dW}}{[V_d - (1-\alpha_{\rho dW})V_{dW}](h_d - h_{dW})}$	
$g_2 = \frac{\alpha_{\rho dW}V_{dW}}{V_d - (1-\alpha_{\rho dW})V_{dW}}$	
$g = g_1 - g_2$	4-4

TABLE A.1-2

WATER-SIDE FEEDWATER-DRUM CIRCUIT SOLUTION (Continued)

RESOLVED EQUATIONS	REFERENCE 10 DEFINING EQUATIONS
$W_{ep} = \frac{1}{2}\{\lambda K_f A_f^2 + [(\lambda K_f A_f^2)^2 + 4K_f A_f^2 (P_{ho} - P_d)]^{\frac{1}{2}}\}$	1-1, 1-3
$W_e = W_{ep} - W_{spa} - W_{rs}$	1-2
$P_{ho} = f_{1,1}(W_{ep})$	1-4 (Depends on Feedwater Pump Operations)
$P_h = P_{ho} + \lambda W_{ep}$	1-3
$h_e = f_{2,1}(W_e)$	2-1
$h_D = \frac{1}{W_D}\{(W_D - W_e)h_{dW} + W_e h_e\}$	2-2
$Q_{ws} = K_w(T_{mws} - T_d)^3$	15-2
$Q_{wr} = K_{wr}(T_{mwr} - T_d)^3$	3-2, 15-2, 16-1
$Q_w = Q_{ws} + Q_{wr}$	3-2
$h_w = \frac{Q_w}{W_D} + h_D$	3-2
$X = \frac{h_w - h_{dw}}{h_d - h_{dw}}$	3-1
$0 = a_1 W_d^4 + a_2 W_d^3 + a_3 W_d^2 - \rho_d(P_d - P_{pso})$	5-1, 5-7 (Solve Quartic for W_d (a_1, a_2, a_3, are constants))
$g_3 = 1 + g(1 - \frac{\rho_d}{\rho_{dW}})$	
$\frac{d}{dt}\rho_d = \frac{\left[\frac{\rho_d}{\rho_{dW}} W_e - W_d + XW_D(1 - \frac{\rho_d}{\rho_{dW}})\right] \times 10^3}{g_3[Vd - (1-\alpha_{\rho dW})V_{dW}]}$	4-5 (10^3 is conversion factor KLBM→LBM)

TABLE A.1-2

WATER-SIDE FEEDWATER-DRUM CIRCUIT SOLUTION (Continued)

RESOLVED EQUATIONS	REFERENCE 10 DEFINING EQUATIONS
$\frac{d}{dt} V_{dW} = \frac{\left[\frac{1+g}{\rho_{dW}} W_e - \frac{g}{\rho_{dW}} W_d - \frac{X}{\rho_{dW}} W_D\right] \times 10^3}{1 + g(1 - \frac{\rho_d}{\rho_{dW}})}$	4-6 (10^3 is conversion factor KLBM→LBM)

TABLE A.1-3

STEAM-SIDE SUPERHEATERS

RESOLVED EQUATIONS	REFERENCE 10 DEFINING EQUATIONS
$T_{pso} = f_{5,1}(h_{pso}, \rho_{pso}, P_{pso})$	5-5
$P_{pso} = f_{5,2}(h_{pso}, \rho_{pso}, P_{pso})$	5-6
$P_{sso} = f_{7,3}(h_{sso}, \rho_{sso})$	7-13
$0 = a_4 W_{pso}^4 + a_5 W_{pso}^3 + a_6 W_{pso}^2 - \rho_{pso}(P_{pso} - P_{sso})$	7-1, 7-14 (Solve quartic for W_{pso} (a_4, a_5, a_6 are constants))
$T_{sso} = f_{7,4}(h_{sso}, \rho_{ss}, P_{sso})$	7-13
$\bar{T}_{ss} = f_{7,4}(\bar{h}_{ss}, \rho_{ss}, (P_{pso} + P_{sso})/2)$	7-13
$P_{ro} = f_{11,1}(h_{ro}, \rho_r, P_{ro})$	
$T_{ro} = f_{11,2}(h_{ro}, \rho_r, P_{ro})$	
$\bar{T}_r = f_{11,3}(P_{ro}, P_{cr}, \bar{h}_r)$	11-7
$\bar{T}_{ps} = (T_d + T_{pso})/2$	
$Q_{ss} = \frac{A_{ss} + K_{ss}(T_{gs} - \bar{T}_{ss})}{\left\{1 + \frac{10^3 K_{ss}}{C_{gs} W_g}\right\}}$	5-10, 7-15, 7-16 (10^3 is conversion factor KBTU→BTU)
$C_{gs} = f_{7,5}(W_f)$	7-17
$T_{gso} = T_{gs} - \frac{2Q_{ss}}{C_{gs} W_g}(10^3)$	5-10 (10^3 is conversion factor KBTU→BTU)
$C_{gr} = f_{11,4}(W_f)$	

TABLE A.1-3

STEAM-SIDE SUPERHEATERS (Continued)

RESOVED EQUATIONS	REFERENCE 10 DEFINING EQUATIONS
$Q_r = \frac{A_r + K_r(T_{gr} - \bar{T}_r)}{\left\{1 + \frac{10^3 K_r}{C_{gr} W_g}\right\}}$	11-5, 11-6
$T_{gro} = T_{gr} - \frac{2Q_r}{C_{gr} W_g} (10^3)$	5-11
$C_{gps} = f_{5,3}(W_f)$	5-12
$j(W_g, W_d) =$ $\frac{K_{rps} K_{ps} (W_g)^{0.6} (W_d)^{0.8}}{K_{rps} (W_g)^{0.6} + K_{ps} (W_d)^{0.8}}$	5-8
$Q_{ps} =$ $\frac{\frac{T_{gso} + T_{gro}}{2} - \bar{T}_{ps}\ j(W_g, W_d)}{\left\{1 + \frac{10^3 j(W_g, W_d)}{2C_{gps} W_g}\right\}}$	5-8; 5-9
$\frac{d}{dt} h_{pso} =$ $[Q_{ps} - W_{pso} h_{pso} + W_d h_d]/M_{ps}$	5-3
$W_{ssi} = W_{pso} + W_{spa}$	6-1
$h_{sse} = (W_{pso} h_{pso} + W_{spa} h_e)/W_{ssi}$	6-2
$\bar{W}_{ss} = (W_{ssi} + W_{sso})/2$	7-4
$\frac{d}{dt} \rho_{ss} = (W_{ssi} - W_{sso})/V_{ss}$	7-9 (Assumes small density variations along superheater)
$\frac{d}{dt} \bar{h}_{ss} =$ $\left[\frac{Q_{ss}}{2} + (h_{sse} - \bar{h}_{ss}) W_{ssi}\right] / \frac{M_{ss}}{2}$	7-11 (Assumes M_{ss} constant)

TABLE A.1-3

STEAM-SIDE SUPERHEATERS (Continued)

RESOLVED EQUATIONS	REFERENCE 10 DEFINING EQUATIONS
$\frac{d}{dt} h_{sso} =$ $\left[\frac{Q_{ss}}{2} + (\bar{h}_{ss} - h_{sso}) \bar{W}_{ss}\right] / \frac{M_{ss}}{2}$	7-12 (Assumes M_{ss} constant)
$W_{rse} = W_{rsi} + W_{rs}$	10-1
$h_{rse} = (W_{rsi} h_{hpe} + W_{rs} h_{ec})/W_{rse}$	10-2
$\frac{d}{dt} \rho_r = (W_{rse} - W_{ro})/V_r$	11-2
$\frac{d}{dt} (\bar{h}_r) =$ $[Q_r - 2(\bar{h}_r - h_{rse}) W_{rse}]/M_r$	11-3 (Assumes M_r constant)
$\frac{d}{dt} (h_{ro}) =$ $[Q_r - (h_{ro} - \bar{h}_r)(W_{rse} + W_{ro})]/M_r$	11-4 (Assumes M_r constant)
$\frac{d}{dt} (\rho_{pso}) = 10^3 (W_d - W_{pso})/V_{ps}$	5-2

TABLE A.1-4

SUPERHEAT FURNACE

RESOLVED EQUATIONS	REFERENCE 10 DEFINING EQUATIONS
$K''_{lw} =$ $K_{lw} \{\Delta + (\sum_{i=5}^{8} M_i(8-i)\delta) / \sum_{i=5}^{8} M_i\} / (\Delta + \frac{3\delta}{2})$	15-5
$K'_{lw} = K''_{lw} (1 - K_{2w} \tan \theta_s)$	15-4
$C_g = f_{15,1} (W_f)$	
$C_{gf} = f_{14,1} (W_f)$	
$T_f = \frac{W_f F \eta}{C_{gf} W_g} + T_f^o$	14-1

TABLE A.1-4
SUPERHEAT FURNACE (Continued)

RESOLVED EQUATIONS	REFERENCE 10 DEFINING EQUATIONS
$V_{gs} = \frac{4}{3}\left[\frac{T_f C_g W_g}{10^3 K'_{1w}} + T^4_{mws}\right]$	(10^3 is conversion factor from KBTU → BTU)
$V_{rs} = \frac{1}{2}\left[\frac{C_g W_g}{10^3 K'_{1w}}\right]^2$	
$U_{s1} = [V^3_{gs} + V^2_{rs}]^{1/2}$	
$U_s = [V_{rs}+U_{s1}]^{1/3}-[U_{s1}-V_{rs}]^{1/3}$	
$T_{gas} = -\frac{1}{2} U_s^{1/2} +$	15-3, 15-6
$\frac{1}{2}[U_s-4(\frac{U_s}{2}-(U_s^2+3V_{gs})^{1/2}/2))]^{1/2}$	
$Q_{rws} = C_g W_g (T_f - T_{gas})/10^3$	15-6
$T_{gs} = 2\,T_{gas} - T_f$	15-7
$\frac{d}{dt} T_{mws} = 2(Q_{rws}-Q_{ws})/(M_w C_{pm})$	15-1 (Assumes M_w constant)

TABLE A.1-5
REHEAT FURNACE

RESOLVED EQUATIONS	REFERENCE 10 DEFINING EQUATIONS
$K''_{1wr} =$ $K_{1wr}\{\Delta+(\sum_{i=1}^{4} M_i(4-i)\delta)/\sum_{i=1}^{4} M_i\}/(\Delta+\frac{3\delta}{2})$	15-5
$K'_{1wr} = K''_{1w}(1 - K_{2wr}\tan\theta_r)$	15-4
$V_{gr} = \frac{4}{3}\left[\frac{T_f C_g W_g}{10^3 K'_{1wr}} + T^4_{mws}\right]$	
$V_{rr} = \frac{1}{2}\left[\frac{C_g W_g}{10^3 K'_{1wr}}\right]^2$	

TABLE A.1-5
REHEAT FURNACE (Continued)

REFERENCE 10 RESOLVED EQUATIONS	DEFINING EQUATIONS
$U_{r1} = [V^3_{gr} + V_{rr}]^{1/2}$	
$U_r = [V_{rr}+U_{r1}]^{1/3}-[U_{r1}-V_{rr}]^{1/3}$	
$T_{gar} = -\frac{1}{2} U_r^{1/2} +$	15-3, 15-6
$\frac{1}{2}[U_r-4(\frac{U_r}{2}-(U_r^2+3V_{gr})^{1/2}/2))]^{1/2}$	
$Q_{rwr} = C_g W_g (T_f - T_{gar})/10^3$	15-6
$T_{gr} = 2\,T_{gar} - T_f$	15-7
$\frac{d}{dt} T_{mwr} = 2(Q_{rwr}-Q_{wr})/(M_w C_{pm})$	15-1

A.2 QUARTIC SOLUTION

Modeling of the pressure drop-steam flow equation is generally quite straightforward:

$$W^2 = \rho(P_2 - P_1)^2/f \qquad (A.2\text{-}1)$$

where

ρ = steam density

P_1, P_2 = conduit inlet and outlet pressures, respectively

f = conduit steam-flow friction coefficient

However, in the Cromby model, two instances occur in which f varies nonlinearly with flow according to

$$f = a_1 W^2 + a_2 W + a_3 \qquad (A.2\text{-}2)$$

The two flows in question are defined by Eqs. 5-1, 5-7, and Eqs. 7-1, 7-14 in Ref. 10 and represent steam flow out of the drum and steam flow out of the primary superheater, respectively. This appendix describes the solution algorithm used to solve Eqs. A.2-1 and A.2-2 for W analytically.

Manipulation of Eqs. A.2-1 and A.2-2 yields

$$a_1 W^4 + a_2 W^3 + a_3 W^2 - \rho(P_2 P_1)^2 = 0 \qquad (A.2\text{-}3)$$

The variable ρ is a state variable and is assumed known at any given time. The pressure variables P_1, P_2 are functions of state variables and are also known at any given time. Therefore, at any time t, let

$$\rho(P_2P_1)^2 = a_4 \qquad \text{(A.2-4)}$$

where a_4 is known at time t.

Thus, Eq. A.2-3 becomes

$$W^4 + a_s W^3 + b_s W^2 + c_s = 0 \qquad \text{(A.2-5)}$$

upon defining $a_s = a_2/a_1$, $b_s = a_3/a_1$, $c_s = a_4/a_1$. Using Eq. A.2-5, W is found according to

$$\alpha^2 = -\frac{4}{3}\left(\frac{a_s c_s}{a_1}\right)^2 b_s - \frac{1}{27}\left(\frac{a_s^2 b_s^3 c_s}{a_1}\right) + \frac{1}{4}\left(\frac{a_s^4 c_s^2}{a_1^2}\right) + \frac{32}{27}\left(\frac{b_s c_s}{a_1}\right)^2 + \frac{4}{27}\left(\frac{b_s^4 c_s}{a_1}\right) + \frac{64}{27}\left(\frac{c_s}{a_1}\right)^3 \qquad \text{(A.2-6)}$$

$$\beta = -\frac{4}{3}\left(\frac{b_s c_s}{a_1}\right) + \frac{1}{2}\left(\frac{a_s^2 c_s}{a_1}\right) - \left(\frac{h_s}{3}\right)^3 \qquad \text{(A.2-7)}$$

$$\gamma = (\alpha-\beta)^{1/3} + (-\alpha-\beta)^{1/3} \qquad \text{(A.2-8)}$$

$$\vartheta^2 = \left(\frac{a_s}{2}\right)^2 - \frac{2}{3} b_s + \gamma \qquad \text{(A.2-9)}$$

$$\varepsilon^2 = -\frac{4}{3} b_s + \frac{a_0 b_\varepsilon}{\vartheta} + \frac{1}{4}\left(\frac{a_s^2}{\vartheta}\right) + \frac{1}{2} a_s^2 - \gamma \qquad \text{(A.2-10)}$$

$$\phi = \frac{a_s}{4} + \frac{\varepsilon-\vartheta}{2} \qquad \text{(A.2-11)}$$

$$W = \phi \ \text{sgn}\ (P_2-P_1) \qquad \text{(A.2-12)}$$

APPENDIX B
MODEL SYMBOL DEFINITIONS

This appendix defines the nomenclature and symbols used in developing the power plant model. The table is adapted from Ref. 26.

TABLE B-1
MODEL NOMENCLATURE

SYMBOL	DESCRIPTION
A	Governing valve area
A_f	Normalized feedwater valve flow area
A_r	Intercept of defining equation for reheater section heat transfer
A_{ss}	Intercept of defining equation for secondary superheater section heat transfer
A_T	Regulating valve area
C	Flow coefficient for sonic flow through valve-nozzle combination
C_1	Flow coefficient for parallel combination of K fully open governing valves and nozzles
C_2	Flow coefficient for series combination of regulating valve and nozzle
C_g	Specific heat of combustion products at average flame furnace temperature (Btu/lb°R)
C_{gf}	Specific heat of combustion products at average flame temperature (Btu/lb°R)
C_{gps}	Specific heat of combustion products at average primary superheater section temperature (Btu/lb°R)
C_{gs},C_{gr}	Specific heat of combustion products at average secondary superheat and reheat section temperature respectively (Btu/lb°R)
C_{pm}	Specific heat of metal in waterwalls (Btu/lb°R)
C_T	Flow coefficient for a regulating valve
f_{ps}	Friction coefficient for steam flow in primary superheater
f_r	Friction coefficient for steam flow in reheater
f_{ss}	Friction coefficient for steam flow in secondary superheater
F	Heating value of coal (Btu/lb)
H_{cr}	Steam enthalpy at discharge of high pressure turbine (Btu/lb)
h^*_{cr}	Ideal steam enthalpy at discharge of high pressure turbine (Btu/lb)

TABLE B-1
MODEL NOMENCLATURE (Continued)

SYMBOL	DESCRIPTION
h_D	Enthalpy of feedwater in downcomer (Btu/lb)
h_d	Enthalpy of saturated steam leaving drum (Btu/lb)
h_{dw}	Enthalpy of drum water (Btu/lb)
h_e	Enthalpy of feedwater leaving economizer (Btu/lb)
h_{hp}	Steam enthalpy in the impulse chamber (Btu/lb)
h^*_{hp}	Ideal steam enthalpy in the impulse chamber (Btu/lb)
h^*_{hp1}	Ideal steam enthalpy entering impulse blading after a regulating valve (Btu/lb)
h^*_{hp2}	Ideal steam enthalpy entering impulse blading (Btu/lb)
h_{pso}	Enthalpy of steam leaving primary superheater (Btu/lb)
$\bar{h}_r$	Average (mid-section) steam enthalpy in reheater (Btu/lb)
h_{ro}	Enthalpy of steam leaving reheater (Btu/lb)
h_{rse}	Enthalpy of steam at outlet from reheat spray (Btu/lb)
$\bar{h}_{ss}$	Average (mid-section) steam enthalpy in secondary superheater (Btu/lb)
h_{sse}	Steam enthalpy at outlet of superheater spray section (Btu/lb)
h_{sso}	Steam enthalpy at outlet of secondary superheater (Btu/lb)
h_{th}	Steam enthalpy after governing valves (equal to h_{sso})(Btu/lb)
h_w	Enthalpy of water-steam mixture leaving waterwalls (Btu/lb)
k	Ratio of specific heats (at constant pressure/at constant volume)
K	Number of fully open governing valves
K_{cf}	Proportionality constant between coal flow rate out of crusher and mass of crushed coal stored
K_f	Flow coefficient for feedwater valve
K_{fs}	Proportionality constant between coal flow into mill and feeder stroke
K_{hp}	Flow coefficient for reaction stages of high pressure turbine

TABLE B-1

MODEL NOMENCLATURE (Continued)

SYMBOL	DESCRIPTION
K	Flow coefficient for low pressure turbine
K_{ps}	Primary superheater heat transfer coefficient on steam side
K_r	Slope of defining equation for reheater section heat transfer
K_{rps}	Primary superheater heat transfer coefficient on gas side
K_{ss}	Slope of defining equation for secondary superheater section heat transfer
K_{wfs}	Proportionality constant between primary air flow and feeder stroke
K_w, K_{wr}	Heat transfer coefficient between tube metal and steam in superheat and reheat furnace waterwalls respectively
K_{1w}, K_{1wr}	Basic heat transfer coefficient between gas and tube metal in superheat and reheat furnace waterwalls respectively
K'_{1w}, K'_{1wr}	Overall heat transfer coefficient between gas and tube metal in superheat and reheat furnace waterwalls respectively
K''_{1w}, K''_{1wr}	Same as K_{1w}, K_{1wr} except including effect of burner geometry
K_{2w}, K_{2wr}	Coefficient relating a change in superheat or reheat burner tilts respectively on waterwall heat transfer
ℓ_{fs}	Normalized feeder stroke
M_{cr}	Mass of coal in crusher zone of mill (lb)
M_{ps}	Effective steam mass (related to actual steam and metal masses) in primary superheater (Klb)
M_r	Effective steam mass (related to actual steam and metal masses) in reheater (Klb)
M_{ss}	Effective steam mass (related to actual steam and metal masses) in secondary superheater (Klb)
M_w	Total effective metal mass of waterwall tubes (Klb)
MW_h, MW_l, MW_t	Equivalent megawatt output of high pressure turbine, low pressure turbine, and the total respectively (MW)
M_1^2	Square of the nozzle exit Mach number for regulating valve
M_2^2	Square of the nozzle exit Mach number for fully open governing valve
n	Number of partially opened valves (regulating valves)

TABLE B-1

MODEL NOMENCLATURE (Continued)

SYMBOL	DESCRIPTION
P_{cr}	Steam pressure at discharge of high pressure turbine (psia)
P_d	Drum pressure (psia)
P_e	Nozzle exit pressure (psia)
P_h	Boiler feed pump discharge pressure (psia)
P_{ho}	Intercept of defining equation for boiler feed pump discharge pressure (psia)
P_{hp}	Steam pressure at exit of throttle valve (1st stage pressure) (psia)
P_{pso}	Steam pressure at outlet of primary superheater (psia)
P_{ro}	Steam pressure at reheater outlet (psia)
P_{sso}	Steam pressure at outlet of secondary superheater (psia)
P_{th}	Governing valve exit pressure (psia)
Q_{ps}	Heat transfer rate from gas to steam in primary superheater (KBtu/sec)
Q_r	Heat transfer rate from gas to steam in reheater (KBtu/sec)
Q_{rws}, Q_{rwr}	Rate of heat transfer from gas to metal in superheat and reheat waterwalls respectively (KBtu/sec)
Q_{ss}	Heat transfer rate from gas to steam in secondary superheater (KBtu/sec)
Q_w	Total rate of heat transfer from tubes to fluid in waterwall section (KBtu/sec)
Q_{ws}, Q_{wr}	Rate of heat transfer from metal to steam in superheat and reheat waterwalls respectively (KBtu/sec)
T_{cr}	Steam temperature of steam at discharge of high pressure turbine (cold reheat)(°R)
T^*_{cr}	Ideal steam temperature at discharge of high pressure turbine (°R)
T_d	Drum steam temperature (°R)
T_e	Nozzle exit temperature (°R)
T_f	Adiabatic flow temperature (°R)
T^o_f	Air heater outlet temperature (°R)
T_{gas}, T_{gar}	Mid-section gas temperature of the waterwall section of the superheat and reheat furnace respectively (°R)
$\bar{T}_{gps}$	Average gas temperature in primary superheater (°R)
T_{gs}, T_{gr}	Superheat and reheat furnace exit gas temperature respectively (°R)

TABLE B-1

MODEL NOMENCLATURE (Continued)

SYMBOL	DESCRIPTION
T_{hp}	Impulse chamber (1st stage) temperature (°R)
T_{mws}, T_{mwr}	Metal temperature of superheat and reheat furnace waterwall tubes respectively (°R)
$\bar{T}_{ps}$	Average steam temperature in primary superheater (°R)
T_{pso}	Steam temperature at primary superheater outlet (°R)
T_{ro}	Steam temperature at reheater outlet (°R)
T_{sso}	Steam temperature at outlet of secondary superheater (discharge of throttle valve)(°R)
T_{th}	Governing valve exit temperature (°R)
V	Mill volume (ft^3)
V_d	Total drum volume (ft^3)
V_{dw}	Drum water volume (ft^3)
V_{ps}	Steam storage volume of primary superheater (Kft^3)
V_r	Steam storage volume of reheater (Kft^3)
V_{ss}	Steam storage volume of secondary superheater (Kft^3)
V_{1s}, V_{2s}	Ideal nozzle discharge velocity for the regulating valves and fully opened valves respectively (ft/sec)
W	Steam flow through K fully open governing valves (Klb/sec)
W'	Steam flow through n regulating valves (Klb/sec)
W_a	Mass rate of air flow through boiler (lb/sec)
W_{ao}	Primary air flow with zero coal flow (lb/sec)
W_{ep}	Water flow through feedwater valve (Klb/sec)
W_D	Constant boiler circulating flow (Klb/sec)
W_d	Steam flow rate leaving drum (Klb/sec)
W_e	Feedwater flow rate to boiler (Klb/sec)
W_f	Mass rate of coal flow to boiler (lb/sec)
W_g	Mass rate of gas flow through boiler (lb/sec)
W_{pao}	Primary air flow through mills (lb/sec)
W_{pso}	Primary superheater outlet steam flow rate (Klb/sec)

TABLE B-1

MODEL NOMENCLATURE (Continued)

SYMBOL	DESCRIPTION
W_{ro}	Reheater outlet steam flow rate (Klb/sec)
W_{rs}	Reheater spray water flow (Klb/sec)
W_{rse}	Steam flow rate at outlet from reheat spray section (Klb/sec)
W_{rsi}	Steam flow from high pressure turbine (Klb/sec)
W_{spa}	Superheater spray water flow rate (Klb/sec)
W_{ssi}	Steam flow rate at inlet to secondary superheater (Klb/sec)
W_{sso}	Steam flow rate at outlet of secondary superheater (Klb/sec)
X	Steam quality at outlet of waterwalls
α_{h_d}	Partial derivative of drum steam enthalpy with respect to drum steam density defined at saturation conditions
$\alpha_{h_{dw}}$	Partial derivative of drum water enthalpy with respect to drum steam density defined at saturation conditions
$\alpha_{\rho_{dw}}$	Partial derivative of drum water density with respect to drum steam density at saturation conditions
Δ	Flow coefficient for a single fully open governing valve and nozzle
Δ'	Flow coefficient for a nozzle for subsonic velocities
η	Combustion efficiency
η_l	Low pressure turbine isentropic efficiency
η_h	High pressure turbine isentropic efficiency (reaction blading)
η_{IMP1}, η_{IMP2}	Impulse turbine efficiency for the regulating valves and for the fully opened valves respectively
θ_s, θ_r	Angle with respect to horizontal of superheat and reheat burner tilts respectively (degrees)
λ	Slope of defining equation for boiler feed pump discharge pressure
v_{cf}	Fraction of total mill volume occupied by coal
ρ_a	Density of primary air (lb/ft^3)
ρ_{cf}	Density of coal (lb/ft^3)
ρ_d	Drum steam density (lb/ft^3)
ρ_{dw}	Drum water density (lb/ft^3)

TABLE B-1

MODEL NOMENCLATURE (Continued)

SYMBOL	DESCRIPTION
ρ_{pso}	Steam density at primary superheater outlet (lb/ft^3)
ρ_r	Average steam density in reheater (lb/ft^3)
ρ_{ss}	Average steam density in secondary superheater (lb/ft^3)
ρ_{th}	Steam density at valve exit (lb/ft^3)

APPENDIX C

COMMAND GENERATOR TRACKER SOLUTIONS TO INPUT AND STATE IDEAL TRAJECTORIES

C.1 CONTINUOUS-TIME *-TRAJECTORIES

This appendix presents derivations of the time-domain expressions of the *-trajectories associated with the command generator tracker (CGT). The *-trajectories $\underline{x}_p^*(t)$ and $\underline{u}_{p1}^*(t)$ must satisfy Eqs. 3.1-1a and 3.1-1b which are repeated here.

$$C_p \underline{x}_p^*(t) = \underline{y}_m(t) \tag{C.1-1a}$$

and

$$\dot{\underline{x}}_p^*(t) = A_p \underline{x}_p^*(t) + B_{p1}\underline{u}_{p1}^*(t) + B_{p2}\underline{u}_{p2}(t) \tag{C.1-1b}$$

A frequency- or s-domain representation of $\underline{x}_p^*$ and $\underline{u}_{p1}^*$ is defined in Ref. 22 as

$$\underline{x}_p^* = S_{11}\,\underline{x}_m + (I_n - s\Omega_{11})^{-1}(S_{12}\,\underline{u}_m + S_{13}\,\underline{u}_{p2}) \tag{C.1-2a}$$

$$\underline{u}_{p1}^* = S_{21}\,\underline{x}_m + S_{22}\,\underline{u}_m + S_{23}\,\underline{u}_{p2} + s\Omega_{21}(I_n - s\Omega_{11})^{-1}(S_{12}\,\underline{u}_m + S_{13}\,\underline{u}_{p2}) \tag{C.1-2b}$$

where the S matrices satisfy

$$\begin{bmatrix} A_p & B_{p1} \\ C_p & 0 \end{bmatrix} \begin{bmatrix} S_{11} & S_{12} & S_{13} \\ S_{21} & S_{22} & S_{23} \end{bmatrix} = \begin{bmatrix} S_{11}A_m & S_{11}B_m & -B_{p2} \\ C_m & 0 & 0 \end{bmatrix} \tag{C.1-3a}$$

and the Ω matrices satisfy

$$\begin{bmatrix} A_p & B_{p1} \\ C_p & 0 \end{bmatrix} \begin{bmatrix} \Omega_{11} & \Omega_{12} \\ \Omega_{21} & \Omega_{22} \end{bmatrix} = \begin{bmatrix} I_n & 0 \\ 0 & I_\ell \end{bmatrix} \tag{C.1-3b}$$

Equation C.1-3a has a solution if none of the plant transmission zeros are equal either to zero, or to any of the reference model poles (Ref. 22). Equation C.1-3b has a solution if none of the plant transmission zeros are equal to zero (Ref. 23).

In order to achieve the results described in Section 3.1, it is necessary to obtain time-domain solutions for $\underline{x}_p^*(t)$ and $\underline{u}_{p1}^*(t)$. Before transforming Eqs. C.1-2a and C.1-2b into the time-domain, a simplifying substitution will be made. Note the following equality

$$\begin{aligned}(I_n - s\Omega_{11})^{-1} &= [(I_n - s\Omega_{11})^{-1} - I_n] + I_n \\ &= [I_n - (I_n - s\Omega_{11})](I_n - s\Omega_{11})^{-1} + I_n \\ &= s\Omega_{11}(I_n - s\Omega_{11})^{-1} + I_n\end{aligned} \tag{C.1-4}$$

Introducing Eq. C.1-4 into Eq. C.1-2a yields

$$\underline{x}_p^* = S_{11}\,\underline{x}_m + [s\Omega_{11}(I_n - s\Omega_{11})^{-1} + I_n] \cdot [S_{12}\,\underline{u}_m + S_{13}\,\underline{u}_{p2}] \tag{C.1-5}$$

Thus, Eqs. C.1-2a and C.1-2b become

$$\underline{x}_p^* = S_{11}\,\underline{x}_m + S_{12}\,\underline{u}_m + S_{13}\,\underline{u}_{p2} + s\Omega_{11}(I_n - s\Omega_{11})^{-1}(S_{12}\,\underline{u}_m + S_{13}\,\underline{u}_{p2}) \tag{C.1-6a}$$

$$\underline{u}_{p1}^* = S_{21}\,\underline{x}_m + S_{22}\,\underline{u}_m + S_{23}\,\underline{u}_{p2} + s\Omega_{21}(I_n - s\Omega_{11})^{-1}(S_{12}\,\underline{u}_m + S_{13}\,\underline{u}_{p2}) \tag{C.1-6b}$$

The *-trajectories are transformed into the time-domain by introducing the filter state $\underline{\theta}(t)$,

$$\underline{\theta}(t) - \Omega_{11}\,\dot{\underline{\theta}}(t) = S_{12}\,\underline{u}_m(t) + S_{13}\,\underline{u}_{p2}(t) \tag{C.1-7}$$

The initial condition of the filter state, $\underline{\theta}(0)$, is arbitrary as long as there exists a quantity, $\dot{\underline{\theta}}(0)$, satisfying Eq. C.1-7 for t=0. Since Ω_{11} is a singular matrix (for the plant described in Eq. 2.3-2), the implementation of this filter is a nontrivial problem (see Ref. 4). Since this analysis leads to a MRC solution that does not require this filter (see Section 3.1), the issue of implementation is not discussed here; however, an implementation does exist.

Transforming Eqs. C.1-6 into the time-domain and substituting Eq. C.1-7, we obtain

$$\underline{x}_p^*(t) = S_{11}\,\underline{x}_m(t) + S_{12}\,\underline{u}_m(t) + S_{13}\,\underline{u}_{p2}(t) + \Omega_{11}\,\dot{\underline{\theta}}(t) \tag{C.1-8a}$$

$$\underline{x}_p^*(0) = S_{11}\,\underline{x}_m(0) + \underline{\theta}(0)$$

$$\underline{u}_{p1}^*(t) = S_{21}\,\underline{x}_m(t) + S_{22}\,\underline{u}_m(t) + S_{23}\,\underline{u}_{p2}(t) + \Omega_{21}\,\dot{\underline{\theta}}(t) \tag{C.1-8b}$$

$$\underline{\theta}(t) - \Omega_{11}\,\dot{\underline{\theta}}(t) = S_{12}\,\underline{u}_m(t) + S_{13}\,\underline{u}_{p2}(t) \tag{C.1-8c}$$

This is the result used in Section 4.1.

C.2 DISCRETE-TIME *-TRAJECTORIES

This section of Appendix C presents a verification that the discrete-time-domain expressions of the *-trajectories satisfy the necessary equations. These equations are repeated here

$$C_p \underline{x}_p^*(k) = \underline{y}_m(k) \quad \text{(C.2-1a)}$$

$$\underline{x}_p^*(k+1) = F_p \underline{x}_p^*(k) + G_{p1} \underline{u}_{p1}^*(k) + G_{p2} \underline{u}_{p2}(k) \quad \text{(C.2-1b)}$$

Note the model dynamics are given by Eq. 3.3-4, that is

$$\underline{x}_m(k+1) = F_m \underline{x}_m(k) + G_m \underline{u}_m(k) \quad \text{(C.2-2a)}$$

$$\underline{y}_m(k) = C_m \underline{x}_m(k) \quad \text{(C.2-2b)}$$

The hypothesized formulation of $\underline{x}_p^*(k)$ and $\underline{u}_p^*(k)$ is

$$\underline{x}_p^*(k) = R_{11} \underline{x}_m(k) + R_{12} \underline{u}_m(k) + R_{13} \underline{u}_{p2}(k) + \Lambda_{11} [\underline{\theta}(k+1) - \underline{\theta}(k)] \quad \text{(C.2-3a)}$$

$$\underline{u}_{p1}^*(k) = R_{21} \underline{x}_m(k) + R_{22} \underline{u}_m(k) + R_{23} \underline{u}_{p2}(k) + \Lambda_{21} [\underline{\theta}(k+1) - \underline{\theta}(k)] \quad \text{(C.2-3b)}$$

where the R-matrices satisfy

$$\begin{bmatrix} F_p - I_n & G_{p1} \\ C_p & 0 \end{bmatrix} \begin{bmatrix} R_{11} & R_{12} & R_{13} \\ R_{21} & R_{22} & R_{23} \end{bmatrix} = \begin{bmatrix} R_{11}(F_m - I_{n_m}) & R_{11} G_m & -G_{p2} \\ C_m & 0 & 0 \end{bmatrix} \quad \text{(C.2-4)}$$

the Λ-matrices satisfy

$$\begin{bmatrix} F_p - I_n & G_{p1} \\ C_p & 0 \end{bmatrix} \begin{bmatrix} \Lambda_{11} & \Lambda_{12} \\ \Lambda_{21} & \Lambda_{22} \end{bmatrix} = \begin{bmatrix} I_n & 0 \\ 0 & I_\ell \end{bmatrix} \quad \text{(C.2-5)}$$

and $\underline{\theta}(k)$ satisfies

$$\underline{\theta}(k) - \Lambda_{11}[\underline{\theta}(k+1) - \underline{\theta}(k)] = R_{12} \underline{u}_m(k) + R_{13} \underline{u}_{p2}(k) \quad \text{(C.2-6)}$$

with arbitrary initial condition $\underline{\theta}(0)$. Note $\underline{\theta}(1)$ must exist such that Eq. C.2-6 is satisfied for $k=0$.

To verify that Eq. C.2-3 satisfies Eq. C.2-1 the former is substituted into the right hand side of Eq. C.2-1b

$$\begin{aligned} \text{RHS} &\triangleq F_p \underline{x}_p^*(k) + G_{p1} \underline{u}_{p1}^*(k) + G_{p2} \underline{u}_{p2}(k) \\ &= F_p(R_{11} \underline{x}_m(k) + R_{12} \underline{u}_m(k) + R_{13} \underline{u}_{p2}(k) \\ &\quad + \Lambda_{11} [\underline{\theta}(k+1) - \underline{\theta}(k)]) + G_{p1}(R_{21} \underline{x}_m(k) \\ &\quad + R_{23} \underline{u}_{p2}(k) + R_{22} \underline{u}_m(k) + \Lambda_{21} [\underline{\theta}(k+1) - \underline{\theta}(k)]) \end{aligned} \quad \text{(C.2-7)}$$

Grouping like terms

$$\begin{aligned} \text{RHS} &= (F_p R_{11} + G_{p1} R_{21}) \underline{x}_m(k) \\ &\quad + (F_p R_{12} + G_{p1} R_{22}) \underline{u}_m(k) \\ &\quad + (F_p R_{13} + G_{p1} R_{23} + G_{p2}) \underline{u}_{p2}(k) \\ &\quad + (F_p \Lambda_{11} + G_{p1} \Lambda_{21}) [\underline{\theta}(k+1) - \underline{\theta}(k)] \end{aligned} \quad \text{(C.2-8)}$$

Using Eq. C.2-4 and Eq. C.2-5

$$\text{RHS} = R_{11} F_m \underline{x}_m(k) + R_{11} G_m \underline{u}_m(k) + R_{12} \underline{u}_m(k) + R_{13} \underline{u}_{p2}(k) + (I_n + \Lambda_{11}) [\underline{\theta}(k+1) - \underline{\theta}(k)] \quad \text{(C.2-9)}$$

Substituting for $R_{12} \underline{u}_m(k) + R_{13} \underline{u}_{p2}(k)$ from Eq. C.2-6 yields

$$\text{RHS} = R_{11} \underline{x}_m(k+1) + \underline{\theta}(k+1) \quad \text{(C.2-10)}$$

Note that substituting Eq. C.2-6 into C.2-3a yields

$$\underline{x}_p^*(k) = R_{11} \underline{x}_m(k) + \underline{\theta}(k) \quad \text{(C.2-11)}$$

Hence, combining Eqs. C.2-10 and C.2-11 yields

$$\text{RHS} = \underline{x}_p^*(k+1) \quad \text{(C.2-12)}$$

which verifies Eq. C.2-1b.

To verify Eq. C.2-1a, note that

$$C_p \underline{x}_p^*(k) = C_p R_{11} \underline{x}_m(k) + C_p R_{12} \underline{u}_m(k) + C_p R_{13} \underline{u}_{p2}(k) + C_p \Lambda_{11} [\underline{\theta}(k+1) - \underline{\theta}(k)]$$

From Eq. C.2-4

$$C_p R_{11} = C_m \quad \text{(C.2-14a)}$$

$$C_p R_{12} = 0 \quad \text{(C.2-14b)}$$

$$C_p R_{13} = 0 \quad \text{(C.2-14c)}$$

and from Eq. C.2-5

$$C_p \Lambda_{11} = 0 \quad \text{(C.2-14d)}$$

Thus, substituting Eqs. C.2-14 into C.2-13 yields

$$C_p \underline{x}_p^*(k) = C_m \underline{x}_m(k) \quad \text{(C.2-15)}$$

or using Eq. C.2-2b

$$C_p \underline{x}_p^*(k) = \underline{y}_m(k) \quad \text{(C.2-16)}$$

and Eq. C.2-1a is verified.

APPENDIX D
DERIVATION OF FEEDBACK GAIN AND REFORMULATION OF FEEDFORWARD GAIN AND ERROR DYNAMICS

D.1 FUNDAMENTAL RELATIONSHIPS

In this appendix, it is shown that under mild sufficient conditions there exists a set of gains satisfying Eq. 3.1-17a (Eq. D.1-1),

$$(\bar{K}\,\Omega_{11} + \Omega_{21})\,\dot{\underline{\theta}}(t) = \underline{0} \qquad \text{(D.1-1)}$$

This result is proved by constructing a set of such gains. In Section D.2 a specific solution is constructed provided C_pB_{p1} is nonsingular, and in Section D.3 the same task is carried out if C_pB_{p1} is singular. Section D.4 provides a set of solutions for $\bar{K}$ satisfying Eq. D-1. In Section D.5, the feedforward gains $\bar{K}_x$, $\bar{K}_u$ and $\bar{K}_{u2}$ are reformulated and in Section D.6 the error dynamics are reformulated.

The following identities required in this appendix are derived from Eqs. 3.1-2d

$$\underline{\theta}(t) = \Omega_{11}\,\dot{\underline{\theta}}(t) + S_{12}\,\underline{u}_m(t) + S_{13}\,\underline{u}_{p2}(t) \qquad \text{(D.1-2)}$$

from Eq. 3.1-3b

$$A_p\,\Omega_{11} + B_{p1}\,\Omega_{21} = I_n \qquad \text{(D.1-3)}$$

$$C_p\,\Omega_{11} = 0 \qquad \text{(D.1-4)}$$

$$A_p\,\Omega_{12} + B_{p1}\,\Omega_{22} = 0 \qquad \text{(D.1-5)}$$

$$C_p\,\Omega_{12} = I_\ell \qquad \text{(D.1-6)}$$

and from Eq. 3.1-3a

$$A_pS_{11} + B_{p1}S_{21} = S_{11}A_m \qquad \text{(D.1-7)}$$

$$C_pS_{11} = C_m \qquad \text{(D.1-8)}$$

$$A_pS_{12} + B_{p1}S_{22} = S_{11}B_m \qquad \text{(D.1-9)}$$

$$C_pS_{12} = 0 \qquad \text{(D.1-10)}$$

$$A_pS_{13} + B_{p1}S_{23} = -B_{p2} \qquad \text{(D.1-11)}$$

$$C_pS_{13} = 0 \qquad \text{(D.1-12)}$$

D.2 C_pB_{p1} IS NONSINGULAR

If C_pB_{p1} is a nonsingular ($\ell\times\ell$) matrix then one choice for $\bar{K}$ is

$$\bar{K} = (C_pB_{p1})^{-1}\,C_pA_p \qquad \text{(D.2-1)}$$

To verify that Eq. D.1-1 is satisfied use Eq. D.1-7 to note that

$$\begin{aligned}\bar{K}\Omega_{11} + \Omega_{12} &= (C_pB_{p1})^{-1}\,C_pA_p\Omega_{11} + \Omega_{21}\\ &= (C_pB_{p1})^{-1}\,C_p(-B_{p1}\Omega_{21} + I) + \Omega_{21}\\ &= (C_pB_{p1})^{-1}\,C_p \qquad \text{(D.2-2)}\end{aligned}$$

Multiplying on both sides of Eq. D.2-2 by $\underline{\theta}(t)$ yields

$$(\bar{K}\Omega_{11} + \Omega_{21})\,\underline{\theta}(t) = (C_pB_{p1})^{-1}\,C_p\,\underline{\theta}(t)$$

and using Eqs. D.1-2, D.1-4, D.1-10, and D.1-12,

$$\begin{aligned}(\bar{K}\Omega_{11} + \Omega_{21})\,\underline{\theta}(t) &= (C_pB_{p1})^{-1}\,C_p[(\Omega_{11}\,\dot{\underline{\theta}}(t)\\ &\quad + S_{12}\,\underline{u}_m(t) + S_{13}\,\underline{u}_{p2}(t)]\\ &= (C_pB_{p1})^{-1}\,\underline{0}\\ &= \underline{0} \qquad \text{(D.2-3)}\end{aligned}$$

Differentiating Eq. D.2-3,

$$(\bar{K}\Omega_{11} + \Omega_{21})\,\dot{\underline{\theta}}(t) = \underline{0} \qquad \text{(D.2-4)}$$

which verifies Eq. D.1-1.

D.3 C_pB_{p1} IS SINGULAR

If C_pB_{p1} is a singular, a methodology presented in Ref. 27 for output decoupling can be used to construct $\bar{K}$. First define the rows of C_p as follows

$$C_p = \begin{bmatrix}\underline{c}_1^T\\ \underline{c}_2^T\\ .\\ .\\ .\\ \underline{c}_m^T\end{bmatrix} \qquad \text{(D.3-1)}$$

Now the indices $d_1, d_2 \ldots d_m$ are defined to be the smallest integers for which

$$\underline{c}_i^T\,A_p^{d_i}\,B_{p1} \neq \underline{0}^T \qquad \text{(D.3-2a)}$$

that is,

$$\underline{c}_i^T\,A_p^{j}\,B_{p1} = \underline{0}^T \qquad j < d_i \qquad \text{(D.3-2b)}$$

The partition of the controls into $\underline{u}_{p1}(t)$ and $\underline{u}_{p2}(t)$ must be made such that

$$\underline{c}_i^T\,A_p^{j}\,B_{p2} = \underline{0}^T \qquad \text{(D.3-3)}$$

The reference the model must be designed to satisfy

$$\underline{c}_{mi}^T\,A_m^{j}\,B_m = \underline{0}^T \qquad j < d_i \qquad \text{(D.3-4)}$$

where

$\underline{c}_{mi}^T$ is the i^{th} row of C_m, i.e.,

$$C_m = \begin{bmatrix} \underline{c}_{m1}^T \\ \underline{c}_{m2}^T \\ . \\ . \\ . \\ \underline{c}_{mm}^T \end{bmatrix} \qquad \text{(D.3-5)}$$

Next, the matrix J is defined using the indices d_i defined in Eq. D.3-2 and D.3-3;

$$J \equiv \begin{bmatrix} \underline{c}_1^T A_p^{d_1} \\ \underline{c}_2^T A_p^{d_2} \\ \vdots \\ \underline{c}_m^T A_p^{d_m} \end{bmatrix} \qquad \text{(D.3-6)}$$

Using J, two other matrices are now defined;

$$L \equiv JB_{p1} \qquad \text{(D.3-7)}$$

$$M \equiv JA_p \qquad \text{(D.3-8)}$$

If L is nonsingular, $\bar{K}$ is selected as

$$\bar{K} = L^{-1} M \qquad \text{(D.3-9)}$$

To verify that this choice of $\bar{K}$ satisfies Eq. D.1-1 note that

$$\bar{K}\Omega_{11} + \Omega_{21} = L^{-1} M\Omega_{11} + \Omega_{21}$$

$$= L^{-1} J A_p \Omega_{11} + \Omega_{21} \qquad \text{(D.3-10)}$$

But from Eq. D.1-3

$$\bar{K}\Omega_{11} + \Omega_{21} = L^{-1} J(I_n - B_p\Omega_{21}) + \Omega_{21}$$

$$= L^{-1} J - L^{-1} JB_p \Omega_{21} + \Omega_{21}$$

$$= L^{-1} J - \Omega_{21} + \Omega_{21}$$

$$= L^{-1} J \qquad \text{(D.3-11)}$$

Next, it will be verified that

$$J\,\dot{\underline{\theta}}(t) = \underline{0} \qquad \text{(D.3-12)}$$

which implies

$$L^{-1} J\,\dot{\underline{\theta}} = 0 \qquad \text{(D.3-13)}$$

Substitution of Eq. D.3-13 into Eq. D.3-11 verifies Eq. D.1-1.

In order to verify Eq. D.3-13, it is first shown that

$$\underline{c}_i^T A_p^{\ell}\,\underline{\theta}(t) = \underline{c}_i^T A_p^{\ell-1}\,\dot{\underline{\theta}}(t) \qquad \text{if } \ell \le d_i \qquad \text{(D.3-14)}$$

This result requires the following identity obtained from Eq. D.1-8, D.3-1 and D.3-5:

$$\underline{c}_i^T S_{11} = \underline{c}_{mi}^T \qquad \text{(D.3-15)}$$

Starting with the left side of Eq. D.3-14 and substituting Eq. D.1-2

$$\underline{c}_i^T A_p^{\ell}\,\underline{\theta}(t) = \underline{c}_i^T A_p^{\ell}\,[(\Omega_{11}\,\dot{\underline{\theta}}(t) + S_{12}\underline{u}_m(t) + S_{13}\,\underline{u}_{p2}(t)]$$

$$= \underline{c}_i^T A_p^{\ell-1}[(A_p\Omega_{11}\,\dot{\underline{\theta}}(t) + A_pS_{12}\,\underline{u}_m(t)) + A_pS_{13}\,\underline{u}_{p2}(t)] \qquad \text{(D.3-16)}$$

Substituting Eqs. D.1-3 and D.1-9 and D.1-11

$$\underline{c}_i^T A_p^{\ell}\,\underline{\theta}(t) = \underline{c}_i^T A_p^{\ell-1}[(I - B_{p1}\Omega_{21})\,\dot{\underline{\theta}}(t) + (S_{11}B_m - B_{p1}S_{22})\underline{u}_m(t) - (B_{p2} + B_{p1}S_{23})\,\underline{u}_{p2}(t)]$$

$$= \underline{c}_i^T A_p^{\ell-1}\,\dot{\underline{\theta}}(t) + \underline{c}_i^T A_p^{\ell-1} S_{11} B_m\,\underline{u}_m(t) - \underline{c}_i^T A_p^{\ell-1} B_{p1}[\Omega_{21}\,\dot{\underline{\theta}}(t) + S_{22}\,\underline{u}_m(t) + S_{23}\,\underline{u}_{p2}(t)] \qquad \text{(D.3-17)}$$

Since $\ell \le d_i$, Eqs. D.3-2 and D.3-3

$$\underline{c}_i^T A_p^{\ell-1} B_{p1} = 0^T \qquad \text{(D.3-18a)}$$

$$\underline{c}_i^T A_p^{\ell-1} B_{p2} = \underline{0}^T \qquad \text{(D.3-18b)}$$

Hence

$$\underline{c}_i^T A_p^{\ell}\,\underline{\theta}(t) = \underline{c}_i^T A_p^{\ell-1}\,\dot{\underline{\theta}}(t) + \underline{c}_i^T A_p^{\ell-1} S_{11} B_m\,\underline{u}_m(t) \qquad \text{(D.3-19)}$$

In order to show that the second term on the right hand side of Eq. D.3-19 is zero, the following equality is established:

$$\underline{c}_i^T A_p^{k} S_{11} A_m^{j} = \underline{c}_i^T A_p^{k-1} S_{11} A_m^{j+1} \qquad \text{if } k \le d_i \qquad \text{(D.3-20)}$$

Starting with the left hand side of Eq. D.3-20,

$$\underline{c}_i^T A_p^k S_{11} A_m^j = \underline{c}_i^T A_p^{k-1} (A_p S_{11})\, A_m^j \qquad \text{(D.3-21)}$$

From Eq. D.1-7

$$\underline{c}_i^T A_p^k\, S_{11}\, A_m^j = \underline{c}_i^T A_p^{k-1} (S_{11} A_m - B_{p1} S_{21})\, A_m^j$$

$$= \underline{c}_i^T A_p^{k-1} S_{11} A_m^{j+1} - \underline{c}_i^T A_p^{k-1} B_{p1} S_{21} A_m^j \qquad \text{(D.3-22)}$$

Since $k \leq d_i$, $\underline{c}_i^T A_p^{k-1} B_{p1} = \underline{0}^T$ and

$$\underline{c}_i^T A_p^k\, S_{11}\, A_m^j = \underline{c}_i^T A_p^{k-1} S_{11} A_m^{j+1} \qquad \text{(D.3-23)}$$

which proves the identity of Eq. D.3-20.

Repeated application of this identity yields

$$\underline{c}_i^T A_p^{\ell-1} S_{11} = \underline{c}_i^T A_p^{\ell-2} S_{11} A_m$$

$$= \underline{c}_i^T A_p^{\ell-3} S_{11} A_m^2$$

$$\vdots$$

$$= \underline{c}_i^T S_{11} A_m^{\ell-1} \qquad \text{(D.3-24)}$$

Substituting Eq. D.3-24 into Eq. D.3-19 produces

$$\underline{c}_i^T A_p\, \underline{\theta}(t) = \underline{c}_i^T A_p^{\ell-1}\, \dot{\underline{\theta}}(t) + \underline{c}_i^T S_{11} A_m^{\ell-1} B_{m-m} \underline{u}_m(t) \qquad \text{(D.3-25)}$$

and combining this result with Eq. D.3-15 yields

$$\underline{c}_i^T A_p^{\ell}\, \underline{\theta}(t) = \underline{c}_i^T A_p^{\ell-1}\, \dot{\underline{\theta}}(t) + \underline{c}_{mi}^T A_m^{\ell-1} B_{m-m} \underline{u}_m(t) \qquad \text{(D.3-26)}$$

Using Eq. D.3-4 eliminates the second term on the right hand side of Eq. D.3-26, reducing it to

$$\underline{c}_i^T A_p^{\ell}\, \underline{\theta}(t) = \underline{c}_i^T A_p^{\ell-1}\, \dot{\underline{\theta}}(t) \qquad \text{(D.3-27)}$$

and the identity of Eq. D.3-14 is verified.

From Eq. D.1-2 it is also true that

$$\underline{c}_i^T\, \underline{\theta}(t) = \underline{c}_i^T\, \Omega_{11}\, \dot{\underline{\theta}}(t) + \underline{c}_i^T\, S_{12}\, \underline{u}_m(t) + \underline{c}_i^T\, S_{13}\, \underline{u}_{p2}(t) \qquad \text{(D.3-28a)}$$

which using Eqs. D.1-4, D.1-10 and D.1-12 reduces to

$$\underline{c}_i^T\, \underline{\theta}(t) = 0 \qquad \text{(D.3-28b)}$$

Differentiating Eq. D.3-28b implies that

$$\underline{c}_i^T\, \dot{\underline{\theta}}(t) = 0 \qquad \text{(D.3-29)}$$

Substituting these results into the right hand side of Eq. D.3-27 with $\ell=1$ yields

$$\underline{c}_i^T\, A_p\, \underline{\theta}(t) = 0 \qquad \text{(D.3-30)}$$

and again differentiating,

$$\underline{c}_i^T\, A_p\, \dot{\underline{\theta}}(t) = 0 \qquad \text{(D.3-31)}$$

Through repetitive application of Eq. D.3-29 to D.3-31,

$$\underline{c}_i^T\, A_p^2\, \dot{\underline{\theta}}(t) = 0$$

$$\underline{c}_i^T\, A_p^3\, \dot{\underline{\theta}}(t) = 0$$

$$\vdots$$

$$\underline{c}_i^T\, A_p^j\, \dot{\underline{\theta}}(t) = 0 \quad j \leq d_i \qquad \text{(D.3-32)}$$

Hence with J being defined by Eq. D.3-6, Eq. D.3-32 implies each row of J times $\dot{\underline{\theta}}(t)$ equals zero. Hence

$$J\, \dot{\underline{\theta}}(t) = \underline{0} \qquad \text{(D.3-33)}$$

Multiplying both sides of D.3-11 by $\dot{\underline{\theta}}(t)$ and using Eq. D.3-33 verifies Eq. D.1-1, that is

$$(\bar{K}\Omega_{11} + \Omega_{21})\, \dot{\underline{\theta}}(t) = L^{-1}\, J\, \dot{\underline{\theta}}(t) = \underline{0} \qquad \text{(D.3-34)}$$

The three restrictions on the above theory are: the reference model must satisfy the structural constraint specification, Eq. D.3-4; the plant controls must be partitioned to satisfy Eq. D.3-3; and L defined in Eq. D.3-6 must be nonsingular. The first two restriction are similar to the relative order restriction in the single-input, single-output MRAC algorithms of Refs. 3 and 14. The first constraint is much weaker than the perfect model following constraint discussed in Ref. 12, and can be satisfied by a judicious choice of the reference model. The second restriction limits the use of this approach for MIMO systems. (Note that for single-input, single-output systems, i.e. $\ell=1$, L is a scalar and is always nonsingular.)

D.4 GENERAL SOLUTION

The selection of $\bar{K}$ as in Eq. D.3-9 satisfies the requirement in Eq. D.1-1. However, this value is not unique; in particular, there are a whole class of gains $\bar{K}$ defined by

$$\bar{K} = L^{-1}(M + QN) \qquad \text{(D.4-1)}$$

where N is the $n_d \times n$ matrix

$$N \equiv \begin{bmatrix} \underline{c}_1^T \\ \underline{c}_1^T A_p \\ \vdots \\ \underline{c}_1^T A_p^{d_1} \\ \underline{c}_2^T \\ \underline{c}_2^T A_p \\ \vdots \\ \underline{c}_2^T A_p^{d_2} \\ \vdots \\ \underline{c}_m^T \\ \underline{c}_m^T A_p \\ \vdots \\ \underline{c}_m^T A_p^{d_m} \end{bmatrix} \qquad (D.4\text{-}2)$$

and Q is any $m \times n_d$ matrix.

Note that

$$n_d = m + \sum_{i=1}^{m} d_i \qquad (D.4\text{-}3)$$

The number of degrees of freedom in the choice of $\bar{K}$ is equal to the number of linearly independent rows of N.

From Eqs. D.3-9 and D.3-27 it is known that

$$(L^{-1}M\Omega_{11} + \Omega_{21})\,\dot{\underline{\theta}} \equiv \underline{0} \qquad (D.4\text{-}4)$$

Thus to prove that $\bar{K}$ as defined in Eq. D.4-1 satisfies Eq. D.1-1, it need only be shown that

$$QN\Omega_{11}\,\dot{\underline{\theta}}(t) \equiv \underline{0} \qquad (D.4\text{-}5)$$

The i^{th} row of $N\Omega_{11}$ is $\underline{c}_i^T A_p^j \Omega_{11}$ where

$$\begin{aligned} &1 \le i \le m \\ &0 \le j \le d_i \end{aligned} \qquad (D.4\text{-}6)$$

If j=0 then using Eq. D.1-4

$$\underline{c}_i^T A_p^j \Omega_{11}\dot{\underline{\theta}}(t) = \underline{c}_i^T \Omega_{11}\,\dot{\underline{\theta}}(t) = 0 \qquad (D.4\text{-}7)$$

If $j \neq 0$, using Eq. D.1-3

$$\underline{c}_i^T A_p^j \Omega_{11} = \underline{c}_i^T A_p^{j-1} - \underline{c}_i^T A_p^{j-1} B_{p1}\,\Omega_{21} \qquad (D.4\text{-}8)$$

Substituting Eq. D.3-3 (note Eq. D.4-6)

$$\underline{c}_i^T A_p^j\,\Omega_{11} = \underline{c}_i^T A_p^{j-1} \qquad (D.4\text{-}9)$$

Using this result and Eq. D.3-32 yields

$$\underline{c}_i^T A_p^j\,\Omega_{11}\,\dot{\underline{\theta}}(t) = \underline{c}_i^T A_p^{j-1}\,\dot{\underline{\theta}}(t) \equiv 0 \qquad (D.4\text{-}10)$$

Hence each element of $N\Omega_{11}\dot{\underline{\theta}}(t)$ is identically zero and Eq. D.4-5 is satisfied.

D.5 FEEDFORWARD GAIN REFORMULATION

In Section 3.1, the MRC algorithm gains are defined to be (Eq. 3.1-16)

$$\bar{K}_x = S_{21} + \bar{K}S_{11} \qquad (D.5\text{-}1)$$

$$\bar{K}_u = S_{22} + \bar{K}S_{12} \qquad (D.5\text{-}2)$$

$$\bar{K}_{u2} = S_{23} + \bar{K}S_{13} \qquad (D.5\text{-}3)$$

In this section, these gains are reformulated such that they can be computed without first computing the S_{ij} matrices. In particular $\bar{K}_x$, $\bar{K}_u$ and $\bar{K}_{u2}$ are functions of L, Q, L_m, M_m, N_m and M_2 where L and Q are defined in Section D.3 and D.4 and L_m, M_m, N_m and M_2 are defined in an analogous fashion to L, M, and N as follows

$$L_m \equiv J_m B_m \qquad (D.5\text{-}4)$$

$$M_m = J_m A_m \qquad (D.5\text{-}5)$$

$$M_2 = JB_{p2} \qquad (D.5\text{-}6)$$

with

$$J_m \equiv \begin{bmatrix} \underline{c}_{m1}^T A_m^{d_1} \\ \underline{c}_{m2}^T A_m^{d_2} \\ \vdots \\ \underline{c}_{m\ell}^T A_m^{d_\ell} \end{bmatrix} \qquad (D.5\text{-}7)$$

and

$$N_m \equiv \begin{bmatrix} \underline{c}_{m1}^T \\ \underline{c}_{m1}^T A_m \\ \vdots \\ \underline{c}_{m1}^T A_m^{d_1} \\ \underline{c}_{m2}^T \\ \underline{c}_{m2}^T A_m \\ \vdots \\ \underline{c}_{m2}^T A_m \\ \vdots \\ \underline{c}_{m\ell}^T \\ \underline{c}_{m\ell}^T A_m \\ \vdots \\ \underline{c}_{m\ell}^T A_m^{d_\ell} \end{bmatrix} \qquad \text{(D.5-8)}$$

Equations D.5-1, D.5-2 and D.5-3 are now shown to be equivalent to

$$\bar{K}_x = L^{-1}(M_m + QN_m) \qquad \text{(D.5-9)}$$

$$\bar{K}_u = L^{-1} L_m \qquad \text{(D.5-10)}$$

$$\bar{K}_{u2} = -L^{-1}M_2 \qquad \text{(D.5-11)}$$

The first step necessary to verify Eqs. D.5-9, 10 and 11 is to show

$$JS_{11} = J_m \qquad \text{(D.5-12)}$$

$$NS_{11} = N_m \qquad \text{(D.5-13)}$$

$$NS_{12} = 0 \qquad \text{(D.5-14)}$$

$$NS_{13} = 0 \qquad \text{(D.5-15)}$$

The rows of N and J are given by $\underline{c}_i^T A_p^j$ where $j \leq d_i$. Hence

$$\underline{c}_i^T A_p^j S_{11} = \underline{c}_i^T A_p^{j-1} (A_p S_{11}) \qquad \text{(D.5-16)}$$

using Eq. D.1-7

$$\underline{c}_i^T A_p^j S_{11} = \underline{c}_i^T A_p^{j-1}(S_{11}A_m - B_{p1}S_{21}) \qquad \text{(D.5-17)}$$

Using Eqs. D.3-2 and D.3-24, Eq. D.5-17 becomes

$$\underline{c}_i^T A_p^j S_{11} = \underline{c}_i^T S_{11} A_m^j \qquad \text{(D.5-18)}$$

and finally using Eq. D.3-15

$$\underline{c}_i^T A_p^j S_{11} = \underline{c}_{mi}^T A_m^j \qquad \text{(D.5-19)}$$

Equation D.5-19 verifies that the rows of JS_{11} are equal to the corresponding rows of J_m and the rows of NS_{11} are equal to the corresponding rows of N_m. Hence Eqs. D.5-12 and D.5-13 are verified.

Applying the same operations on the rows of NS_{12} (use Eq. D.1-9 instead of D.1-7)

$$\begin{aligned} \underline{c}_i^T A_p^j S_{12} &= \underline{c}_i^T A_p^{j-1}(A_p S_{12}) \quad j \leq d_i \\ &= \underline{c}_i^T A_p^{j-1} (S_{11}B_m - B_{p1}S_{22}) \\ &= \underline{c}_i^T S_{11} A_m^{j-1} B_m \\ &= \underline{c}_{mi}^T A_m^{j-1} B_m \end{aligned} \qquad \text{(D.5-20)}$$

The reference model structure constraint Eq. D.3-4 states the right hand side of Eq. D.5-20 is zero; thus

$$\underline{c}_i^T A_p^j S_{12} = 0 \qquad \text{(D.5-21)}$$

which verifies Eq. D.5-14.

Applying the same sequence of equations on the rows of NS_{13} (use Eq. D.1-11)

$$\begin{aligned} \underline{c}_i^T A_p^j S_{13} &= \underline{c}_i^T A_p^{j-1}(A_p S_{13}) \\ &= \underline{c}_i^T A_p^{j-1}(-B_{p2} + B_{p1}S_{23}) \end{aligned} \qquad \text{(D.5-22)}$$

Next Eqs. D.3-2 and D.3-3 are used to show

$$\underline{c}_i^T A_p^j S_{13} = 0 \qquad \text{(D.5-23)}$$

which verifies Eq. D.5-15.

Using the definition of $\bar{K}$ (Eq. D.4-1), $\bar{K}_x$ (Eq. D.5-1) becomes

$$\begin{aligned} \bar{K}_x &= S_{21} + L^{-1}(M+QN)S_{11} \\ &= S_{21} + L^{-1}MS_{11} + L^{-1}QNS_{11} \end{aligned} \qquad \text{(D.5-24)}$$

Substituting Eqs. D.3-8 and D.5-13

$$\bar{K}_x = S_{21} + L^{-1}JA_pS_{11} + L^{-1}QN_m \qquad \text{(D.5-25)}$$

Furthermore substituting Eq. D.1-7

$$\bar{K}_x = S_{21} + L^{-1}J(S_{11}A_m - B_{p1}S_{21}) + L^{-1}QN_m \quad (D.5\text{-}26)$$

Next substitute Eqs. D.3-7 and D.5-12

$$\bar{K}_x = S_{21} + L^{-1}(J_mA_m - LS_{21}) + L^{-1}QN_m$$

Finally substituting the definition of M_m (Eq. D.5-5) and regrouping terms

$$\bar{K}_x = L^{-1}(M_m + QN_m) \quad (D.5\text{-}27)$$

verifying Eq. D.5-9

A similar sequence of substitutions can be applied to $\bar{K}_u$ (Eq. D.5-2) and $\bar{K}_{u2}$ (Eq. D.5-3). Using Eqs. D.4-1, D.3-8, D.5-14, D.1-9, D.5-12, D.3-7 and D.5-4

$$\begin{aligned}
\bar{K}_u &= S_{22} + L^{-1}(M+QN)S_{12} \\
&= S_{22} + L^{-1}(MS_{12} + QNS_{12}) \\
&= S_{22} + L^{-1}JA_pS_{12} \\
&= S_{22} + L^{-1}J(S_{11}B_m - B_{p1}S_{22}) \\
&= S_{22} + L^{-1}(J_mB_m - LS_{22}) \\
&= L^{-1}J_mB_m \\
&= L^{-1}L_m
\end{aligned}$$

verifies Eq. D.5-10

Using Eqs. D.4-1, D.3-8, D.5-15, D.1-11, D.5-6 and D.3-7

$$\begin{aligned}
\bar{K}_{u2} &= S_{23} + L^{-1}(M+QN)S_{13} \\
&= S_{23} + L^{-1}(MS_{13} + QNS_{13}) \\
&= S_{23} + L^{-1}JA_pS_{13} \\
&= S_{23} + L^{-1}J(-B_{p2} - B_{p1}S_{23}) \\
&= S_{23} - L^{-1}M_2 - L^{-1}LS_{23} \\
&= -L^{-1}M_2
\end{aligned}$$

verifies Eq. D.5-11. A result similar to this has recently been reported by Kawahta (Ref. 28)

D.6 TRANSFORMATION OF OUTPUT ERROR DYNAMICS

In Section 3.1, the error dynamics are shown to be governed by Eq. 4.3-1

$$\underline{e}_y(t) = C_p\underline{e}(t) \quad (D.6\text{-}1a)$$

$$\dot{\underline{e}}(t) = (A_p - B_{p1}\bar{K})\underline{e}(t) + B_{p1}[\underline{\bar{u}}_{p1}(t) - \underline{u}_{p1}(t)] + B_{p1}\bar{K}W_1\underline{e}_z(t) \quad (D.6\text{-}1b)$$

The selection of $\bar{K}$ as (Eq. D.4-1)

$$\bar{K} = L^{-1}(M+QN) \quad (D.6\text{-}2)$$

where L, M, N and Q are defined in Sections D.3 and D.4, causes Eqs. D.6-1 to be a nonminimal system. In particular, for each transmission zero there exists a eigenvalue equal to it and hence a corresponding mode which is unobservable in $\underline{e}_y$. In this section these dynamics are reformulated into a minimal and simplified format.

Before reformulating the error dynamics the matrices A_N, B_N and C_N are defined and identifies using these matrices are established. First A_N is a $n_d \times n_d$ matrix given by

$$A_N = \begin{bmatrix} A_{N1} & 0 & \cdots & 0 \\ 0 & A_{N2} & \cdots & 0 \\ \vdots & \vdots & & \vdots \\ 0 & 0 & \cdots & A_{N\ell} \end{bmatrix} \quad (D.6\text{-}3)$$

where A_{Ni} is a $d_i \times d_i$ matrix with ones on the superdiagonal and zeroes elsewhere

$$A_{Ni} = \begin{bmatrix} 0 & 1 & 0 & \cdots & 0 \\ 0 & 0 & 1 & \cdots & 0 \\ \vdots & & & & \vdots \\ 0 & 0 & 0 & \cdots & 1 \\ 0 & 0 & 0 & \cdots & 0 \end{bmatrix} \quad (D.6\text{-}4)$$

Next B_N is a $n_d \times \ell$ matrix defined by

$$B_N = \begin{bmatrix} \underline{b}_{N1} & 0 & \cdots & 0 \\ 0 & \underline{b}_{N2} & \cdots & 0 \\ \vdots & \vdots & & \vdots \\ 0 & 0 & \cdots & \underline{b}_{N\ell} \end{bmatrix} \quad (D.6\text{-}5)$$

where $\underline{b}_{Ni}$ is a $d_i \times 1$ vector of all zeroes except in the last element

$$\underline{b}_{Ni} = \begin{bmatrix} 0 \\ 0 \\ . \\ . \\ . \\ 1 \end{bmatrix} \qquad \text{(D.6-6)}$$

Finally C_N is a $\ell \times n_d$ matrix defined by

$$C_N = \begin{bmatrix} \underline{c}_{N1}^T & 0 & \cdots & 0 \\ 0 & \underline{c}_{N2}^T & \cdots & 0 \\ . & . & & . \\ . & . & & . \\ . & . & & . \\ 0 & 0 & \cdots & \underline{c}_{N\ell}^T \end{bmatrix} \qquad \text{(D.6-7)}$$

Where $\underline{c}_{ni}^T$ is a $1 \times d_i$ row vector of all zeroes except the first element

$$\underline{c}_{Ni}^T = [1 \quad 0 \quad \cdots \quad 0] \qquad \text{(D.6-8)}$$

Using these definitions and the definitions of N, J, L and M (Eqs. D.4-2, D.3-6, D.3-7 and D.3-8) along with the condition in Eq. D.3-2a the following identities are established

$$NA_p = A_N N + B_N M \qquad \text{(D.6-9)}$$

$$NB_{p1} = B_N L \qquad \text{(D.6-10)}$$

$$C_p = C_N N \qquad \text{(D.6-11)}$$

Using the definition of $\bar{K}$ in Eq. D.4-1 and these identities, the following equality is derived

$$\begin{aligned} N(A_p - B_{p1}\bar{K}) &= NA_p - NB_{p1}L^{-1}(M+QN) \\ &= A_N N + B_N M - B_N(M+QN) \\ &= (A_N - B_N Q)N \end{aligned} \qquad \text{(D.6-12)}$$

Next the transformed error $\underline{e}_N(t)$ is defined as

$$\underline{e}_N(t) = N\underline{e}(t) \qquad \text{(D.6-13)}$$

If Eq. D.6-1b is multiplied by N the result is

$$\begin{aligned} N\dot{\underline{e}}(t) &= N(A_p - B_{p1}\bar{K})\underline{e}(t) \\ &\quad + NB_{p1}[\bar{\underline{u}}_{p1}(t) - \underline{u}_{p1}(t)] \\ &\quad + NB_{p1}\bar{K}W_1\underline{e}_z(t) \end{aligned} \qquad \text{(D.6-14)}$$

Using Eqs. D.6-10, D.6-12 and D.6-13, Eq. D.6-14 is transformed into

$$\begin{aligned} \dot{\underline{e}}_N(t) &= (A_N - B_N Q)\underline{e}_N(t) \\ &\quad + B_N L[\bar{\underline{u}}_{p1}(t) - \underline{u}_{p1}(t)] \\ &\quad + B_N L\bar{K}W_1\underline{e}_z(t) \end{aligned} \qquad \text{(D.6-15)}$$

Using Eqs. D.6-11 and D.6-13 transforms Eq. D.6-1a into

$$\underline{e}_y(t) = C_N\underline{e}_N(t) \qquad \text{(D.6-16)}$$

Hence the output error dynamics described in Eqs. D.6-1 have been transformed into Eqs. D.6-15 and D.6-16. Each set of matrices A_{Ni}, $\underline{b}_{Ni}$, $\underline{C}_{Ni}^T$ represent a canonical system for the i^{th} output error. An appropriate choice for Q keeps these error dynamics decoupled.

D.7 SUMMARY

This appendix demonstrates that any $\bar{K}$ given by Eq. D.4-1 satisfies Eq. D.1-1 provided L (defined in Eq. D.3-7) is nonsingular. The degrees of freedom in the choice of $\bar{K}$ is a function of the linearly independent rows of N, Eq. D.4-2. The stability of $A_p - B_p\bar{K}$ is dependent on the stability of the transmission zeroes between $\underline{u}_{p1}$ and $\underline{y}_p$ and the choice of Q. The reformulation in Section D.6 eliminates the unobservable modes related to the transmission zeroes and provides a formulation from which a stable Q can be chosen, i.e., Q must stabilize $A_N - B_N Q$.

APPENDIX E

OTHER MRAC ALGORITHMS

In order that this report include all the efforts in this research project, Appendix E presents the MRAC algorithms developed earlier in this study and presented in an earlier report. The stability of these algorithms required complex constraints and are restricted to bounded error type stability. The algorithm presented in Chapter 4 has a more complex structure than these algorithms but the stability constraints are much easier to satisfy. However, the three algorithms presented before are repeated here for completeness.

The algorithms are based on a slightly different MRC solution. In particular no observer is used, hence, the $\underline{z}(t)$ terms in Eq. 3.1-6 are not used. Instead the matrix $\bar{K}_y$ is assumed to exist such that

$$\bar{K} = \bar{K}_y H_p \qquad (E\text{-}1)$$

Furthermore, $\bar{K}$ is assumed to satisfy Eq. E-1 and Eq. 3.1-17a. This condition may require the reference model control being fixed (which makes $\dot{\underline{\theta}}(t) = \underline{0}$). Also, the number of inputs and outputs are assumed to be the same ($m=\ell$).

E.1 CONTINUOUS ALGORITHM I

This section presents an adaptive algorithm for the continuous time control previously defined in Eq. 2.3-1 and a Lyapunov stability analysis of the closed loop system. The algorithm and the analysis are based on the work by Mabius in Ref. 6. However, introducing the MRC solution presented in Section 3.1 into the stability analysis demonstrates asymptotic stability of the output error to zero.

The control algorithm is

$$\underline{u}_p(t) = K_y(t)\underline{y}_s(t) + K_x(t)\underline{x}_m(t) + K_u(t)\underline{u}_m(t) \qquad (E.1\text{-}1)$$

As in Ref. 6, $\underline{r}(t)$, $K_r(t)$ and $\bar{K}_r$ are now defined to provide more compact notation for the adaptive controller, viz,

$$\underline{r}(t) \equiv \begin{bmatrix} \underline{y}_s(t) \\ \underline{x}_m(t) \\ \underline{u}_m(t) \end{bmatrix} \qquad (E.1\text{-}2a)$$

$$K_r(t) = [K_y(t),\ K_x(t),\ K_u(t)] \qquad (E.1\text{-}2b)$$

$$\bar{K}_r = [\bar{K}_y,\ \bar{K}_x,\ \bar{K}_u] \qquad (E.1\text{-}2c)$$

$K_r(t)$ represents a concatenation of the adaptive gains with these definitions

$$\bar{\underline{u}}_p(t) = \bar{K}_r\ \underline{r}(t) \qquad (E.1\text{-}3a)$$

$$\underline{u}_p(t) = K_r(t)\ \underline{r}(t) \qquad (E.1\text{-}3b)$$

The mechanism by which $K_r(t)$ is adapted is defined by

$$K_r(t) = K_p(t) + K_I(t) \qquad (E.1\text{-}4a)$$

$$K_p(t) = \underline{v}(t)\underline{r}^T(t)T_p \qquad (E.1\text{-}4b)$$

$$\dot{K}_I(t) = \underline{v}(t)\underline{r}^T(t)T_I \qquad (E.1\text{-}4c)$$

$$K_I(0) = K_{I_o} \qquad (E.1\text{-}4d)$$

$$\underline{v}(t) = Q_C(\underline{y}_m(t) - \underline{y}_p(t)) \qquad (E.1\text{-}4e)$$

where T_P is positive semidefinite, T_I is positive definite, Q_C is any nonsingular $m \times m$ matrix that satisfies a constraint described below and K_{I_o} is any initial guess at $K_r(t)$. Note that $K_p(t)$ is a proportional gain and $K_I(t)$ is an integral gain, and the choice of T_p and T_I affects the transient behavior of the adaptive algorithm. The adaptive algorithm is depicted in Fig. E.1-1. It is now shown that the this adaptive control system is asymptotically stable to zero using the Lyapunov approach of Ref. 6.

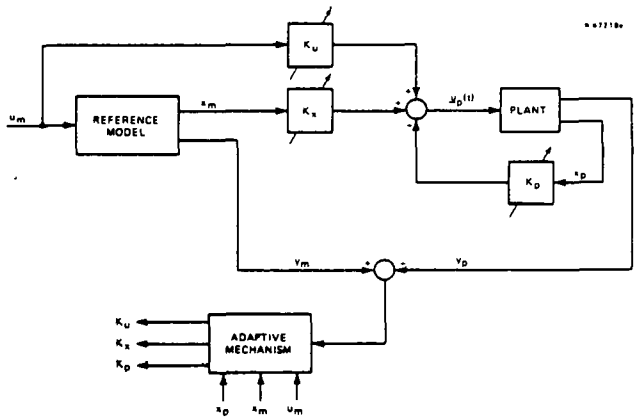

Figure E.1-1 Block Diagram of Continuous Algorithm I

The stability proof is based upon the dynamics of the error as it is defined in Eq. 3.1-23a, that is

$$\underline{e}(t) = \underline{x}_p^*(t) - \underline{x}_p(t) \qquad (E.1\text{-}5)$$

$$\dot{\underline{e}}(t) = (A_p - B_p\bar{K})\underline{e}(t) + B_p[\bar{\underline{u}}_p(t) - \underline{u}_p(t)] \qquad (E.1\text{-}6)$$

Into this error equation, we substitute the CGT controller, Eq. E.1-3a and the time-varying control law, Eq. E.1-3b resulting in

$$\dot{\underline{e}}(t) = (A_p - B_p\bar{K})\ \underline{e}(t) + B_p[\bar{K}_r - K_r(t)]\underline{r}(t) \qquad (E.1\text{-}7a)$$

Note that Eq. 4.1-13c is still invoked

$$C_p\underline{e}(t) = \underline{y}_m(t) - \underline{y}_p(t) \qquad (E.1\text{-}7b)$$

The Lyapunov function V, which is quadratic in the state variables of the adaptive controller, is defined by†

$$V = \underline{e}^T(t)P\underline{e}(t) + Tr[S_v(K_I(t) - \bar{K}_r)T_I^{-1}(K_I(t) - \bar{K}_r)^T S_v^T] \quad (E.1\text{-}8)$$

where S_v is any nonsingular m × m matrix and P is a positive definite symmetric matrix. The selection of these two matrices is related to the stability constraints to be discussed below.

It can be shown that if

$$S_v^T S_v Q_C C_p = B_p^T P \quad (E.1\text{-}9)$$

then

$$\dot{V} = \underline{e}^T(t)\,[P(A_p - B_p\bar{K}) + (A_p - B_p\bar{K})^T P]\,\underline{e}(t) - \underline{e}^T(t)\,C_p^T Q_C^T S_v^T S_v Q_C C_p \underline{e}(t)\,\underline{r}^T(t)\,T_p\underline{r}(t) \quad (E.1\text{-}10)$$

Analysis in Ref. 6 shows that if V is positive definite in $\underline{e}(t)$ and $\dot{V}$ is negative definite in $\underline{e}(t)$, then $\underline{e}(t)$ will approach zero asymptotically. By its definition, Eq. E.1-8, V is positive definite in $\underline{e}(t)$. If Q, defined as

$$P(A_p - B_p\bar{K}) + (A_p - B_p\bar{K})^T P = -Q \quad (E.1\text{-}11)$$

is positive definite then $\dot{V}$ is negative definite in e(t) and thus, the adaptive controller is stable. This constraint is the positive real constraint and is discussed in detail in Section E.4. Summarizing this stability analysis: if Eqs. E.1-9 and E.1-11 are satisfied and Q in Eq. E.1-11 is positive definite, the adaptive control law formulated in Eqs. E.1-1, E.1-2, E.1-3 and E.1-4 is asymptotically stable.

E.2 CONTINUOUS ALGORITHM II

This section presents a modified version of Continuous Algorithm I with a less restrictive stability constraint than Eqs. E.1-9 and E.1-11. The algorithm requires a nominal value of $\bar{\underline{u}}_p(t)$ and yields only a bounded output error. The bound depends on the accuracy of the nominal value.

Section E.2.1 presents the algorithm structure and the constraint for stability. The proof of stability appears in Section E.2.2 when $\bar{\underline{u}}_p(t)$ is known exactly, and an algorithmic anomaly in computing $\underline{u}_p(t)$ is resolved in Section E.2.3. Stability of the algorithm with only a nominal value of $\bar{\underline{u}}_p(t)$ is presented in Section E.2.4.

†Tr(A) refers to the trace of the matrix A which is the sum of the diagonal elements.

E.2.1 Algorithm Structure

Again the form of the adaptive rules for adjusting $K_p(t)$ and $K_I(t)$ is the same as given by Eq. E.1-4, except for the following modifications:

1) It is now assumed that $\underline{y}_p(t) = \underline{y}_s(t)$ i.e., that the measurement and controlled vector are the same (then $C_p = H_p$).

2) $$\underline{v}(t) = Q_M(\underline{y}_m(t) - \underline{y}_p(t)) + G[\bar{\underline{u}}_p(t) - \underline{u}_p(t)] \quad (E.2\text{-}1)$$

where G is any m × m matrix satisfying the constraint developed below and Q_M is a m × m positive definite matrix.

Note that the above adjustment algorithm directly implements the quantity $\bar{\underline{u}}_p(t)$, the computation of which is dependent upon some apriori knowledge of the process matrices A_p and B_p. Since in reality $\bar{\underline{u}}_p(t)$ would be unknown, a subsequent analysis shows that if $\bar{\underline{u}}_p(t)$ is replaced in Eq. E.2-1 by an approximation, the resulting errors can still be guaranteed to be within bounds.

As in the previous section, stability is established using the error dynamics in conjunction with a Lyapunov function. Recall the error dynamics defined by Eq. 3.1-23a,

$$\dot{\underline{e}}(t) = (A_p - B_pK)\,\underline{e}(t) + B_p\,[\bar{\underline{u}}_p(t) - \underline{u}_p(t)] = \tilde{A}_p\,\underline{e}(t) + B_p\,\underline{z}(t) \text{ where } \tilde{A}_p = A_p - B_p\bar{K} \quad (E.2\text{-}2a)$$

and

$$\underline{z}(t) = \bar{\underline{u}}_p(t) - \underline{u}_p(t) \quad (E.2\text{-}2b)$$

Introducing the control algorithm into the error equation and recalling from Eq. E.1-3a that $\bar{\underline{u}}_p(t) = \bar{K}_r\,\underline{r}(t)$

$$\dot{\underline{e}}(t) = \tilde{A}_p\,\underline{e}(t) - B_p[\bar{K}_r\,\underline{r}(t) - K_r(t)\,\underline{r}(t) - \underline{v}(t)\,\underline{r}^T(t)\,T_p\,\underline{r}(t)] \quad (E.2\text{-}3)$$

Asymptotic stability is proven in Section E.2.2, subject to the conditions:

$$J + C_p(sI - A_p + B_p\bar{K})^{-1}\,B_p \quad (E.2\text{-}4)$$

is strictly positive real and

$$Q_M^{-1}G > J$$

This constraint is not as severe as that in Eq. E.1-11, as will be discussed in Section E.5.

4.3.2 Stability Proof

The first step in the analysis is, as before, to form a quadratic function which is positive definite in the state variables of the adaptive system,

$\underline{e}(t)$ and $K_I(t)$. Assuming that T_I is a positive definite matrix, a valid Lyapunov candidate is:

$$V(\underline{e}, K_I) = \underline{e}^T(t)\, P\underline{e}(t) + Tr[S_M(K_I(t) - \bar{K}_r)T_I^{-1}\,(K_I(t) - \bar{K}_r)^T\, S_M^T] \qquad (E.2\text{-}5)$$

where

P is an n × n positive definite symmetric matrix

$\bar{K}_r$ is an m × n_r matrix

S_M is an m × m nonsingular matrix satisfying $S_M^T S_M = Q_M^{-1}$

The matrix $\bar{K}_r$ has the same dimensions, as $K_r(t)$ and can therefore be partitioned as $\bar{K}_r = [\bar{K}_y, \bar{K}_x, \bar{K}_u]$ so that

$$\bar{u}_p(t) = \bar{K}_r\underline{r}(t) = \bar{K}_y\, \underline{y}_s(t) + \bar{K}_u\, \underline{u}_m(t) + \bar{K}_x\, \underline{x}_m(t) \qquad (E.2\text{-}6)$$

The algorithm to be established is repeated here for convenience:

$$K_p = \underline{v}(t)\, \underline{r}^T(t)\, T_p \qquad (E.2\text{-}7a)$$

$$\dot{K}_I(t) = \underline{v}(t)\, \underline{r}^T(t)\, T_I \qquad (E.2\text{-}7b)$$

$$\underline{v}(t) = Q_M C_p\, \underline{e}(t) + G(\bar{\underline{u}}_p(t) - \underline{u}_p(t)) \qquad (E.2\text{-}7c)$$

As an aid to establishing conditions under which the derivative $\dot{V}$ is negative definite, the positive real lemma is introduced (Ref. 29):

Lemma: The transfer matrix $Z(s) = J + C(sI-A)^{-1}B$, having no poles with positive real parts, and only simple poles on the imaginary axis, is positive real if, and only if, there exists a real symmetric positive definite matrix P and real matrices L and W such that

$$PA + A^TP = -LL^T \qquad (E.2\text{-}8a)$$

$$PB = C^T - LW \qquad (E.2\text{-}8b)$$

$$W^TW = J + J^T \qquad (E.2\text{-}8c)$$

If in addition to Z(s) being positive real, it is also true that Z(s) has no poles on the imaginary axis, then Z(s) is strictly positive real and

$$PA + A^TP = -LL^T < 0 \qquad (E.2\text{-}9)$$

Assuming that the transfer matrix $Z(s) = J + C_p\,(sI-A_p+B_p\bar{K})^{-1}B_p$ is strictly positive real for some matrices $\bar{K}$ and J, and using E.2-8, it can be shown that $\dot{V}$ becomes:

$$\dot{V} = -[L^T\underline{e}(t) + W\underline{z}(t)]^T\, [L^T\underline{e}(t) + W\underline{z}(t)] - 2\, \underline{v}^T(t)\, S_M^TS_M\, \underline{v}(t)\, \underline{r}^T(t)\, T_p\underline{r}(t) - 2\, \underline{z}^T(t)\, (S_M^TS_M\, G - J)\underline{z}(t) \qquad (E.2\text{-}10)$$

Since L is nonsingular, $\dot{V}$ is negative definite in $\underline{e}(t)$ and $\underline{z}(t)$ provided that

$$G^T\, S_M^TS_M > J \qquad (E.2\text{-}11a)$$

and

$$T_p \geq 0 \qquad (E.2\text{-}11b)$$

From Eq. E.2-10 and Eq. E.2-11 we observe that $V(\underline{e}, K_I)$ cannot increase beyond its initial value $V(\underline{e}(t_0), K_I(t_0))$. Thus it follows that the adaptive gain matrix $K_I(t)$ is also bounded.

It is interesting to note that if the stabilized plant transfer matrix $Z(s) = C_p(sI - A_p + B_p\bar{K})^{-1}B_p$ is strictly positive real for some matrix $\bar{K}$, then from Eq. E.2-8 we may choose G=J=W=0. With this choice of matrices Eq. E.2-10 reduces to

$$\dot{V} = \underline{e}^T(t)[P(A_p - B_p\bar{K}) + (A_p - B_p\,\bar{K})^T\, P]\underline{e}(t) - 2\, \underline{e}^T(t)\, P\, B_p(S_M^TS_M)^{-1}\, B_p^T\, P\, \underline{e}(t)\, \underline{r}^T(t)\, T_p\, \underline{r}(t) \qquad (E.2\text{-}12)$$

which basically is the derivative of the Lyapunov function obtained for Continuous Algorithm I.

To summarize, the closed loop system which results from Algorithm II gives rise to an asymptotically stable error provided the following sufficient conditions are satisfied:

$$\underline{v}(t) = (S_M^TS_M)^{-1}\, C_p\, \underline{e}(t) + G[\bar{\underline{u}}_p(t) - \underline{u}_p(t)] \qquad (E.2\text{-}13a)$$

$$Z(s) = J + C_p(sI - A_p + B_p\bar{K})\, B_p \qquad (E.2\text{-}13b)$$

is strictly positive real for some matrices J and $\bar{K}$ with

$$G^T\, S_M^TS_M > J \qquad (E.2\text{-}13c)$$

Furthermore, $\bar{K}$ must satisfy Eq. 3.1-17a or $\underline{u}_m(t)$ is restricted to a constant and $\bar{K}$ must be such that Eqs. E-1 and 3.1-17b can be satisfied.

E.2.3 Computation of the Plant Control Law

In this section the problem involved in the implementation of the signal $\underline{v}(t)$ from Eq. E.2-13a

will be considered. Recall from Eqs. E.1-3b and E.1-4 that

$$\underline{u}_p(t) = [\underline{v}(t)\ \underline{r}^T(t)\ T_p + K_I(t)]\ \underline{r}(t) \qquad \text{(E.2-14)}$$

and from Eq. E.2-1

$$\underline{v}(t) = \underline{v}_1(t) - G\ \underline{u}_p(t) \qquad \text{(E.2-15)}$$

where

$$\underline{v}_1(t) = (S_M^T S_M)^{-1}\ C_p\ \underline{e}(t) + G[\bar{\underline{u}}_p(t) - \underline{u}_p(t)] \qquad \text{(E.2-16)}$$

We see from Eq. E.2-14 that $\underline{u}_p(t)$ is a function of $\underline{v}(t)$, while from Eq. E.2-15 we note that $\underline{v}(t)$ is a function of $\underline{u}_p(t)$. From Eqs. E.2-14 and E.2-15 we obtain

$$\underline{u}_p(t) = [\underline{v}_1(t) - G\ \underline{u}_p(t)]\ \underline{r}^T(t)\ T_p\ \underline{r}(t) + K_I(t)\ \underline{r}(t) \qquad \text{(E.2-17)}$$

or solving for $\underline{u}_p(t)$

$$\underline{u}_p(t) = [I + \underline{r}^T(t)\ T_p\ \underline{r}(t)\ G]^{-1}\ [K_I(t)\ \underline{r}(t) + \underline{v}_1(t)\ \underline{r}^T(t)\ T_p\ \underline{r}(t)] \qquad \text{(E.2-18)}$$

It should be noted that a unique solution of Eq. E.2-18 requires the nonsingularity of the matrix $[I + \underline{r}^T(t)\ T_p \underline{r}(t)\ G]$ for all t.

E.2.4 Effects of Approximating Ideal Plant Control

Computation of the control law using Eq. E.1-18 requires implementation of $\bar{\underline{u}}_p(t)$ as can be seen from Eq. E.2-16. This is not feasible because the gains used in the computation $\bar{\underline{u}}_p(t)$ are functions of the plant parameters Eq. 3.1-14. However, given a nominal set of plant parameters, it may be possible to find values of $\bar{K}_y$, $\bar{K}_x$ and $\bar{K}_u$ such that the nominal $\bar{\underline{u}}_p(t)$ is not too far from the true value. Thus, the control would be modified as follows:

$$\underline{v}(t) = (S_M^T S_M)^{-1}\ C_p\ \underline{e}(t) + G[\bar{\underline{u}}_{pnom}(t) - \underline{u}_p(t)]$$

$$= (S_M^T S_M)^{-1}\ C_p\ \underline{e}(t) + G[\bar{\underline{u}}_{pnom}(t) - \bar{\underline{u}}_p(t)] + G[\bar{\underline{u}}_p(t) - \underline{u}_p(t)] \qquad \text{(E.2-19)}$$

If we use the definition from Eq. E.2-2b that

$$\underline{z}(t) = \bar{\underline{u}}_p(t) - \underline{u}_p(t)$$

and define $\Delta\underline{u}(t) = \bar{\underline{u}}_{pnom}(t) - \bar{\underline{u}}_p(t)$, then Eq. E.2-19 reduces to

$$\underline{v}(t) = (S_M^T S_M)^{-1}\ C_p\ \underline{e}(t) + G[\Delta\underline{u}(t) + \underline{z}(t)] \qquad \text{(E.2-20)}$$

Using the modified control law with the original Lyapunov function (E.2-5) results in

$$\dot{V} = -[L^T\underline{e}(t) + W\underline{z}(t)]^T\ [L^T\underline{e}(t) + W\underline{z}(t)] - 2\ \underline{v}^T(t)\ S_M^T S_M\ \underline{v}(t)\ \underline{r}^T(t)\ T_p\ \underline{r}(t) - 2\ \underline{z}^T(t)\ (G^T\ S_M^T S_M - J)\underline{z}(t) - 2\ \Delta\underline{u}^T(t)\ G^T\ S_M^T S_M\ \underline{z}(t) \qquad \text{(E.2-21)}$$

Observe that $\dot{V}$ is the same as that given by Eq. E.2-10 except for one additional term which is linear in $\underline{z}(t)$. From a result due to LaSalle (Ref. 30), we can state that $\underline{e}(t)$ and $\underline{z}(t)$ are ultimately bounded. That is, there exists a $t_1 > 0$ with the property that $||\underline{e}(t)|| < b_1$ and $||\underline{z}(t)|| < b_2$ for all $t > t_1$.

The errors resulting from approximating the ideal control have been reduced in simulation examples by redefining the plant output to be a linear combination of the original output and its integral. That is,

$$\underline{y}_p(t) = \alpha_1\ C_p\ \underline{x}_p(t) + \alpha_2 \int_0^t C_p\ \underline{x}_p(t)\ dt \qquad \text{(E.2-22)}$$

where α_1 and α_2 are a constant scalars. Similarly, the reference model output is defined as

$$\underline{y}_m(t) = \alpha_1 C_m\ \underline{x}_m + \alpha_2 \int_0^t [(C_m\ \underline{x}_m(t)]\ dt \qquad \text{(E.2-23)}$$

A theoretical investigation of this compensation technique is continuing.

E.3 DIGITAL ALGORITHM I

This section presents an adaptive algorithm for the discrete-time control defined in Eq. 3.2-14. The algorithm and its stability proof are similar to Continuous Algorithm II and its stability proof. As in Section E.2 asymptotic stability is proven, subject to the condition that the ideal plant control $\underline{u}_p(k)$ is known. Next, stability with respect to a bounded error is guaranteed when only a nominal value for $\bar{\underline{u}}_p(k)$ is known.

E.3.1 Algorithm Structure

The control algorithm is

$$\underline{u}_p(k) = K_x(k)\ \underline{x}_m(k) + K_u(k)\ \underline{u}_m(k) + K_y(k)\ \underline{y}_s(k) \qquad \text{(E.3-1)}$$

with the gains $K_x(k)$, $K_u(k)$, and $K_y(k)$ being adaptive. To simplify later computations, the adaptive gains are concatenated into the $(m \times n_r)$ matrix $K_r(k)$ which is defined as:

$$K_r(k) = [K_y(k), K_x(k), K_u(k)] \qquad \text{(E.3-2a)}$$

Similarly $\bar{K}_r$ is defined as a concatenation of the MRC solution gains

$$\bar{K}_r = [\bar{K}_y, \bar{K}_x, \bar{K}_u] \qquad \text{(E.3-2b)}$$

Correspondingly, the states are put into respective locations in the $n_r \times 1$ vector $\underline{r}(k)$, defined as:

$$\underline{r}(k) = \begin{matrix} \underline{y}_s(k) \\ \underline{x}_m(k) \\ \underline{u}_m(k) \end{matrix} \qquad \text{(E.3-3)}$$

Then Eq. E.3-1 becomes

$$\underline{u}_p(k) = K_r(k)\ \underline{r}(k) \qquad \text{(E.3-4a)}$$

and the MRC solution Eq. 4.1-20 becomes

$$\bar{\underline{u}}_p(k) = \bar{K}_r\ \underline{r}(k) \qquad \text{(E.3-4b)}$$

The adaptive gain is again defined as the sum of a proportional gain, $K_p(k)$, and an integral type gain, $K_I(k)$, each of which will be adapted as follows:

$$K_r(k) = K_p(k) + K_I(k) \qquad \text{(E.3-5)}$$

$$K_p(k) = \underline{v}(k)\ \underline{r}^T(k)\ T_p \qquad \text{(E.3-6)}$$

$$K_I(k+1) = K_I(k) + \underline{v}(k)\ \underline{r}^T(k)\ T_I \qquad \text{(E.3-7)}$$

$$K_I(0) = K_{Io} \qquad \text{(E.3-8)}$$

$$\underline{v}(k) = F\underline{e}(k) + G\underline{z}(k) \qquad \text{(E.3-9)}$$

$$\underline{z}(k) = \bar{\underline{u}}_p(k) - \underline{u}_p(k) \qquad \text{(E.3-10)}$$

where

T_p, T_I are $n_r \times n_r$ time invariant weighting matrices

K_{Io} is the initial integral gain

F and G are matrices of appropriate dimensions.

Selection of F, G, and the weighting matrices T_p and T_I, will, as before, be limited by the sufficient conditions for stability.

Unlike the continuous time case, stability cannot be ensured if Eq. E.3-9 is replaced by $\underline{v}(k) = C_p\ \underline{e}(k)$. This result is a direct consequence of the important role played by the continuous and discrete positive real lemmas in the stability proofs.

The error dynamics in the discrete-time formulation are given by Eq. 3.2-23a:

$$\underline{e}(k+1) = (F_p - G_p \bar{K})\ \underline{e}(k) + G_p\ [\bar{\underline{u}}_p(k) - \underline{u}_p(k)]$$

$$= \tilde{F}_p\ \underline{e}(k) + G_p\ \underline{z}(k) \qquad \text{(E.3-11a)}$$

where

$$\tilde{F}_p = F_p - G_p \bar{K} \qquad \text{(E.3-11b)}$$

and

$$\underline{z}(k) = \bar{\underline{u}}_p(k) - \underline{u}_p(k) \qquad \text{(E.3-11c)}$$

Introducing the control algorithm into the error equation and substituting for $\bar{\underline{u}}_p(k)$ from Eq. 4.4-4b yields

$$\underline{e}(k+1) = \tilde{F}_p\ e(k) + G_p[\bar{K}_r\ \underline{r}(k) - K_I(k)\ \underline{z}(k) - \underline{v}(k)\ \underline{r}^T(k)\ T_p\ \underline{r}(k)] \qquad \text{(E.3-12)}$$

The error dynamics defined in Eq. E.3-12 are used in the subsequent stability proof.

E.3.2 Stability Proof

The first step in the analysis is to form a quadratic function which is positive definite in the state variables, $\underline{e}(k)$ and $K_I(k)$. Assuming that T_I is positive definite, a valid Lyapunov candidate is:

$$V[\underline{e}(k), K_I(k)] = \underline{e}^T(k)\ P\underline{e}(k) + \mathrm{Tr}\ [S_D(K_I(k) - \bar{K}_r)\ T_I^{-1}\ (K_I(k) - \bar{K}_r)^T S_D^T] \qquad \text{(E.3-13)}$$

where

P is an $n \times n$ positive definite symmetric matrix

S_D is an $m \times m$ nonsingular matrix

Stability of the algorithm can be proved by establishing conditions under which the function is decreasing. To aid in this goal, the discrete positive real lemma is stated as follows (Ref. 31):

Lemma: The transfer matrix $S(z) = J + C(zI - A)^{-1} B$, with no poles for $|z| > 1$, and only simple poles on $|z| = 1$, is discrete positive real if and only if there exists a real symmetric positive definite matrix P and real matrices L and W such that

$$A^T PA - P = -LL^T \qquad \text{(E.3-14a)}$$

$$A^T PB = C^T - LW \qquad \text{(E.3-14b)}$$

$$W^T W = J + J^T - B^T PB \qquad \text{(E.3-14c)}$$

If in addition to S(z) being discrete positive real, it is also true that S(z) has no poles for $z = 1$, then S(z) is strictly positive real and

$$A^T PA - P = -LL^T < 0 \qquad (E.3\text{-}15)$$

Using Eqs. E.3-14 and E.3-15 along with the assumption that the transfer matrix $S(z) = J + C_p (zI - F_p + G_p \bar{K})^{-1} B_p$ is discrete strictly positive real for some matrix J and that

$$\underline{v}(k) = F\underline{e}(k) + G\underline{z}(k) \qquad (E.3\text{-}16)$$

where

$$F = (S_D^T S_D)^{-1} C_p \qquad (E.3\text{-}17)$$

it can be shown that

$$\Delta V \equiv V(k+1) - V(k) = -[L^T\underline{e}(k) + W\underline{z}(k)]^T [L^T\underline{e}(k) + W\underline{z}(k)] - \underline{v}^T(k) S_D^T S_D \underline{v}(k) \underline{r}^T(k) (2T_P - T_I)\underline{r}(k) - 2\underline{z}^T(k)(S_D^T S_D G - J)\underline{z}(k) \qquad (E.3\text{-}18)$$

For V(k) to be decreasing, ΔV must be negative definite in $\underline{e}(k)$ and $\underline{z}(k)$, which will be true provided that

$$S_D^T S_D G > J \qquad (E.3\text{-}19)$$

and

$$2T_P - T_I \geq 0 \qquad (E.3\text{-}20)$$

Hence $\underline{e}(k) \to 0$ and $\underline{z}(k) \to 0$ as $k \to \infty$. In addition, Eq. E.3-19 and Eq. E.3-20 imply that $V[\underline{e}(k), K_I(k)]$ cannot increase beyond its initial value $V[\underline{e}(k_o), K_I(k_o)]$. Thus, from Eq. E.3-13 it follows that the adaptive gain matrix $K_I(k)$ will be bounded.

It is interesting to note that if J=0, then Eq. E.3-14 cannot be satisfied and S(z) cannot be discrete positive real. Hence, there does not exist a discrete counterpart to Continuous Algorithm I.

To summarize, the closed loop system which results from the algorithm gives rise to an asymptotically stable error provided that the following sufficient conditions are satisfied:

$$\underline{v}(k) = (S_D^T S_D)^{-1} C_p \underline{e}(k) + G[\bar{\underline{u}}_p(k) - \underline{u}_p(k)] \qquad (E.3\text{-}21)$$

$$S(z) = J + C_p(zI - F_p + G_p \bar{K})^{-1} G_p \qquad (E.3\text{-}22)$$

is strictly positive real for some gain $\bar{K}$

$$S_D^T S_D G > J \qquad (E.3\text{-}23)$$

$$2T_P - T_I \geq 0 \qquad (E.3\text{-}24)$$

Furthermore, $\bar{K}$ must satisfy Eqs. 3.2-17a and 3.2-17b or $\underline{u}_m(k)$ must be restricted to a constant and H_p must be such that Eqs. E-1 and 3.2-17b can be satisfied.

E.3.3 Computation of the Plant Control Law

In this section we address the problem involved in the implementation of the signal $\underline{v}(k)$ from Eq. E.3-21. From the previous subsections we observe that

$$\underline{u}_p(k) = \underline{v}(k)\, \underline{r}^T(k)\, T_P\, \underline{r}(k) + K_I(k)\, \underline{r}(k) \qquad (E.3\text{-}25)$$

and

$$\underline{v}(k) = \underline{v}_1(k) - G\, \underline{u}_p(k) \qquad (E.3\text{-}26)$$

where

$$\underline{v}_1(k) = (S_D^T S_D)^{-1} C_p\, \underline{e}(k) + G\bar{\underline{u}}_p(k) \qquad (E.3\text{-}27)$$

We see from Eq. E.3-25 that $\underline{u}_p(k)$ is a function of $\underline{v}(k)$, while from Eq. E.3-26 we note that $\underline{v}(k)$ is a function of $\underline{u}_p(k)$. From Eq. E.3-25, and E.3-26 we obtain

$$\underline{u}_p(k) = [\underline{v}_1(k) - G\, \underline{u}_p(k)]\, \underline{r}^T(k)\, T_P\, \underline{r}(k) + K_I(k)\, \underline{r}(k) \qquad (E.3\text{-}28)$$

or, solving for $\underline{u}_p(k)$,

$$\underline{u}_p(k) = [I + \underline{r}^T(k)\, T_P\, \underline{r}(k)\, G]^{-1} [K_I(k)\, \underline{r}(k) + \underline{v}_1(k)\, \underline{r}^T(k)\, T_P\, \underline{r}(k)] \qquad (E.3\text{-}29)$$

It should be noted that a unique solution of Eq. E.3-29 requires that the matrix $[I + \underline{r}(k)^T T_P\, \underline{r}(k)\, G]$ be nonsingular.

E.3.4 Effects of Approximating Ideal Plant Control

Computation of the control law using Eq. E.3-29 requires implementation of $\bar{\underline{u}}_p(k)$, as can be seen from Eq. E.3-27. This is not feasible because the gains used in the computation of $\bar{\underline{u}}_p(k)$ are functions of the plant parameters. However, given a nominal set of plant parameters, it may be possible to find values of $\bar{K}_y$, $\bar{K}_x$ and $\bar{K}_u$ such that the nominal $\bar{\underline{u}}_p(k)$ is not too far from the true value. Thus, the control would be modified as follows:

$$\underline{v}(k) = (S_D^T S_D)^{-1} C_p\, \underline{e}(k) + G[\bar{\underline{u}}_{pnom}(k) - \underline{u}_p(k)] \qquad (E.3\text{-}30)$$

$$\underline{v}(k) = (S_D^T S_D)^{-1} C_p\, \underline{e}(k) + G[\underline{u}_{pnom}(k) - \bar{\underline{u}}_p(k)] + G[\bar{\underline{u}}_p(k) - \underline{u}_p(k)] \qquad (E.3\text{-}31)$$

If we use the definition from Eq. E.3-11c that:

$$\underline{z}(k) = \bar{\underline{u}}_p(k) - \underline{u}_p(k) \qquad (E.3\text{-}32)$$

and define $\Delta\underline{u}(k) = \bar{\underline{u}}_{pnom}(k) - \bar{\underline{u}}_p(k)$, then Eq. E.3-31 reduces to

$$\underline{v}(k) = (S_D^T S_D)^{-1} C_p\, \underline{e}(k) + G[\Delta\underline{u}(k) + \underline{z}(k)] \qquad (E.3\text{-}33)$$

Using the modified control law with the original Lyapunov candidate results in

$$\Delta V = -[L^T \underline{e}(k) + W\underline{z}(k)]^T [L^T \underline{e}(k) + W\underline{z}(k)] - \underline{v}(k)^T S^T S\, \underline{v}(k)\, \underline{r}(k)^T(2T_p - T_I)\, \underline{r}(k) - 2\underline{z}(k)^T(-J + G^T S^T S)\underline{z}(k) - 2\Delta\underline{u}(k)^T G^T S^T S\, \underline{z}(k) \qquad (E.3\text{-}34)$$

Observe that ΔV is the same as given by Eq. E.3-18 except for one additional term which is linear in $\underline{z}(k)$. As an extension to a result for continuous systems due to LaSalle (Ref. 30), we can state that $\underline{e}(k)$ and $\underline{z}(k)$ will be ultimately bounded. That is, there exists a $k_1 > 0$ with the property that $||\underline{e}(k)|| < b_1$ and $||\underline{z}(k)|| < b_2$ for all $k > k_1$. Again, as with the continuous time case, these ultimate bounds might be reduced through the redefinition of a new output equal to a linear sum of all past outputs.

E.4 CONSTRAINTS FOR STABILITY OF CONTINUOUS ALGORITHM I

Two types of constraints must be met for asymptotic stability of Continuous Algorithm I, presented in Section E.1. The first type involves structural relationships, given by Eq. E-1 and 3.1-17, between the plant and reference model dynamics. Satisfying these constraints ensures the existence of a control $\bar{\underline{u}}_p(t)$, defined in Eq. 3.1-14, which solves the model reference control problem. In application, these constraints impact the design of the reference model either in terms of the parameters selected or by restricting the command to be a constant. In either case the constraints do not limit the application of the adaptive algorithm if Eq. 3.1-17b can be satisfied (i.e., the system is stabilizable with the measured outputs). The second, more restricting set of constraints in Eqs. E.1-9 and E.1-11 are functions of the plant parameters and are restated here.

A matrix Q_C must be selected such that for every set of plant parameters A_p, B_p and C_p, there exist positive definite matrices P, Q and $S_v^T S_v$ and a feedback matrix $\bar{K}_H$ (satisfying Eq. E-1 and 3.1-17) such that

$$Q_C S_v^T S_v C_p = B_p^T P \qquad (E.4\text{-}1a)$$

and

$$P(A_p - B_p \bar{K}_H H_p) + (A_p - B_p \bar{K}_H H_p)^T P = -Q \qquad (E.4\text{-}1b)$$

where

$S_v^T S_v$ is $m \times m$

P is $n \times n$

$\bar{K}_H$ is $m \times \ell$

Q is $n \times n$

Q_C is $m \times m$

This section presents techniques which determine whether this constraint can be, or is, satisfied. Section E.4.1 shows that this condition is equivalent to a positive real constraint. Section E.4.2 presents possible alternate design procedures to follow if this constraint cannot be satisfied.

E.4.1 Positive Real Approach

Frequency- and time-domain approaches for satisfying the constraint are discussed below. Both approaches are based on the positive real lemma theory (Ref. 29). Mabius has used this theory (Ref. 6) to prove the following lemma:

Lemma: Define

$$Z_1(s) = \bar{C}(sI - \bar{A})^{-1}\bar{B}$$

Let $\bar{A}$, $\bar{B}$ and $\bar{C}$ be a minimal realization of $Z_1(s)$. Then $Z_1(s)$ is strictly positive real if and only if there exists a positive definite $\bar{P}$ and a positive semidefinite $\bar{Q}$ such that

$$\bar{P}\bar{A} + \bar{A}^T\bar{P} = \bar{Q} \qquad (E.4\text{-}2a)$$

and

$$\bar{C} = \bar{B}^T\bar{P} \qquad (E.4\text{-}2b)$$

This Lemma can be used in conjunction with the constraint of Eq. E.4-1 by choosing

$$\bar{A} = A_p - B_p\bar{K}_H H_p \qquad (E.4\text{-}3a)$$

$$\bar{B} = B_p \qquad (E.4\text{-}3b)$$

$$\bar{C} = S^T S\, Q_C\, C_p \qquad (E.4\text{-}3c)$$

Note that $(\bar{A}, \bar{B})$ is controllable because (A_p, B_p) is controllable and since $Q_C S_v^T S_v$ is nonsingular and (C_p, A_p) is observable, $(\bar{C}, \bar{A})$ is observable. Hence, the constraint E.4-1 is equivalent to $Z_1(s)$ being strictly positive real where

$$Z_1(s) = S_v^T S_v\, Q_C\, C_p\, (sI - A_p + B_p\bar{K}_H H_p)^{-1} B_p \qquad (E.4\text{-}4)$$

Thus Eq. E.4-1 is referred to as the PR (positive real) constraint.

Constraint Satisfaction Using Frequency-Domain Considerations - Similar to the method proposed by Mabius (Ref. 6), the following procedure is sufficient to verify that given choices of Q_C and K_H satisfy the PR constraint:

Step 1. Verify that the eigenvalues of $A_p - B_p \bar{K}_H H_p$ have negative real parts for all A_p, B_p and H_p.

Step 2. Define $F(\omega) = Z_1(j\omega) + Z_1^T(-j\omega)$

Step 3. Validate that
(a) $[(A_p - B_p \bar{K}_H H_p), S^T S Q_C C_p]$ is observable for all possible A_p, B_p, C_p and H_p.
(b) $F(\omega)$ is positive definite for all ω.

Step 3(b) is perhaps best carried out by checking that all m principal minors of $F(\omega)$ are positive. Each such minor can be expanded as a ratio of two polynomials in ω^2, each coefficient being a function of C_p, A_p, B_p and $\bar{K}_H$. In such an expansion, the denominator can always be made positive and the numerator can then be written as

$$\sum_{i=o}^{N_m} f_i(H_p, A_p, B_p C_p)\, \omega^{2i} \qquad \text{(E.4-5)}$$

where N_m depends on the number of states and the order of the minor. In order to guarantee that $F(\omega)$ is positive for all ω, it is sufficient that each coefficient, f_i, in each minor be positive for all A_p, B_p C_p and H_p. If each coefficient is not positive, it may be desirable to test for positive realness using the Routh algorithms suggested by Siljak (Ref. 32).

Constraint Satisfaction Based Upon Time-Domain Considerations - This section presents a time-domain approach for determining whether the PR constraint is satisfied for a specific choice of A_p, B_p, C_p, H_p, Q_C, S and $\bar{K}_H$. It is hoped that further study will allow this procedure to apply to a range of these parameters.

The time-domain approach for showing positive realness of the transfer function

$$Z(s) = J + H(sI - F)^{-1}G \qquad \text{(E.4-6)}$$

is based upon the following result. Assume $Z(\infty) < \infty$ and that (F, G, H, J) is a minimal realization of Z(s). Then Z(s) is a positive real matrix of rational functions of s if, and only if, there exists a negative definite matrix π satisfying the equation (Ref. 29):

$$\pi(F - GR^{-1}H) + (F^T - H^T R^{-1} G^T)\pi - \pi GR^{-1} G^T\pi - H^T R^{-1} H = 0 \qquad \text{(E.4-7)}$$

and R is nonsingular where $R = J + J^T$. However, since $J = 0$ in the problem of interest, R is singular. Thus an alternate approach is suggested based upon a test for the discrete positive realness of a transformed system (Ref. 29).

Define the following quantities:

$$A = (I + F)(I - F)^{-1} \qquad \text{(E.4-8a)}$$

$$B = \frac{1}{\sqrt{2}}(A + I)G \qquad \text{(E.4-8b)}$$

$$C = \frac{1}{\sqrt{2}}(A^T + I)H^T \qquad \text{(E.4-8c)}$$

$$U = R + C^T (A + I)^{-1}B + B^T(A^T + I)^{-1} C \qquad \text{(E.4-8d)}$$

Then Z(s) as defined in Eq. E.4-6 will be positive real (for any J including J = 0) if, and only if, the following recursive difference equation has a negative definite steady state solution (Ref. 29):

$$\pi(n + 1) = A^T \pi(n)A - [A^T \pi(n) B + C][U + B^T\pi(n) B]^{-1}[B^T\pi(n) A + C^T] \qquad \text{(E.4-9)}$$

$$\pi(0) = 0$$

To apply this test to the model reference adaptive control problem, A, B, C and are be computed using the following definitions of F, G, H and J:

$$F = A_p - B_p\bar{K}_H H_p \qquad \text{(E.4-10a)}$$

$$G = B_p \qquad \text{(E.4-10b)}$$

$$H = C_p \qquad \text{(E.4-10c)}$$

$$J = 0 \qquad \text{(E.4-10d)}$$

If the π-sequence generated by Eq. E.4-9 converges with these choices, the PR constraint is satisfied for the given A_p, B_p, C_p, H_p and $\bar{K}_H$.

E.4.2 Design of Suitable Output Configurations

In the event that the original system description does not yield a strictly positive real transfer matrix, then it becomes necessary to redesign the output configuration in order to utilize Continuous Algorithm I. This possibility is discussed for the case when measurements are available for all states. At this point we introduce the constraint $\underline{u}_m(t) = 0$. This removes the structural constraint on $\bar{K}$, Eq. 3.1-17a, so that $\bar{K}$ must only satisfy Eqs. E-1 and 3.1-17b.

If measurements for all states are available (assume $H_p = I$), then it may be possible to define a new output matrix that will satisfy the PR constraint. That is, it may be possible to reformulate the model reference control problem with C_p selected as a different linear combination of the measured states;

$$C_p = K_C H_p = K_C \qquad \text{(E.4-11)}$$

The intended result is that the constraint in Eq. 4.5-1 be satisfied. In this section a promising procedure for obtaining K_C is presented.

First, we choose

$$Q_C = I \qquad \text{(E.4-12)}$$

With Eqs. E.4-11 and E.4-12, the constraint (Eq. E.4-1) becomes

$$S_v^T S_v \, K_C = B_p^T P \qquad \text{(E.4-13a)}$$

and

$$P(A_p - B_p \bar{K}_H) + (A_p - B_p \bar{K}_H)^T P = -Q \qquad \text{(E.4-13b)}$$

The selection of K_C uses the theory of the following linear quadratic regulator problem. Consider the problem of choosing $\underline{u}(t)$ to minimize the integral

$$\int_0^\infty (\underline{x}^T Q_R \, \underline{x} + \underline{u}^T R \underline{u}) dt \qquad \text{(E.4-14a)}$$

where Q_R is positive semidefinite and R is positive definite, subject to:

$$\dot{\underline{x}} = A_p \, \underline{x} + B_p \, \underline{u} \qquad \text{(E.4-14b)}$$

The well known solution (when it exists) to this problem is

$$\underline{u} = -K \, \underline{x} \qquad \text{(E.4-15c)}$$

where

$$K \equiv R^{-1} B_p^T P \qquad \text{(E.4-16)}$$

Furthermore,

$$A_p - B_p K \text{ is stable} \qquad \text{(E.4-17)}$$

and

$$A_p^T P + P A_p - P B_p R^{-1} B_p^T P + Q_R = 0 \qquad \text{(E.4-18)}$$

If both K_C and $\bar{K}_H$ are chosen to be equal to K (Eq. E.4-16),

S_v is selected such that $S_v^T S_v = R$, and $Q = Q_R + PB_p R^{-1} B_p^T P$, then

$$S_v^T S_v \, K_C = R(R^{-1} B_p^T P) = B_p^T P$$

and

$$P(A_p - B_p R^{-1} B_p^T P) + (A_p - B_p R^{-1} B_p^T P)^T P$$

$$= A_p^T P + P A_p - 2 P B_p R^{-1} B_p^T P$$

$$= -P B_p R^{-1} B_p^T P - Q_R$$

$$= -Q$$

Hence Eqs. E.4-13a and E.4-13b are satisfied.

Since the above choice of C_p (as defined in Eq. E.4-11) requires a priori knowledge of A_p and B_p, its use is contingent upon the availability of nominal values of A_p and B_p. The robustness of this output matrix for deviations in A_p and B_p must then be examined. As an illustration of how this robustness can be determined, assume that Eq. E.4-18 has been solved for nominal values $\bar{A}_p$ and $\bar{B}_p$, i.e.,

$$\bar{A}_p^T P + P \bar{A}_p - P \bar{B}_p R^{-1} \bar{B}_p^T P + Q_R = 0 \qquad \text{(E.4-19a)}$$

and

$$K_C = \bar{K}_H = R^{-1} \bar{B}_p^T P \qquad \text{(E.4-19b)}$$

Assume further that for all parameters A_p and B_p

$$A_p = \bar{A}_p + \Delta A_p \qquad \text{(E.4-20a)}$$

$$B_p = \bar{B}_p B \qquad \text{(E.4-20b)}$$

where B is a positive definite symmetric matrix. (The form of B_p is motivated by the subsequent solution). Then constraint E.4-13b becomes:

$$P(A_p + \Delta A_p - \bar{B}_p B \bar{K}_H) + (\bar{A}_p + \Delta A_p + \bar{B}_p B \bar{K}_H)^T P = -Q \qquad \text{(E.4-21)}$$

Using Eq. E.4-19b, the above may be rewritten as:

$$P \bar{A}_p + \bar{A}_p^T P - P \bar{B}_p B R^{-1} \bar{B}_p^T P - P \bar{B}_p R^{-1} B \bar{B}_p^T P \qquad \text{(E.4-22)}$$

$$+ P \Delta A_p + \Delta A_p^T P = -Q$$

Adding and subtracting $P \bar{B}_p R^{-1} \bar{B}_p^T P$ to this equation and using Eq. E.4-19a gives:

$$-Q_R + P \bar{B}_p R^{-1} \bar{B}_p^T P - P \bar{B}_p B R^{-1} \bar{B}_p^T P$$

$$-P \bar{B}_p R^{-1} B \bar{B}_p^T P + P \Delta A_p + \Delta A_p^T P = -Q \qquad \text{(E.4-23)}$$

Thus constraint Eq. E.4-13b will be satisfied if A_p and B_p (defined by Eq. E.4-20) are such that:

$$-Q_R + P\,\Delta A_p + \Delta A_p^T P$$

$$+ P\,\bar{B}_p\,R^{-1}\,\bar{B}_p^T P - P\,\bar{B}_p\,[B\,R^{-1} + R^{-1}\,B]\bar{B}_p^T P = -Q$$

With regard to the constraint of Eq. E.4-13a, it should be noted that from Eq. E.4-19b

$$\bar{K}_H = K_C = R^{-1}\,\bar{B}_p^T P \qquad (E.4\text{-}24)$$

or

$$\bar{K}_H = K_C = R^{-1}(B_p\,B^{-1})^T P = R^{-1}\,B^{-1}\,B_p^T P \qquad (E.4\text{-}25)$$

Consequently, if the variation in B is such that the matrix RB is symmetric and positive definite, then S^TS can be defined

$$S_v^T S_v = RB \qquad (E.4\text{-}26)$$

This yields

$$S_v^T S_v\,K_C = B_p^T P \qquad (E.4\text{-}27)$$

which satisfies the constraint, Eq. E.4-13a.

Under the conditions, Eqs. E.4-26 and E.4-27, Eq. E.4-24 may be simplified to:

$$-Q_R + P\,\Delta A_p + \Delta A_p^T P + P\,\bar{B}_p\,R^{-1}\,\bar{B}_p^T P$$

$$- 2\,P\bar{B}_p\,[BR^{-1}]\bar{B}_p^T P = -Q \qquad (E.4\text{-}28)$$

Thus, the matrices $\bar{K}_H$ and K_C (recall they are equal to each other) can be determined by solving the LQR problem:

$$\min J = \int_0^\infty (\underline{x}^T\,Q_R\,\underline{x} + \underline{u}^T\,R\underline{u})\,dt$$

subject to

$$\dot{\underline{x}} = \bar{A}_p\,\underline{x} + \bar{B}_p\,\underline{u}$$

will result in the satsifaction of the constraint Eq. E.4-1 for all A_p and B_p given by Eq. E.4-20 provided that there exists a positive definite P and positive definite symmetric BR such that

$$-Q_R + P\,\Delta A_p + \Delta A_p\,P + P\,\bar{B}_p\,R^{-1}\,\bar{B}_p^T P$$

$$- 2\,P\,\bar{B}_p\,[BR^{-1}]\,\bar{B}_p^T P = -Q \qquad (E.4\text{-}28)$$

E.5 CONSTRAINTS FOR STABILITY OF CONTINUOUS ALGORITHM II

In order to satisfy the strictly positive real constraint, Eq. E.2-4, for Continuous Algorithm II, with a time-invariant A_p and B_p, it is sufficient that this constraint be satisfied for all possible values of A_p and B_p. Thus, an implementable procedure is needed in order to determine that

$$Z(s) = J + C_p(sI - A_p + B_p\,\bar{K})^{-1}\,B_p \qquad (E.5\text{-}1)$$

is strictly positive real. To this effect we shall discuss two procedures.

Recall from Section 3.1 that $\bar{K}$ is chosen to satisfy Eq. E-1 and 3.1-17, or is chosen to satisfy Eqs. E-1 and 3.1-17b with $\underline{u}_m(t)$ restricted to a constant. In the following analysis, $\bar{K}$ is selected to satisfy Eqs. E-1 and 3.1-17b and the PR constraint (Eq. E.5-1).

E.5.1 Frequency-Domain Approach

As an extension to the frequency-domain approach for satisfying the strictly positive real property for Continuous Algorithm I, the following procedure is proposed for validating that the strictly positive real property is satisfied for some matrices J and $\bar{K}_H$ ($\bar{K} = \bar{K}_H\,H_p$).

Step 1. Choose the matrix product $\bar{K}_H H_p$ such that the eigenvalues of $A_p - B_p\bar{K}_H H_p$ have negative real parts.

Step 2. Define $Z(s) = J + C_p\,(sI - A_p + B_p\bar{K})^{-1}\,B_p$ and define $F(\omega) = Z(j\omega) + Z^T(-j\omega)$

Step 3. Validate that C_p and J are such that $F(\omega)$ is positive definite for all ω.

E.5.2 Time-Domain Approach

A time-domain approach for determining a matrix J which results in the strict positive realness of the transfer matrix

$$Z(s) = J + C_p(sI - A_p + B_p\,\bar{K})^{-1}\,B_p$$

is based upon existence of P, L, W such that

$$P(A_p - B_p\,\bar{K}) + (A_p - B_p\,\bar{K})^T P = -LL^T < 0 \qquad (E.5\text{-}2a)$$

$$PB_p = C_p^T - LW \qquad (E.5\text{-}2b)$$

$$W^TW = J + J^T \qquad (E.5\text{-}2c)$$

The procedure for choosing the matrix J is given below.

Step 1 If A_p is a stable matrix, choose $\bar{K}$=0. If A_p is not stable then choose $\bar{K}$ to output-stabilize the plant.

Step 2 Choose L such that L^{-1} exists. Solve the Lyapunov equation, Eq. E.5-2a, for the positive definite symmetric matrix P

Step 3 Solve Eq. E.5-2b for W, yielding $W = L^{-1}(C_p^T - PB_p)$

Step 4 Find any matrix J which solves Eq. E.5-2c. Choosing J to be a symmetric matrix yields $J = \frac{1}{2} W^T W$.

Since the above choice of J requires a priori knowledge of A_p and B_p, its use is contingent upon the availability of nominal A_p and B_p matrices. The robustness of this matrix J, in the sense of retaining the strict positive realness of Z(s) for deviations in A_p and B_p, must then be examined.

As an illustration of how a matrix J (which results in Z(s) being strictly positive real for all A_p and B_p) can be determined, assume that there exist nominal values $\bar{A}_p$ and $\bar{B}_p$ for A_p and B_p, and that all possible variations of these parameters are defined by

$$A_p = \bar{A}_p + \Delta A_p \qquad \text{(E.5-3a)}$$

$$B_p = \bar{B}_p B \qquad \text{(E.5-3b)}$$

where B is a positive definite symmetric matrix. Assume further that there is a known matrix $\bar{K}_H$ which output-stabilizes the plant $(A_p - B_p \bar{K}_H H_p)$ for all parameter variations defined in Eq. E.5-3. The three steps described below define J as a function of a variation in the plant parameters, $J(\Delta A_p, B)$:

Step 1 Choose a nonsingular matrix L. Solve Eq. E.5-2a with A_p and B_p defined by Eq. E.5-3.

Step 2 Set $W(\Delta A_p, \bar{B}) = L^{-1}[C_p^T - P(\Delta A_p, B)\bar{B}_p B]$

Step 3 Set $J = \frac{1}{2} W^T W$

Using these three steps to define J, find the maximum value of J (according to some norm) over the possible parameter variations, ΔA_p and B. That is,

$$J_{max} = \max_{\Delta A_p, B} J$$

Finally choose G such that

$$S_M^T S_M G > J_{max}$$

It may also be possible to obtain a different matrix $S_M^T S_M G$ which will result in improved performance by choosing L in Step 1 to minimize J_{max}. Define this J to be $\tilde{J}$; that is,

$$\tilde{J} = \min_L J_{max}$$

Now choose G such that

$$S_M^T S_M G > \tilde{J}$$

E.6 CONSTRAINT SATISFACTION FOR DIGITAL ALGORITHM I

In order to satisfy the strictly positive real property with a time-invariant F_p and G_p, it is sufficient that this property be satisfied for all F_p and G_p. Thus given all possible values F_p and G_p, an implementable procedure is needed in order to determine that

$$S(z) = J + C_p(zI - F_p + G_p \bar{K})^{-1} G_p$$

be strictly positive real. Since such procedures are parallel to those discussed in Section E.5.2, they are not detailed in this report.

REFERENCES

1. Osborne, R.L., "Controlling Central Station Steam Turbine-Generators," Instruments and Control Systems, Vol. 48, No. 11, November 1975, pp. 29-32.

2. Monopoli, R.V., "Direct Model Reference Adaptive Control: Progress, Problems, and Prospects," Proceedings of the 1979 IEEE Conference on Decision and Control (Ft. Lauderdale), December 1979, pp. 196-201.

3. Narendra, K.S., and Lin, Y.H., "Design of Stable Model Reference Adaptive Controllers," Proceedings of the Workshop on Applications of Adaptive Control (Yale University), August 1979, pp. 15-32.

4. Mabius, L.E., and Kaufman, H., "An Implicit Adaptation Algorithm for a Linear Model Reference Control System," Proceedings of the 1975 IEEE Conference on Decision and Control (Houston), December 1975, pp. 864-865.

5. Mabius, L.E., and Kaufman, H., "An Adaptive Flight Controller for the F-8 Without Explicit Parameter Identification," Proceedings of the 1976 IEEE Conference on Decision and Control (Clearwater), December 1976, pp. 9-14.

6. Mabius, L.E., "An Implicitly Adaptive Model Reference Control Design for Linear Multi-Input Multi-Output Systems," Ph.D. Thesis, Rensselaer Polytechnic Institute, June 1976.

7. Broussard, J.R., and Berry, P.W., "Command Generator Tracking-Continuous Time Case," The Analytic Sciences Corporation, Technical Report TIM-612-1, January 1976.

8. Broussard, J.R., "Command Generator Tracking-Discrete Time Case," The Analytic Sciences Corporation, Technical Report TIM-612-2, January 1976.

9. McDonald, J.P., Kwatny, H.G., and Spare, J.H., "A Nonlinear Model for Reheat-Boiler-Turbine-Generator Systems; Part I - General Description and Evaluation," Proceedings of the 12th Joint Automatic Control Conference (St. Louis), August 1971, pp. 219-226.

10. McDonald, J.P., Kwatny, H.G., and Spare, J.H. "A Nonlinear Model for Reheat Boiler-Turbine-Generator Systems; Part II - Development," Proceedings of the 12th Joint Automatic Control Conference (St. Louis), August 1971, pp. 227-236.

11. Aström, K.T., "Self-Tuning Regulators - Design Principles and Applications," Proceedings of the Workshop on Applications of Adaptive Control (Yale University), August 1979, pp. 1-14.

12. Landau, L.D., and Courtiol, B., "Adaptive Model Following Systems for Flight Control and Simulation," Proceedings of the AAIA 10th Aerospace Sciences Meeting (San Diego), No. 72-95, January 1972.

13. Landau, L.D., Adaptive Control: The Model Reference Approach, Dekker, New York, 1978.

14. Monopoli, R.V., "Model Reference Adaptive Control with an Augmented Error Signal," IEEE Transactions on Automatic Control, Vol. AC-19, No. 5, October 1974, pp. 474-484.

15. Monopoli, R.V., and Hsing, C.C., "Parameter Adaptive Control of Multivariable Systems," International Journal of Control, Vol. 22, No. 3, September 1975, pp. 313-327.

16. Narendra, K.S., Proceedings of the Workshop on Applications of Adaptive Control (Yale University), August 1979.

17. Harris, T.J., MacGregor, J.F., and Wright, J.D., "An Application of Self-Tuning Regulators to Catalytic Reactor Control," Proceedings of 1978 Joint Automatic Control Conference (Philadelphia), Vol. 2, October 1978, pp. 43-58.

18. Waites, H.B., "Application of Model Reference Adaptive Control System to Instrument Pointing Systems" Proceedings of 17th Aerospace Sciences Meeting (New Orleans), January 1979.

19. Amaral, W.C., Magalhaes, L.P., and Mendes, M.J., "Implementation of Self Tuning Regulators in a Mini Computer," Proceedings of 1978 Joint Automatic Control Conference (Philadelphia), Vol. 3, October 1978, pp. 221-228.

20. Elliott, H., "A Model Reference Adaptive Controller with Arbitrary Small Error," Proceedings of 1978 Joint Automatic Control Conference (Philadelphia), Vol. 4, October 1978, pp. 175-182.

21. Price, C.F., "Advanced Concepts for Guidance and Control of Tactical Missiles," The Analytic Sciences Corporation, Technical Report TR-170-5, June 1973.

22. O'Brien, M.J., and Broussard, J.R., "Feedforward Control to Track the Output of a Forced Model," Proceedings of the 1978 IEEE Conference on Decision and Control (San Diego), January 1979, pp. 1149-1155.

23. Broussard, J.R., "The Generalized State Space Representation of the Inverse of Linear Systems," IEEE Transactions on Automatic Control, Vol. AC-24, No. 5, October 1979, pp. 784-785.

24. Tuel, W.G., "On the Trasformation to (Phase-Variable) Canonical Form," IEEE Transactions on Automatic Control, Vol. AC-11, No. 3, July 1966, pg. 607.

25. Kalnitsky, K.C., and Kwatny, H.G., "Development and Implementation of a First Principle Model of a Compound Turbine," Drexel University, Report No. 76-545-1, January 1976.

26. McDonald, J.P., Kwatny, H.G., and Spare, J.H., "Nonlinear Model of a Reheat-Boiler-Turbine-Generator System," Philadelphia Electric Co., Research Division, Report No. E-196, September 1970 (Revised 3rd Printing, October 1973).

27. Fossard, A.J., Multivariable System Control, North-Holland Publishing Company, Oxford, 1977.